KEK Report 95-17
February 1996
H/M

FERMILAB
APR 22 1996
LIBRARY

Study of the Mass of the Electron Neutrino in Japan

Fermilab Library
0 1160 0042432 9

edited by

S. YASUMI & H. MAEZAWA

NAME	I.D.No.	M.S.
A.L Read	00005	323

RETURN TO FERMILAB LIBRARY

NATIONAL LABORATORY FOR
HIGH ENERGY PHYSICS

KEK Report 95-17 The Mass of the Electron Neutrino S.YASUMI & H.MAEZAWA(eds.)

Study of the Mass of the Electron Neutrino in Japan

Preface

This report describes a study of the mass of the electron neutrino using electron capture in ^{163}Ho in Japan for the period from 1981 to 1994.

This monograph has two purposes, one is to supplement the papers on the mass of the electron neutrino already published by us and another is to make a record on some details of our experiments for future.

Electron capture in a nucleus takes place in a rather small space inside an atom, where atomic physics, nuclear physics and particle physics work closely together.

Therefore, this study needed an intimate collaboration of atomic physicists, nuclear physicists and particle physicists. In addition, it was necessary for this study to use various fine techniques, including metallurgy, production of ^{163}Ho activity, micro-analysis by wet chemistry, isotope-dilution mass spectrometry, undulator radiation source technology, the soft X-ray monochromator technology, a counting technique for very intense soft X-rays and so on.

As a result, our collaboration consisted of many researchers from various fields as follows; M. Ando, H. Arai, M. Fujioka, N. Hashimoto, H. Ikeda, Y. Inagaki, K. Ishii, K. Itoh, G. Izawa, O. Kawakami, S. Kishimoto, H. Kitamura, H. Maezawa, M. Maruyama, A. Masuda, K. Masumoto, A. Mikuni, T. Mizogawa, T. Mukoyama, F. Ochiai, T. Ohta, T. Omori, G. Rajasekaran, K. Sera, K. Shima, T. Shinozuka, P. M. Stefan, I. Sugai, H. Taketani, M. Yagi, and S. Yasumi.

Without such an excellent collaboration, this study would not have been completed.

We would like to express our sincere gratitude to Professor T. Sasaki for supporting this study and recommending the undulator beam line of 2.5 GeV Photon Factory Storage Ring as a light source to be used in the experiment.

We also would like to thank Dr. A. Yagishita and Dr. Y. Kitajima who are responsible for the BL-2 beamline.

Finally we are grateful to Ms. M. Noji for her patient typewriting of manuscripts written by hand.

February 1996

Shinjiro Yasumi and Hideki Maezawa

Contents

Preface

Chapters

1. History. 1
S. Yasumi

2. Preparation of a Dysprosium Metal Target and its Bonding to a Cooling Block for the Production of ^{163}Ho. 5
K. Ishii, M. Fujioka, K. Sera, T. Shinozuka and K. Katsube

3. Production of a Long-Lived Isotope ^{163}Ho by a Simple Method of Internal Irradiation. 11
M. Fujioka, K. Ishii, T. Shinozuka and K. Sera

4. Chemical Separation of ^{163}Ho and its Source Preparation. 15
T. Omori, G. Izawa, M. Yagi, K. Masumoto, M. Fujioka, K. Ishii and K. Sera

5. Study in the Period from 1981 to 1983. 27
S. Yasumi and F. Ochiai

6. Study in the Period from 1984 to 1986. 33
S. Yasumi and Y. Inagaki

7. Response Functions of a Si(Li) Detector for Low Energy X-rays. 43
Y. Inagaki

8. Influence of the Window Effect of Si(Li) X-ray Detector on the Response Function and Detection Efficiency. 47
K. Shima, Y. Inagaki, H. Maezawa and S. Yasumi

9. N_0 and $T_{1/2}$ of ^{163}Ho Source. 55
O. Kawakami and A. Masuda

10. Description of the Soft X-ray Undulator Beamline. 65
H. Maezawa and S. Kishimoto

11. Study in the Period from 1987 to 1990. 69
S. Yasumi and S. Kishimoto

12. Estimation of Atomic Parameters for Electron Capture Decay of ^{163}Ho. 71
T. Mukoyama

13. Study in the Period from 1991 to 1995. 83
S. Yasumi and H. Maezawa

Supplements

1. On the log(*ft*) Values of Gamow-Teller Transitions around ^{163}Ho. 109
M. Fujioka and S. Yasumi

2. Milestones. 112

3. Publications. 117

Chapter 1

History

S. Yasumi

Teikyo University/KEK

In 1980, Lubimov et al. [1] of Moskow firstly reported a lower limit for the electron antineutrino mass of 14 eV from a study of the shape of the tritium beta spectrum at the end point.

Also in the same year, Reines and others [2] reported indications of neutrino instability, that is, the neutrino oscillation. They measured cross sections for the charged - and neutral - current branches of the interactions of fission neutrinos with deuterons:

$$\bar{\nu}_e + d \begin{cases} \nearrow n + n + e^+ & \text{(ccd)}, \\ \searrow n + p + \bar{\nu}_e & \text{(ncd)}. \end{cases}$$

Based on the departure of the measured ratio (ccd/ncd) from the expected value at 2 - 3 standard deviation level, they reached the above conclusion. If the neutrino oscillation does exist, it means that neutrinos have some finite masses.

Furthermore, it was discussed that the missing-mass problems in cosmology could be solved if neutrinos had masses of the order of some tens of electronvolt [3],[4].

In 1981, A. De Rújula [5] of CERN proposed a new way to measure the electron neutrino mass by using the internal bremsstrahlung in electron capture (abbreviated as IBEC). The endpoint shape of an IBEC photon spectrum is governed by the three-body kinematics and is sensitive to the neutrino mass in precisely the same way as in the beta decay process discussed by Fermi. Generally the intensity of IBEC is very low. However, De Rújula pointed out that when the Q-value of a nucleus lies close to the binding energy of one of S-states of an atom, the intensity of IBEC is resonantly enhanced and becomes intense enough to measure for obtaining the mass of the electron neutrino. He recommended to experimenters ^{193}Pt and ^{163}Ho as possible candidates of electron capturing nuclei for measuring the electron neutrino mass.

Under such a situation, three groups which intended to measure the electron neutrino mass, started; CERN-Aarhus group in Europe, Princeton-Livermore group of United States, and our Japanese group.

European group [6] estimated the partial M-capture half-life of ^{163}Ho from electron capture rates and the number of active atoms in a ^{163}Ho source. Using the matrix element which they deduced from the measured reduced transition probability of ^{161}Ho and pairing model calculations, they evaluated the Q-value of ^{163}Ho. They also performed a direct determination of the Q-value using nuclear reaction experiments, obtaining 2.3 ± 1.0 keV, which is consistent with the above Q-value. From these results they deduced a half-life of (7 ± 2) x 10^3 yr and an upper limit for the electron neutrino mass of 1.3 keV.

Next, European group [7), 14)] proved the validity of IBEC theory developed by De Rújula [5] by using ^{193}Pt. They also reported an upper limit for the electron neutrino mass of 500 eV (90% C.L.) from the above ^{193}Pt experiment.

The American group, at an early stage, intended to measure the mass of the electron neutrino using relative capture ratio from different electron orbits in ^{163}Ho [8]. They measured M X-ray from ^{163}Ho with a Si (Li)-detector [6] and also measured a half-life of 4570 ± 50 yr (95% C.L.) for ^{163}Ho using isotope-dilution mass spectrometry [9]. From this value of the half-life, they inferred a Q-value of approximately 2.65 keV using known atomic physics parameters and an estimate of the nuclear matrix element based on the systematics of electron-capturing log ft values of other Ho isotopes. Thus it turned out that the Q-value of ^{163}Ho is not so low, then they abandoned their initial approach and began pursuing the measurement of the internal bremsstrahlung in electron capture for ^{163}Ho [10].

They measured an IBEC photon spectrum from ^{163}Ho in the 5p-3s characteristic X-ray region with a Si (Li)-detector in air. From this measurement, they claimed that an upper limit for the electron neutrino mass of 225 eV was obtained.[10), 11)]

By K. Riisager [12], however, this upper limit seems to be unreliable for the following reasons: 1) this upper limit is too much dependent on the Q-value of Hartmann and Naumann (~ 2.6 keV) which was deduced from the measured ratio of N-capture to M-capture in the decay of ^{163}Ho [13]. In addition this Q-value is probably too low; 2) that the sign of the interference term is opposite to that predicted by the theory also seems not to be persuasive.

In 1985 Riisager et al. [14] found that there is the presence of an interference minimum near the end-point in an IBEC spectrum from ^{163}Ho, which reduces the expected intensity and also complicates the shape of a spectrum, hence making the IBEC approach to obtain the electron neutrino mass less attractive.

In May 1981, our Japanese group started, aiming at the electron neutrino mass measurement using the IBEC approach proposed by A. De Rújula [5].

In the seminar on the electron neutrino mass held on July 22nd 1981 at the Cyclotron and Radioisotope Center in Tohoku University, the Tohoku University

group decided to join the $m_{\nu e}$-Collaboration in KEK and to be in charge of the production of ^{163}Ho activity (CYRIC) and the preparation of ^{163}Ho sources (Chemistry Department and Laboratory of Nuclear Science).

References

1) V. A. Lubimov et al., Phys. Lett. **94**B (1980) 266.
2) F. Reines, H. W. Sobel, and E. Pasierb, Phys. Rev. Lett. **45** (1980) 1307.
3) P. H. Frampton and P. Vogel, Phys. Reports, **84** (1982) 342.
4) W. J. Marciano, Comments on Nuclear and Particle Physics **IX**, No. 5 (1981) 169.
5) A. De Rújula, Nucl. Phys. B**188** (1981) 414.
6) J. U. Andersen et al., phys. Lett. **113**B (1982) 72.
7) B. Jonson et al., Nucl. Phys. A**396** (1983) 479C.
8) C. L. Bennett et al., Phys. Lett. **107**B (1981) 19.
9) P. A. Basiden et al., Phys. Rev. C**28** (1983) 337.
10) C. L. Bennett, Neutrino Mass & Low Energy Weak Interactions Telemark, 1984 p. 128 edited V. Barger and D. Cline.
11) Springer et al., Phys. Rev. A**35** (1987) 679.
12) K. Riisager, Private communication, April 14, 1986.
13) F. X. Hartmann and R. A. Naumann, Phys. Rev. C**31** (1985) 1594.
14) K. Riisager et al., Physica Scripta, **31**, (1985) 321.

Chapter 2.

Preparation of a Dysprosium Metal Target and its Bonding to a Cooling Block for the Production of ^{163}Ho

K. Ishii, M. Fujioka, K.Sera and T. Shinozuka

Cyclotron and Radioisotpe center, Tohoku University

K. Katsube

Department of Physics, Tohoku University

Recently two new methods have been proposed by Rújula et.al. [1] and by Hallin et.al. [2] for the determination of the mass of the electron neutrino from the electron-capture decay of the long-lived isotope ^{163}Ho. The decay of this isotope was first studied by Hopke et.al. [3]; they prepared a ^{163}Ho source by neutron activation via ^{162}Er(n,γ)^{163}Er(E.C.)^{163}Ho. Since the natural abundance of ^{162}Er is extremely small, the source is inevitably accompanied by another long-lived isotope ^{166}Ho via ^{164}Er(n,γ)^{165}Er(E.C.)^{165}Ho(n,γ)^{166}Ho. We produced ^{163}Ho by the ^{164}Dy(p, 2n) ^{163}Ho reaction which is free from ^{166}Ho. In order to obtain ^{163}Ho as much as possible it was necessary to irradiate a Dy target by a proton beam of 20 MeV × 100 μA inside the vacuum chamber. For this purpose we developed a method of high-temperature bonding of a Dy metal target onto a cooling block of Cu together with a technique of dis-bonding after irradiaton.

From the thermal design of target cooling [4], temperature as high as 600°C was expected at the Dy-Cu interface due to high thermal flux of ~ 4 kW/cm^2 by the beam heating that the ordinary low-temperature soldering cannot withstand. Therefore we used as a brazing filler metal BAg-8 which has the temperature of solidus and liquidus of 779°C [5]. Since the rare-earth metals are easily oxidized and alloyed at high temperature, it was necessary to use an induction furnace under argon atmosphere and to perform bonding or dis-bonding as swiftly as possible; Dy begins to alloy with Cu at 750°C to form DyCu to $DyCu_6$. To our knowledge such a high-temperature bonding of a rare-earth metal has not been reported [6].

The starting material was $^{164}Dy_2O_3$ from ORNL, which was fluorinated into $^{164}DyF_3$. The method of fluorination is as follows. About 1.2 times of theoretical quantity of HNO_3 dissolves $^{164}Dy_2O_3$ and about 1.2 times of theoretical quantity of HF is added , and the precipitate is decantated with H_2O until pH becomes about 3.5. Washing with water the final sample of $^{164}DyF_3$ is obtained after drying in vacuum. $^{164}DyF_3$ was then reduced to metal by a Ca reduction method [7]. The metal pellet thus obtained was pressed and rolled into a plate of 30 mm × 10mm × 0.1 mm. The power supply of the furnace has a capacity of 5 kW and a frequency of 400 kHz. The furnace is a quartz tube of 50 mm in inner diameter wound by a water-cooled Cu coil of 10 turns × 4 mm in outer diameter; the flow rate of argon is ~ 1ℓ/min at 1 atm. Fig. 1 illustrates the arrangement of bonding. By a quartz pole is supported the Cu block (30 × 32 × 40 high), onto which are placed a foil of BAg-8 (11 × 29 × 0.05 thick), the Dy target plate and a quartz plate (30 × 30 × 3 thick). The center of the quartz plate was pressed by a quartz stick in order to obtain a tight contact of Dy, BAg-8 and Cu. Since these metals have different values of specific resistivity, the speed of temperature rise is different for the different metal elements if the Cu block assembly is placed at the center of the induction coil, leading to a failure of bonding. Therefore, the Cu block assembly should be positioned in such that the Dy-BAg-Cu region be 10-15 mm above the upper border of the induction coil. In this way only the Cu block is directly heated by induction, and BAg-8 and Dy are heated by conduction from the Cu block. About 3 min after switching on the power supply in its full power of 5 kW the BAg-8 begins to melt, and it is essential to switch off the power instantly; otherwise the Dy metal is strongly alloyed with BAg-8 and the surface of the Cu block, and dis-bonding becomes very difficult. After several trials we found an optimum thickness of 0.05 mm of BAg-8; a too small thickness gives an incomplete bonding on the one hand, and a too large thickness a strong alloying. Also the use of any flux material is not recommended because of oxidation of Dy. We also note that the coupling between the grid and the plate circuits of the power supply should be matched with the effective input impedance of the load consisting of the induction coil and the Cu block, in order to effectively supply power into the Cu block. Fig. 2 shows a Dy target bonded to the Cu block and Fig. 3 shows microscopic pictures of the Dy-BAg-Cu bonding structure. Whereas in (a) of Fig. 3 any region of alloying between Dy and BAg-8 is not discernible, a layer of alloy region is clearly seen in (b) of Fig. 3 for which the power supply of the furnace was switched off 10 s after the moment of the melting of BAg-8. However, we consider that a minimum amount of alloying should be necessary for a firm bonding of Dy to the Cu block. The ^{164}Dy target prepared in this way was found to withstand a proton irradiation of 20 MeV × 100μA × 24 h without any visible damage.

After irradiation we *dis-bonded* the target from the Cu block using the same induction furnace under the same condition as for the bonding. We scraped off the target using a quartz stick at the one end of which a small rectangular plate of tungsten was firmly fastened. We would like to stress again that it is important to do the job as fast as possible at the instant of melting of BAg-8. It is rather easy to catch the instant of melting by eyes.

The present method of bonding and dis-bonding should be applicable to other target metals which are easily oxidized or alloyed for an efficient cooling of the target in a high-current irradiation by charged particles.

We are grateful to Mr. H. Noro of Japan Yttrium Co. Ltd. for a metallurgical guidance of rare earths, to Dr. M. Kasaya of Department of Physics for his cooperation in the initial phase of the present development, and to Dr. T. Omori of Department of Chemistry for the preparation of $^{164}DyF_3$ Thanks are due to Prof. T. Ishimatsu, director of this center, and Prof. S. Yasumi of National Laboratory for High Energy Physics for encouragement.

References.

[1] A. De Rújula, Nucl. Phys. **B188** (1981) 414.

[2] A. L. Hallin, C. L. Bennett, P. T. Springer and R. A. Naumann, Princeton Nucl. Phys. Proposal (1980) 75, unpublished.

[3] P. K. Hopke, J. S. Evans and R. A. Naumann, Phys. Rev. **171** (1968) 1290.

[4] M. Fujioka et.al., Cyclotron and Radioisotope Center Ann. Rept. (1981).

Cleveland, 1977-1978) 172.

[5] R. C. Weast, ed., CRC handbook of chemistry and physics, 58th ed. (CRC Press, Cleveland, 1977-1978) 172

[6] J. Jaklovsky, Preparation of nuclear targets - A comprehensive bibliography (IFI, Plinum, New York, Washington, London, (1981).

[7] A. H. Daane and F. H. Spedding, J. Electrochem. Soc., 100 (1953) 422. See also E. C. Subbarao and W. E. Wallace (eds.) Science and technology of rare earch materials (Academic Press, New York, 1980).

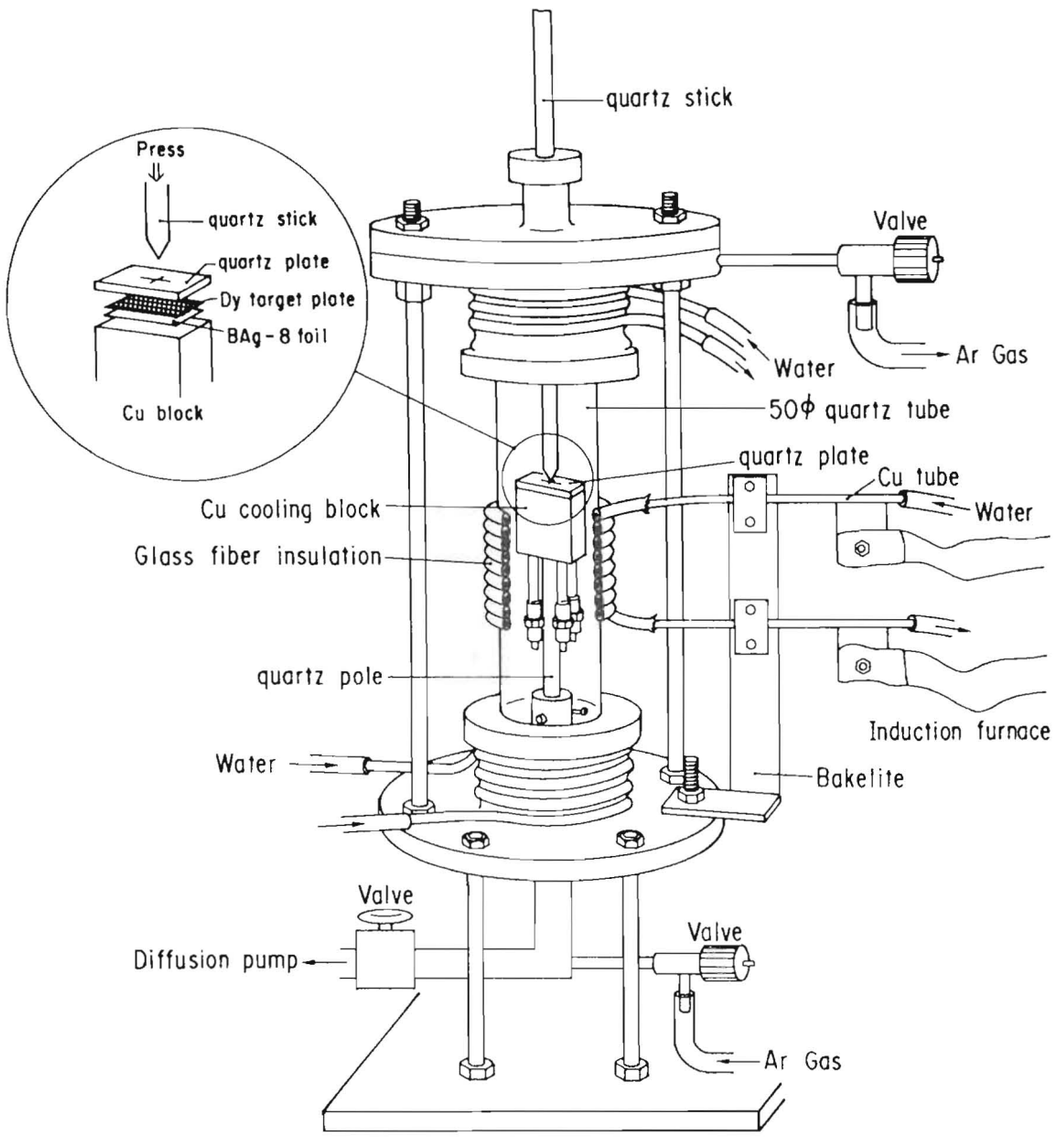

Fig. 1. Arrangement for the bonding of a Dy metal plate onto a Cu cooling block.

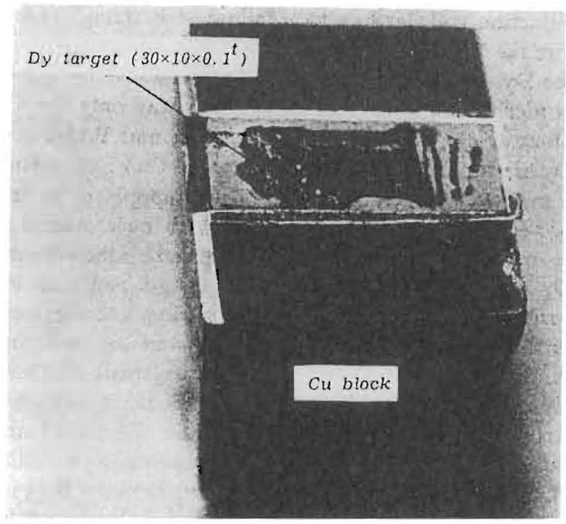

Fig. 2. Dy target as bonded onto the Cu block. In this case natural Dy was used.

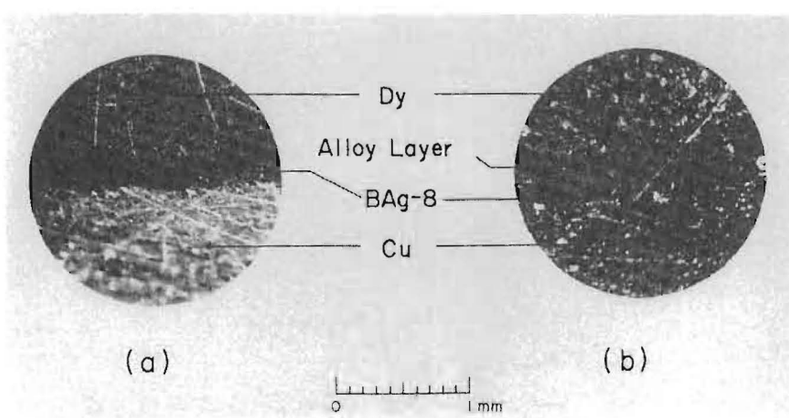

Fig. 3 Microscope picture of the bonding layer of Dy-BAg-Cu. (a) The power supply of the induction furnace was switched off at the moment of the melting of BAg-8. (b) The power supply was switched off 10 s after the melting of BAg-8. It is noted that in (b) the surface was etched by HCl in order to make clear the region of the alloy layer. The different appearance of the Cu layer in (a) and (b) is due to different angles of illumination and is spurious.

Chapter 3

Production of a Long-Lived Isotope ^{163}Ho by a Simple Method of Internal Irradiation

M. Fujioka, K. Ishii, T. Shinozuka and K. Sera
Cyclotron and Radioisotope Center, Tohoku University, Sendai 980 Japan

1. Introduction

The electron-capture decay of long-lived ^{163}Ho ($T_{1/2} = 5\times10^3$ y) has been proposed as a new method for determining the mass of electron neutrino.[1] For producing this isotope we developed a simple method of internal irradiation by modifying the cooling block of the main diagnostic probe of our cyclotron on the basis of a thermal design calculation of cooling.

2. Modification of the main probe

The relevant part of the modified main probe is shown in fig. 1. The results of modification are; i) the cooling water channel has a form of sheet parallel to the surface of the cooling block of Cu where the target is mounted, ii) the block can be disconnected from the stem so that the target can be mounted and dismounted conveniently, and iii) an interlock will rapidly exaust water in the cooling line in the event of vacuum failure of the cyclotron. From test irradiations the beam grazing angle θ was chosen to be 8.5°. The most important parameter D, the depth of the water channel below the surface, was determined to be 8 mm as described below.

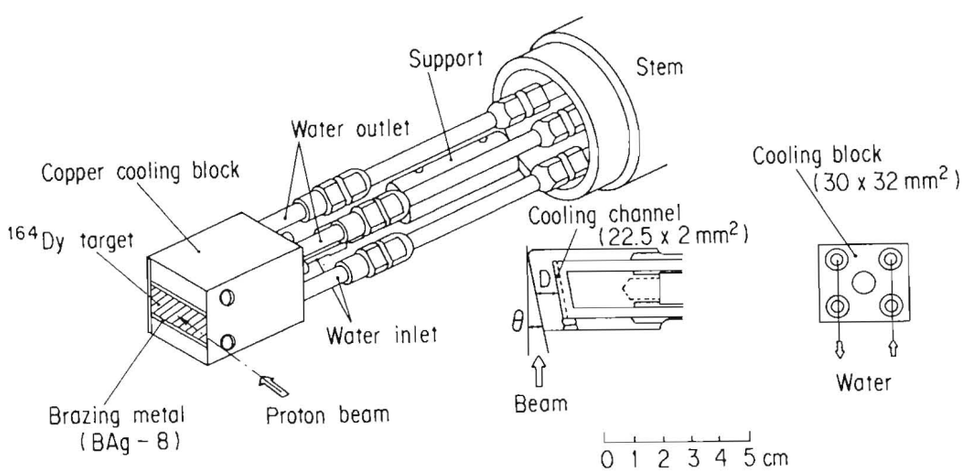

Fig. 1. Modified main probe for internal irradiation. The target assembly is for the production of ^{163}Ho by ^{164}Dy(p,2n)^{163}Ho.

3. Thermal design calculation

Through the wall of cooling channel the heat generated by the beam is transferred to water by a mechanism of *subcool nucleate boiling*, but if the thermal flux density on the wall q_{wall} becomes larger than a *critical burnout flux density* q_{BO} the nucleate boiling goes over irreversively into a membranous boiling with a resultant catastrophe of burnout. Therefore D should be such that q_{wall} be smaller than q_{BO}. The relevant empirical formula for q_{BO}[2] and heat transfer[3] by subcool nucleate boiling are

$$q_{BO} = 0.719\ V^{1/2}\ \Delta T_{sat} \text{ with } \Delta T_{sat} \equiv T_{sat} - T_0\ , \tag{1}$$

$$\Delta T_{boil} \equiv T_{wall} - T_{sat} = 7.86\ e^{-P/61}\ q_{wall}^{1/4}\ , \tag{2}$$

where V is the velocity (cm/s), T_{sat} the saturation temperature (°C), T_0 the main-stream temperature, and P the absolute pressure (atm) of the cooling water; q's are in W/cm^2, T_{wall} is the wall temperature, and T_0 can be identified with the average temperature of cooling water as long as the temperature rise is small.

On the other hand the maximum temperature on the surface of cooling block T_{surf}^{max} and the maximum flux density on the wall q_{wall}^{max} can be estimated from a solution of thermal conduction in a finite cylinder;

$$T_{surf}^{max} \simeq T_{wall}^{max} + \frac{q_0 B}{\lambda}\left[\left(\frac{B}{A}\right)^2 + \frac{2B}{D}\sum_{m=1}^{\infty}\frac{J_1\left(\frac{B}{A}j_{1,m}\right)}{j_{1,m}^2 J_0^2(j_{1,m})}\tanh\left(\frac{D}{A}j_{1,m}\right)\right]\ , \tag{3}$$

$$q_{wall}^{max} \simeq q_0\left[\left(\frac{B}{A}\right)^2 + \frac{2B}{A}\sum_{m=1}^{\infty}\frac{J_1\left(\frac{B}{A}j_{1,m}\right)}{j_{1,m}J_0^2(j_{1,m})\cosh\left(\frac{D}{A}j_{1,m}\right)}\right]\ , \tag{4}$$

where the conduction layer (thermal conductivity λ) is approximated by an equivalent cylinder (disk) of radius A and thickness D, the beam heating by a flux density of q_0 over a circle of radius B on the surface, $J_n(x)$ is the Bessel function of order n, and $j_{1,m}$ the m-th *positive* root of $J_1(x) = 0$.

From these equations one obtains D, provided a safety factor $F_{safe} > 1$ defined by $F_{safe} = q_{BO}/q_{wall}^{max}$ is assumed.

3. Choice of D and production of ^{163}Ho

For a safe production of ^{163}Ho by the $^{164}Dy(p,2n)^{163}Ho$ reaction, we chose D [hereafter denoted as D(Cu)] assuming a beam spot area of $\pi B^2 = 0.5\ cm^2$,

hence q_0 = 4 kW/cm^2, under the condition of πA^2 = 3.0×3.2 cm, a water flow of 11.6 ℓ/min over a cross section of 2.25×0.2 cm^2, P = 4 atm and T_0 = 30°C. The thermal conduction through the ^{164}Dy layer and a bonding layer (BAg-8)[4] on top of the Cu block was calculated using an approximation of homogeneous heat generation in these layers. Thus the necessary quantities were calculated as a function of D(Cu), and from this we selected D(Cu) to be 0.8 cm; see table 1.

Table 1. Design parameters of cooling for internal proton irradiation of a ^{164}Dy metal target[a)]

Quantity	Design value	Quantity	Design value
E_p	20 MeV	V	430 cm/s
I_p	100 μA	P	4 atm
	8.5°	T_{sat}	144°C
A	1.75 cm	q_0	4.0 kW/cm^2
B	0.40 cm	q^{max}_{wall}	1.7 kW/cm^2
D(Dy)	0.010 cm	F_{safe}	2.2
D(BAg-8)	0.005 cm	T(vac./Dy)	652°C
D(Cu)	0.80 cm	T(Dy/BAg-8)	581°C
T_0	30°C		

a) Effective thickness of Dy as a target is D_{eff}(Dy) = D(Dy)/sinθ. Thermal conductivities used are λ(Dy) = 0.11, λ(BAg-8) = 0.58 and λ(Cu) = 3.57 in W/cm°C.

We successfully irradiated a ^{164}Dy metal target of 96 mg/cm^2 (D = 0.011 cm; cf. table 1) using a 100 μA proton beam for 42 h at R_{irrad} = 64.5 cm, where E_p = 20 MeV, with an estimated production quantity of ^{163}Ho of 24 μg. From MX-ray measurement in the electron-capture decay of ^{163}Ho we deduced[5] an upper limit of the mass of electron neutrino as $m_{\nu_e}c^2 \lesssim 1.25$ keV.

References

1) A. De Rújula, Nucl. Phys. B188 (1981) 414.

2) F. C. Gunther, Trans. ASME 73-2 (1951) 115.

3) W. H. Jens and P. A. Lottes, ANL-46 (1951).

4) K. Ishii, M. Fujioka, K. Sera, T. Shinozuka and K. Katsube, Nucl. Instr. Meth. 205 (1983) 563.

5) S. Yasumi et al., Phys. Letters 122B (1983) 461.

Chapter 4

Chemical Separation of ^{163}Ho and its Source Preparation

Takashi OMORI, Gunzo IZAWA
Department of Chemistry, Tohoku University
Masuo YAGI, Kazuyoshi MASUMOTO
Nuclear Science Laboratory, Tohoku University
Manabu FUJIOKA. Keizo ISHII, and Koichiro SERA
Cyclotron and Radioisotope Center, Tohoku University

1. Introduction

Preparation of sources of carrier-free ^{163}Ho was tried to determine the mass of electron neutrino. However, this method was considered to overcome many difficulties which differ extensively from usual source preparation as follows:

1) In addition to difficulties in mutual separations of lanthanoids resulting from their chemical similarities, carrier-free ^{163}Ho must be separated from a large excess of target ^{164}Dy.

2) Since no γ-rays are emitted from ^{163}Ho, chemical behavior of ^{163}Ho must be traced by measuring Dy M X-rays, of which energy is 2.3 keV. This means that detection of ^{63}Ho in solutions is actually impossible.

3) Preliminary separation of macroamount of Ag and Cu which are main component of the brazing metal BAg-8 and are necessarily accompanied with the target ^{164}Dy is required. Furthermore, it should be taken into consideration that very strong radioactivities are also induced in the brazing metal.

4) A large number of radioactivities derived from ultramicro amount(less than ppb) of element in the target must be identified and eliminated.

5) In the final source, no X- and γ-rays other than M X-rays of Dy should be detected. If the detection limit of radioisotope is considered to be 1 pCi(3.7 Bq), expected radioactivities of 1 mCi must be eliminated less than $1/10^9$. It should, of course, be a point source and is preferable to minimize the contamination of non-radioisotopes other than Dy.

From the view point of these considerations, the following procedure has been established.

1) Final separation of ^{163}Ho from the parent ^{164}Dy is desirable by means of a cation exchange method. However, preliminary separation of the component of brazing material is

recommended to maintaining safe-working condition and should be a simple and convenient method. A candidate for the preliminary separation of the brazing material was the coprecipitation of ^{163}Ho with ^{164}Dy as hydroxide in an ammonium solution, so that the brazing material such as Ag, Cu and ^{65}Zn which would be produced by (p, xn) reactions remain the solution as ammine complexes.

2) The ^{163}Ho coprecipitated in $Dy(OH)_3$ was dissolved in a diluted hydrochloric acid and the solution was placed onto a cation exchange column. By using hydrochloric acid in this procedure, silver coprecipitated in $Dy(OH)_3$ can completely be removed from the solution, forming silver chloride precipitation.

3) An electrodeposition method is considered to be adequate for the preparation of ^{163}Ho source to obtain a thin and point source.

2. Preliminary study for separation condition using a cation exchanger

Among various separation methods of lanthanoids, the cation exchange method demonstrates the highest separation efficiency in the wider range from carrier-free concentration to macroamount element[1, 2]. General procedures can be described as follows: First, lanthanoids are adsorbed on a cation exchange column and then they are eluted by an appropriate organic weak acid as an eluent. In the present study, AG50W-X8 (100-200 mesh) was employed as a cation exchanger, because it has a uniform size and the highest purity among available exchangers. The resin column (1 cmϕ × 100 cm) was equipped with a water jacket to circulate water at a constant temperature. A constant volume of the eluate was collected with a fraction collector and the flow rate of the eluate was kept constant with a regulating pump. The radioactivity of each fraction was measured with a single channel γ-ray spectrometer with a well type NaI(Tl) scintillator or by a multichannel pulse height analyzer with a Ge(Li) or a LEPS.

Ethylenediaminetetraacetic acid (EDTA)[3, 4], citric acid [3, 5] and 2-hydroxy-methylpropionic acid (α-hydroxyisobutylic acid, AHIB) [6-8] have been employed as an eluent in the cation exchange separation of lanthanoids. Though AHIB was said to be effective in the separation of heavy rare earths, there still be a problem that yttrium is eluted between holmium and dysprosium[8].

It is necessary to determine accurately the elution positions of erbium, holmium and dysprosium under the present experimental condition. Thus, the radioactive tracers required for this purpose were produced by the reactions of $^{162}Eu(\gamma, n)^{161}Eu$ ($T_{1/2}$ = 3.2 h), $^{168}Er(\gamma,$

p)^{167}Ho (3.1 h), and ^{158}Dy(γ, n)^{157}Dy (8.1 h) using a LINAC of Nuclear Science Laboratory, Tohoku University. These tracers were separated using EDTA or citric acid as the eluent, but satisfactory elution curve could not be obtained. One of the reasons for failure in the separation was ascribed to low specific activities. These required long time separation with a low flow rate, but their short half-lives could not allow the separation procedure.

Dysprosium metal of natural abundance, therefore, was irradiated with protons using a cyclotron of the Cyclotron and Radioisotope Center, Tohoku University, and AHIB was chosen as an eluent. The irradiated dysprosium metal was dissolved in nitric acid and then dysprosium was precipitated with ammonium hydroxide to leave silver and copper in the solution. The elution curve for the lanthanoid fraction was seen in Fig. 1.

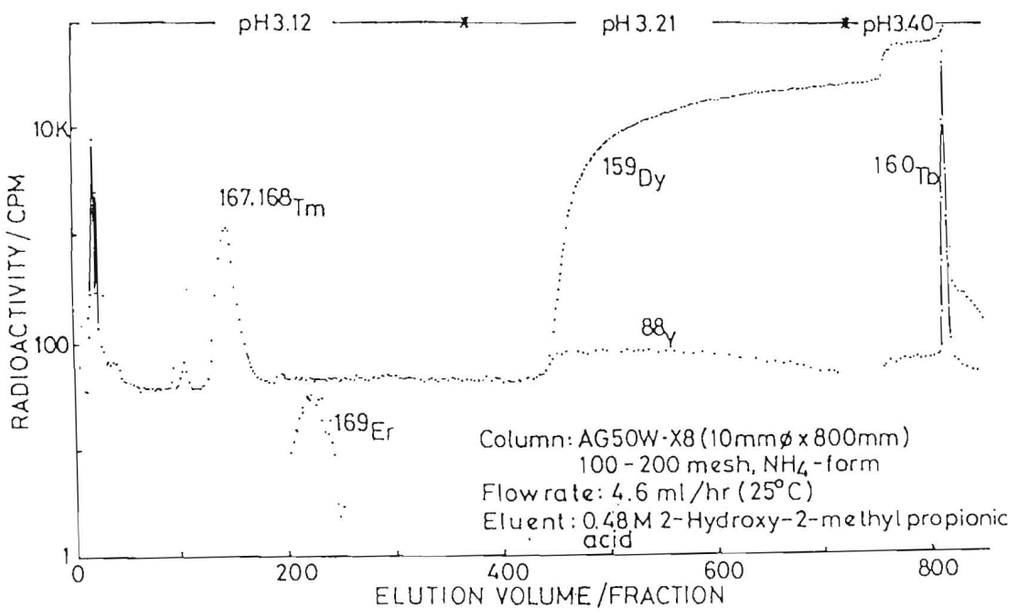

Fig. 1. Elution curve for natural Dy target.

The elements such as zirconium and hafnium having large formation constants with AHIB were eluted first, and then lanthanoids were eluted in the reverse order of the atomic number. Thulium was followed by ^{169}Er, of which activities was measured with a GM counter. The elution curve of dysprosium did not exhibit a Gaussian distribution, because of a very large concentration of its carrier, but the eluted position of dysprosium was separated enough away from that of erbium. Thus, the fundamental separation procedure had been established by considering that ^{163}Ho would appear in a position far away from both erbium

and dysprosium. In order to use ^{168}Tm as a tracer in the practical separation, the thulium fractions were collected and concentrated.

3. Preparation of ^{163}Ho source

3.1. Separation of lanthanoids by hydroxide co-precipitation.

Figure 2 summarizes the chemical separation procedures for ^{164}Dy used as a target.

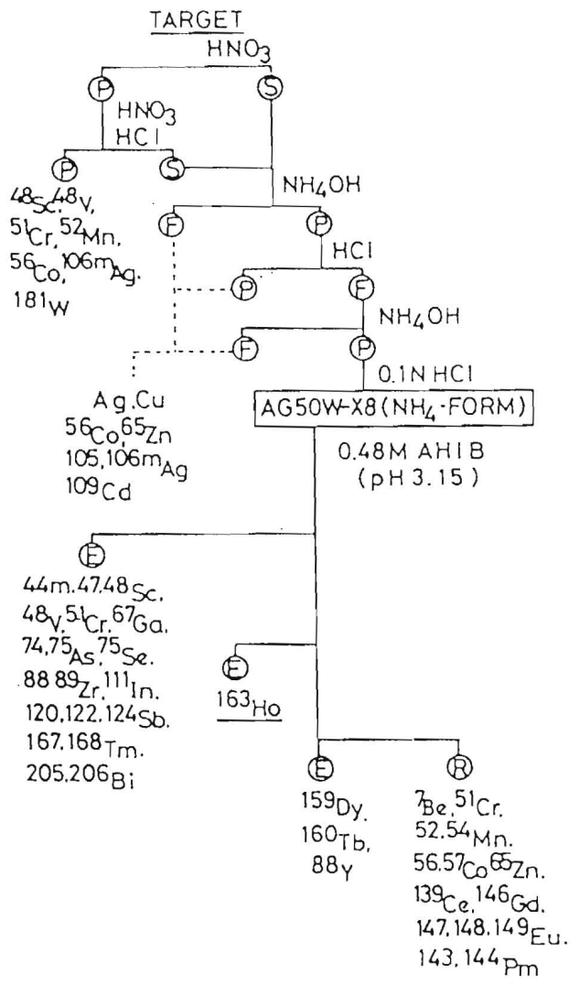

Fig. 2. Procedure for the chemical separation of ^{163}Ho.

The target was dissolved in concentrated nitric acid, but the black residue remained slightly. In the residue ^{48}Sc, ^{48}V, ^{51}Cr, ^{52}Mn, ^{54}Mn, ^{56}Co, and ^{65}Zn were detected by the γ-ray

spectrometry. As Fig. 3 shows, a large peak of tantalum seemed to be due to the contamination of target from a tantalum crucible used in the calcium reduction of dysprosium fluoride.

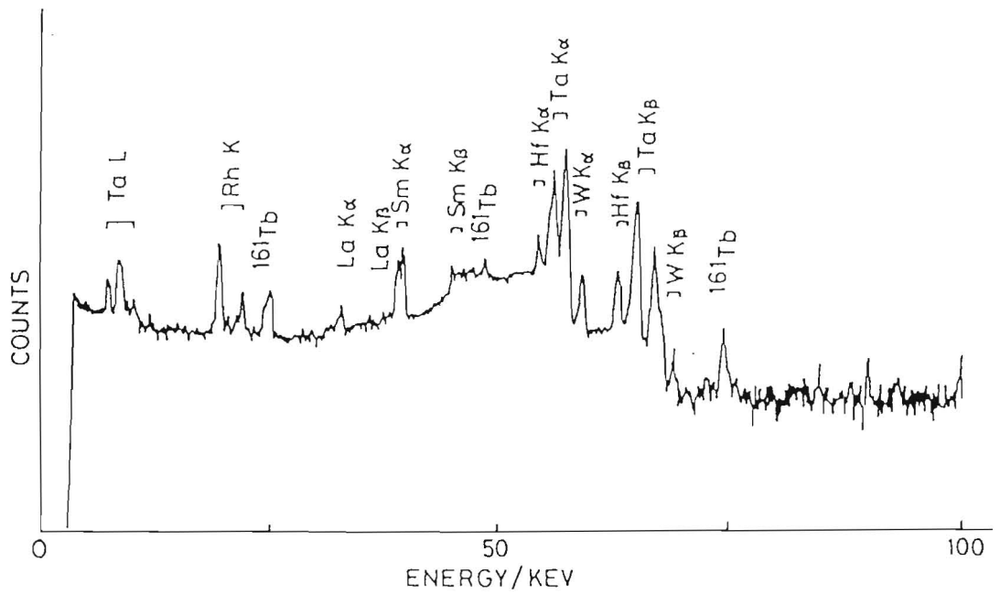

Fig. 3. X-ray spectrum of the residue of ^{164}Dy target.

On addition of ammonium hydroxide to the solution of the target, the solution became violet, showing the formation of tetra(ammine)copper(II) complex. After the dysprosium hydroxide was dissolved in hydrochloric acid, ammonium hydroxide was added again to the solution to remove completely silver and copper. The white dysprosium hydroxide remained after filtration. The precipitate of dysprosium hydroxide was dissolved in 0.1 M hydrochloric acid.

Though ^{56}Co and ^{65}Zn were detected in the silver and copper fraction, no γ-ray peaks of lanthanoids were found, as shown in Fig. 4. Accordingly, the lanthanoids were considered to be coprecipitated effectively with dysprosium hydroxide. On the other hand, various nuclides were identified in the γ-ray spectrum of the hydrochloric acid solution, as shown in Fig. 5. However, the peaks of ^{205,206}Bi could not be identified at that stage, because a fair number of those peaks overlapped with those of ^{160}Tb and those were not found in the preliminary experiment.

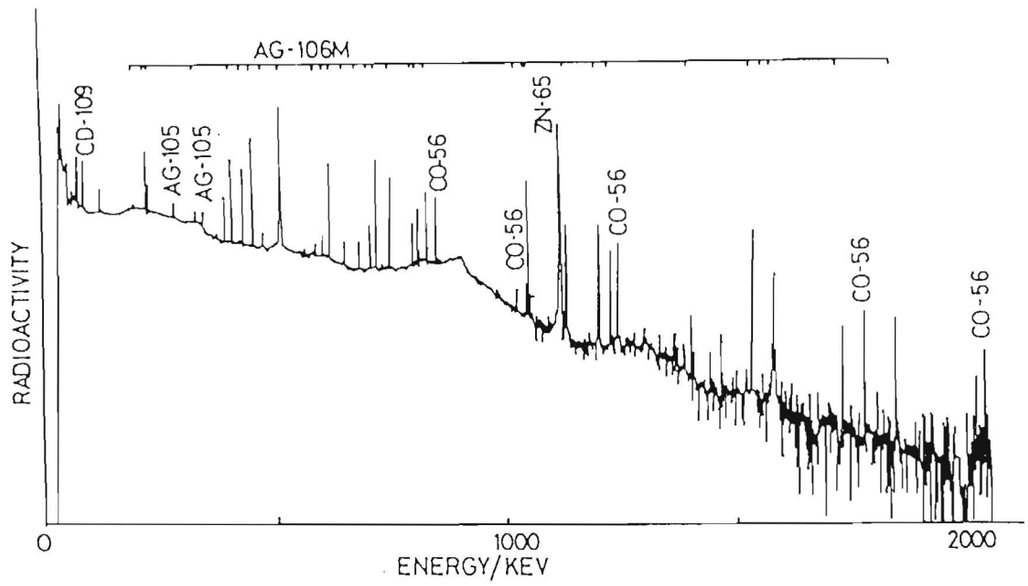

Fig. 4. γ –Ray spectrum of the silver and copper fraction.

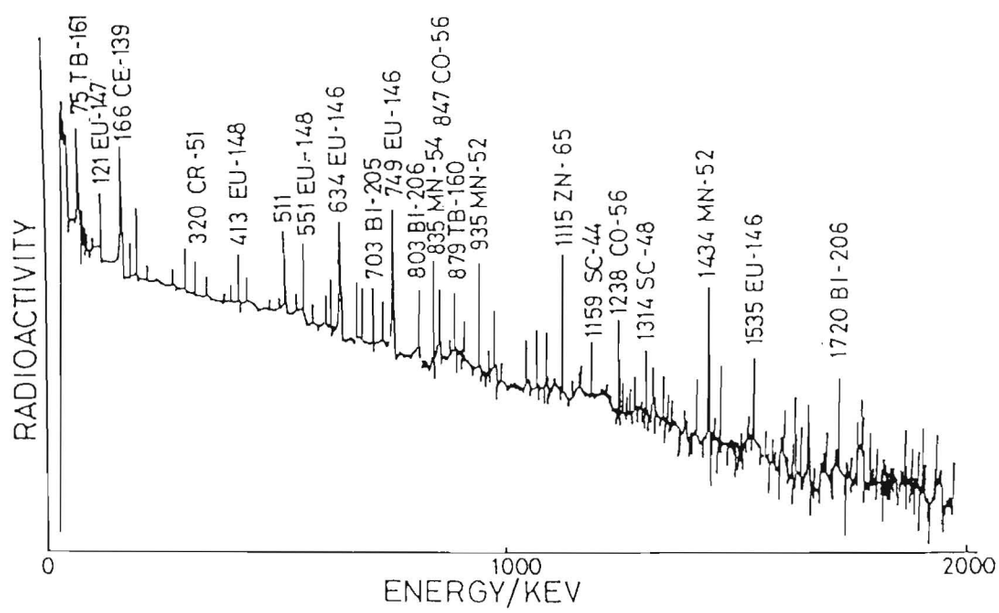

Fig. 5. γ –Ray spectrum of the lanthanoid fraction.

3. 2. Separation of ^{163}Ho by means of the cation exchange method

A cation exchange column (AG50W-X8, 100-200 mesh, NH_4-form, 10 mmϕ × 800 mm) was pre-treated with a 0.1 M hydrochloric acid solution and the lanthanoids were placed on the top of the column. The elution condition was fundamentally similar to the preliminary experiment and the flow rate was controlled at 4.6 ml/h. However, pH of the eluent was adjusted to 3.15 to accelerate the elution of ^{163}Ho. The effluent was collected by every 1.5 ml using a fraction collector. The elution curve was constructed by measuring the radioactivities at intervals of several fractions.

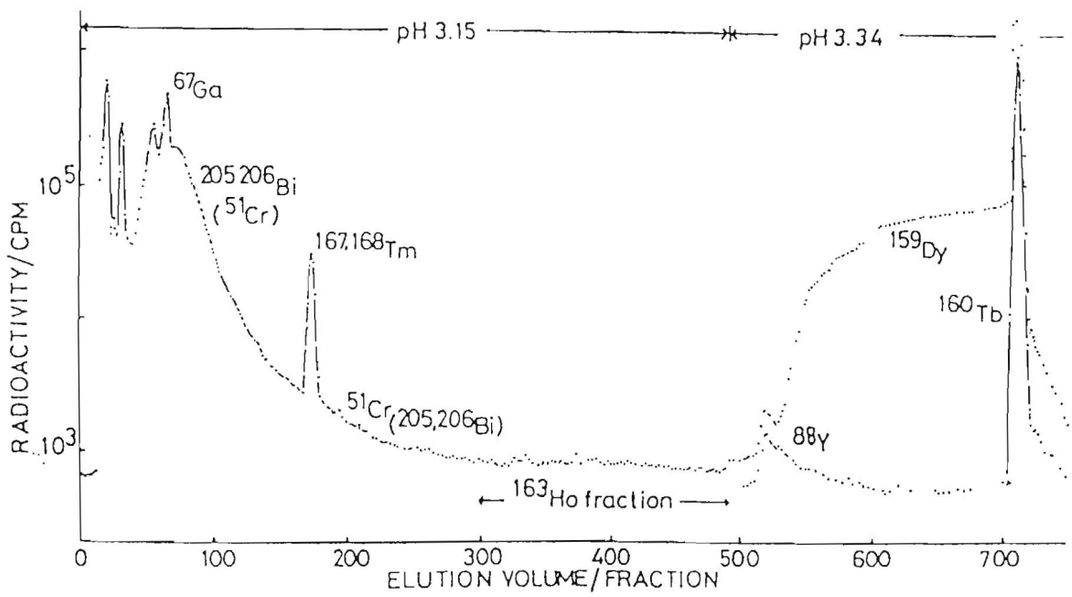

Fig. 6. The elution curve for ^{164}Dy target.

Column: AG50W-X8 (10 mmϕ × 800 mm, 100-200 mesh, NH_4-form)

Flow rate: 4.62 ml/h (25℃); Eluent: α-hydroxyisobutylic acid)

The elution curve is shown in Fig. 6. In addition to a lot of nuclides which had been detected in the stage shown in Fig. 5, new nuclides were also identified in the course of the cation exchange process. The first peak in Fig. 6 consisted of $^{44m,47,48}Sc$, ^{48}V, ^{51}Cr, ^{67}Ga, $^{74,75}As$, ^{74}Se, $^{88,89}Zr$, and $^{120,122,124}Sb$, the second and third peaks consisted of $^{44m,47,48}Sc$, ^{51}Cr, and $^{205,206}Bi$. ^{111}In distributed in the range from the fraction No. 85 to 115, with a maximum at the fraction No. 99. The peak of $^{205,206}Bi$ was recognized at the fraction No.75

and the most of $^{205,206}Bi$ was eluted by the fraction No. 105. However, trace amount of $^{205,206}Bi$ tailed until the fraction of ^{163}Ho appeared. Chromium demonstrated curious behavior that two peaks exhibited. In the preliminary experiment, ^{51}Cr remained at the top of the column. Different behavior of ^{51}Cr would be explained by considering a possibility that in the present system, chromium was oxidized to hexavalent state, when the target was dissolved in aqua regia instead of nitric acid. Since chromate is an anion, it should be eluted at first. However, while passing through the column, a strong oxidizing agent, Cr(VI), might be reduced to Cr(III) with an interaction with resin or HIBA. Actually, it was confirmed that some chromium(III) remained at the top of the column.

Total γ-activities decreased gradually to a level of natural background. Consequently, in the fractions from No. 300 to 500, no detectable radioactivities were found with the NaI(Tl) detector. The elution procedure that started on December 21 continued to December 28. At that time the separation was intermitted for a short while and then resumed on January 11.

The fact that the full-width at half-maximum for the peak of thulium shown in Fig. 6 was smaller than that shown in Fig. 1 means that in the former case the separation was carried out under the optimum condition. On the other hand, it brought difficulty for precise determination of the elution volume of ^{163}Ho. Consequently, 300 ml effluent collected from No. 300 to 499 were concentrated. The γ-ray spectrum of the ^{163}Ho was shown in Fig. 7. In this fraction, ^{51}Cr and $^{205,206}Bi$ were detected. The amounts for these nuclides were roughly estimated to be 0.08 μCi for ^{51}Cr, 0.003 μCi for ^{205}Bi, and 0.0007 μCi for ^{206}Bi. In addition, the contamination of ^{88}Y was also observed. As far as the elution curve was examined, ^{88}Y could be separated from ^{163}Ho. Actually, no γ-rays from ^{88}Y could be detected in each fraction. The amount of ^{88}Y was estimated to be about 10^{-5} μCi. ^{88}Y was considered to be produced by the decay of the parent ^{88}Zr. Since ^{88}Zr forms a very stable complex with AHIB, it could be eluted first. However, there is a possibility that ^{88}Y produced during elution was distributed throughout the column. This is the reason why a small amount of ^{88}Y was eluted earlier than its normal position of elution.

Because time limitation, decontamination of ^{51}Cr and $^{205,206}Bi$ was then tried. Furthermore, ^{88}Y would be available as an indicator for determination of electrodeposition efficiency, though the amount of ^{88}Y was too small to use as a tracer.

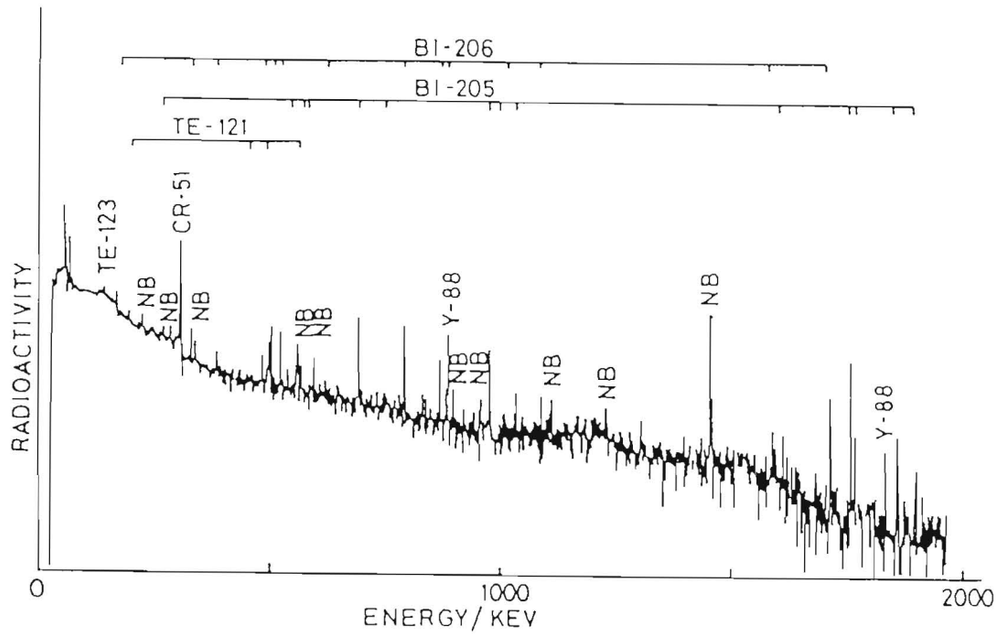

Fig. 7. γ -Ray spectrum of ^{163}Ho.

3. 3. Purification of ^{163}Ho

A volume used for electrodeposition of ^{163}Ho was 150 μl. Accordingly, the concentration of 300 ml ^{163}Ho fraction was done together with the decontamination of ^{51}Cr and ^{205,206}Bi. These procedures were summarized in Fig. 8.

At first the concentration of ^{163}Ho fraction together with the separation of ^{51}Cr was tried by means of a cation exchange method by considering that Cr(III)–AHIB complex much more stable than that of lanthanoid. However, by this method complete separation of ^{51}Cr from ^{163}Ho was impossible, though ^{121,121m,123}Te were removed.

After AHIB of ^{163}Ho fraction was decomposed by hydrochloric acid and fumed nitric acid, potassium chromate was added as a carrier for the iron(III) hydroxide coprecipitation method. The chromate was reduced by hydrogen peroxide and then chromium(III) was oxidized again to chromate using aqueous bromine in the basic media. To the solution 2 mg iron(III) was added and iron(III) hydroxide was precipitated on addition of potassium hydroxide solution. In this procedure, ^{163}Ho coprecipitated in iron(III) hydroxide, while chromate remained in the solution. The precipitate of iron(III) hydroxide was dissolved in 1 M hydrochloric acid and the solution was passed through an anion exchange column(Dowex

1-X8, 100-200 mesh, Cl-form, 7 mmϕ × 60 mm). Under this condition, bismuth could be adsorbed on the column[9], while ^{163}Ho and iron should passed through the column. In order to remove the macro amount of iron(III), the effluent was evaporated to dryness and then 6 M hydrochloric acid was added. Iron(III) in 6 M hydrochloric acid could be adsorbed on the anion exchange column (Dowex 1-X8, 100-200 mesh, Cl-form, 7 mmϕ × 60 mm). The sample for electroplating was prepared by evaporation to dryness of the effluent containing ^{163}Ho. These procedures were done with caution so that all the glass wares were employed and these once used were disposed. However, in the final sample ^{51}Cr (7 × 10^{-5} μCi), ^{139}Ce and small amounts of unidentified nuclides were detected by the γ-ray spectrometry. This contamination was considered to be brought from dust of the laboratory. Thus, it was necessary to start over again from the separation of ^{51}Cr in another laboratory.

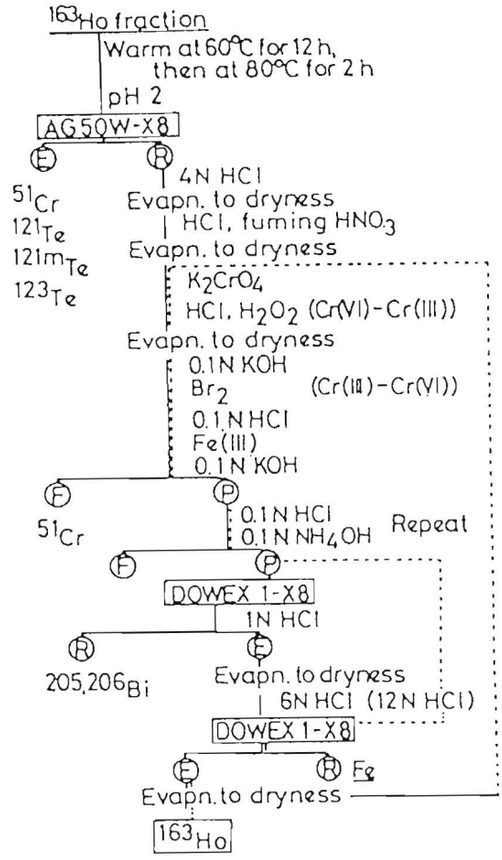

Fig. 8. Purification procedure of ^{163}Ho.

A similar separation procedure as described above was repeated, but iron(III) hydroxide was dissolved in 12 M hydrochloric acid to remove unidentified nuclides on the anion exchange column. After the effluent was evaporated to dryness and organic compounds containing in the residue was decomposed by hydrochloric acid and fumed nitric acid, the sample for electroplating was prepared. Thus, the finally purified sample was completely free from ^{51}Cr, ^{205,206}Bi and unidentified nuclides, though ^{139}Ce (8.6 × 10^{-6} μCi) and ^{88}Y (9.5 × 10^{-5} μCi) were still contained in it.

3. 4. Electrodeposition of ^{163}Ho

A cell used for electrodeposition of ^{163}Ho is shown in Fig. 9. To the sample for electrodeposition 200 μl of previously treated 0.1 M ammonium lactate (pH 4.0) was added.

The ^{163}Ho–lactate solution (150 μl) was electrodeposited in the cell at 12 V, 10 mA for 90 min[10,11]. Finally, four ^{163}Ho sources were prepared. No. 1 source was electrodeposited using 50 μl out of the ^{163}Ho solution. The electrodeposition yield was estimated by measuring the γ-activity of ^{88}Y. The residual 150 μl was used for the preparation of No. 2 source. Since ^{88}Y could not be detected in the source, it was concluded that the electrodeposition was failed. Using a newly prepared solution obtained by the decomposition of lactic acid in the residual solution, No. 3 source was prepared in a similar way. Furthermore, No. 4 source was prepared from all the remaining solutions.

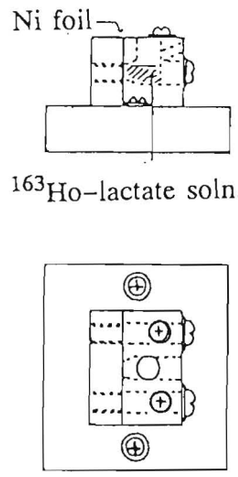

Fig. 9. The cell for electrodeposition.

The recovery yields of ^{88}Y are summarized as follows:

The loss in the purification procedure of ^{163}Ho	24.3	%
No. 1 source	9.8	%
No. 2 source	x	%
No. 3 source	30.9	%
No. 4 source	8.0	%
The remainder in the solution	21.4	%
Total	93.5 + x	%

It has been accepted that chemical behavior of ^{88}Y is the same as that of lanthanoids including ^{163}Ho. X–Ray measurement and PIXE of the ^{163}Ho source, however, demonstrated different behavior of ^{163}Ho from ^{88}Y in the electrodeposition process[12]. Since the X–ray intensity of No. 2 source was comparable to that of No. 1 source and the X–ray intensity ratio of No. 1 to No.3 was about 1:7, the amount of ^{163}Ho in the remaining solution was considered to be less than the estimation. This means that ^{163}Ho could be electrodeposited more effectively than ^{88}Y. An example of the γ-ray spectrum of No. 1 source is shown in Fig. 10.

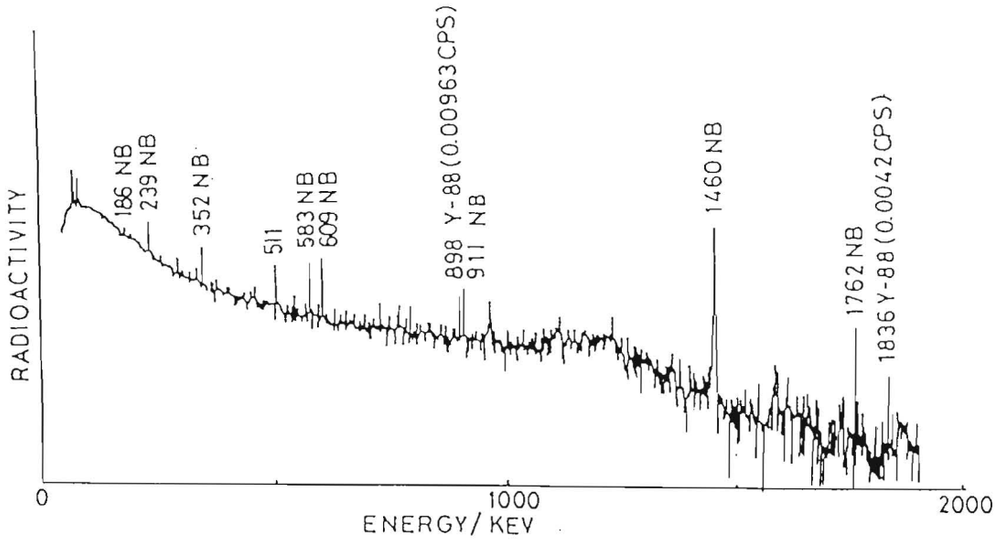

Fig. 10. γ-ray spectrum of ^{163}Ho source (No. 1).

References

[1] W. Rieman III, H. F. Walton, Ion Exchange in Analytical Chemistry, Pergamon Press, New York, 1970.

[2] H. Natsume, JEARI-Memo 1915(1965).

[3] F. W. Cornishi, G. Phillips, A. Thomas, *Can. J. Chem.*, **34**(1956)1471.

[4] J. E. Powell, H. R. Bukholder, *J. Chromatog.*, **29**(1967)210.

[5] B. H. Kettelle, G. E. Boyd, *J. Amer. Chem. Soc.*, **73**(1951)1862.

[6] G. R. Choppin, B. G. Harvey, S. G. Thompson, *J. Inorg. Nucl. Chem.*, **2**(1956)66.

[7] G. R. Choppin, R. Silva, *J. Inorg. Nucl. Chem.*, **3**(1956)153.

[8] H. L. Smith, D. C. Hoffman, *J. Inorg. Nucl. Chem.*, **3**(1956)243.

[9] K. A. Kraus, F. Nelson, Proc. 1st Int. Conf. on Peaceful Uses of Atomic Energy, **7**(1955)113.

[10] A. F. Novgarodov, V. L. Kochetkov, N. A. Lebedev, V. A. Khalkin, *Radiokhimiya*, **6**(1964)73.

[11] M. Fujioka, *Nucl. Phys.*, **A153**(1970)337.

[12] K. Ishii *et al.*, Proc. of the 4th Workshop on the Mass of the Electron Neutrino, KEK82-8(1982).

Chapter 5

Study in the period from 1981 to 1983

S. Yasumi
F. Ochiai*

Teikyo University/KEK
**Tezukayama University*

At the beginning of our $m_{\nu e}$-study there were only contradictory data on the Q-value and the half-life of ^{163}Ho. Therefore we intended to estimate these two quantities using the intensity of M X-rays from ^{163}Ho atoms and the total number of ^{163}Ho atoms in a source.

Tohoku university group prepared several ^{163}Ho sources. Among them, source No. 3 was the most intense and was used throughout the experiment.

At first we estimated the total number of ^{163}Ho atoms in the source No. 3 using the PIXE method in the following way. Another ^{163}Ho source (No. 4) whose intensity of M X-rays was already measured, and a reference holmium foil whose dimension is the same as that of a ^{163}Ho source (all ^{163}Ho sources are 3 mm in diameter) and whose weight is known, were irradiated with 38 MeV protons under the same beam conditions. By comparing the Ho K X-ray intensities of irradiated two samples, namely ^{163}Ho source No. 4 and a reference Ho foil, and using the ratio of M X-ray intensities of the two ^{163}Ho sources (No. 3 and No. 4), the total weight of ^{163}Ho atoms in the source No. 3 was estimated to be $(2.37 \pm 0.70)\mu g$. Thus we concluded that the total number of ^{163}Ho atoms in the source No. 3 is $(0.88 \pm 0.26) \times 10^{16}$ [1].*

Next, a photon spectrum from the source No. 3 was measured with a Si(Li)-detector (EG&G ORTEC) having a Be window 0.3 mil thick. The photon spectrum from ^{163}Ho has five peaks in the case of the measurement with a Si(Li) detector.

---

* Another PIXE measurement [2] of the total number of ^{163}Ho atoms in the source No. 3 was performed. ^{163}Ho source No. 11 having a Pd backing and a reference Ho foil were irradiated with 3 MeV protons under the same beam conditions. By comparing the holmium L_α X-ray intensities from these two samples, the total number of ^{163}Ho atoms in the source No. 11 was estimated. Next, by comparing M X-ray intensities from sources No. 11 and No. 3, the total number of ^{163}Ho atoms in the source No. 3 was determined. This result was consistent with the previous value[1] within experimental uncertainties.

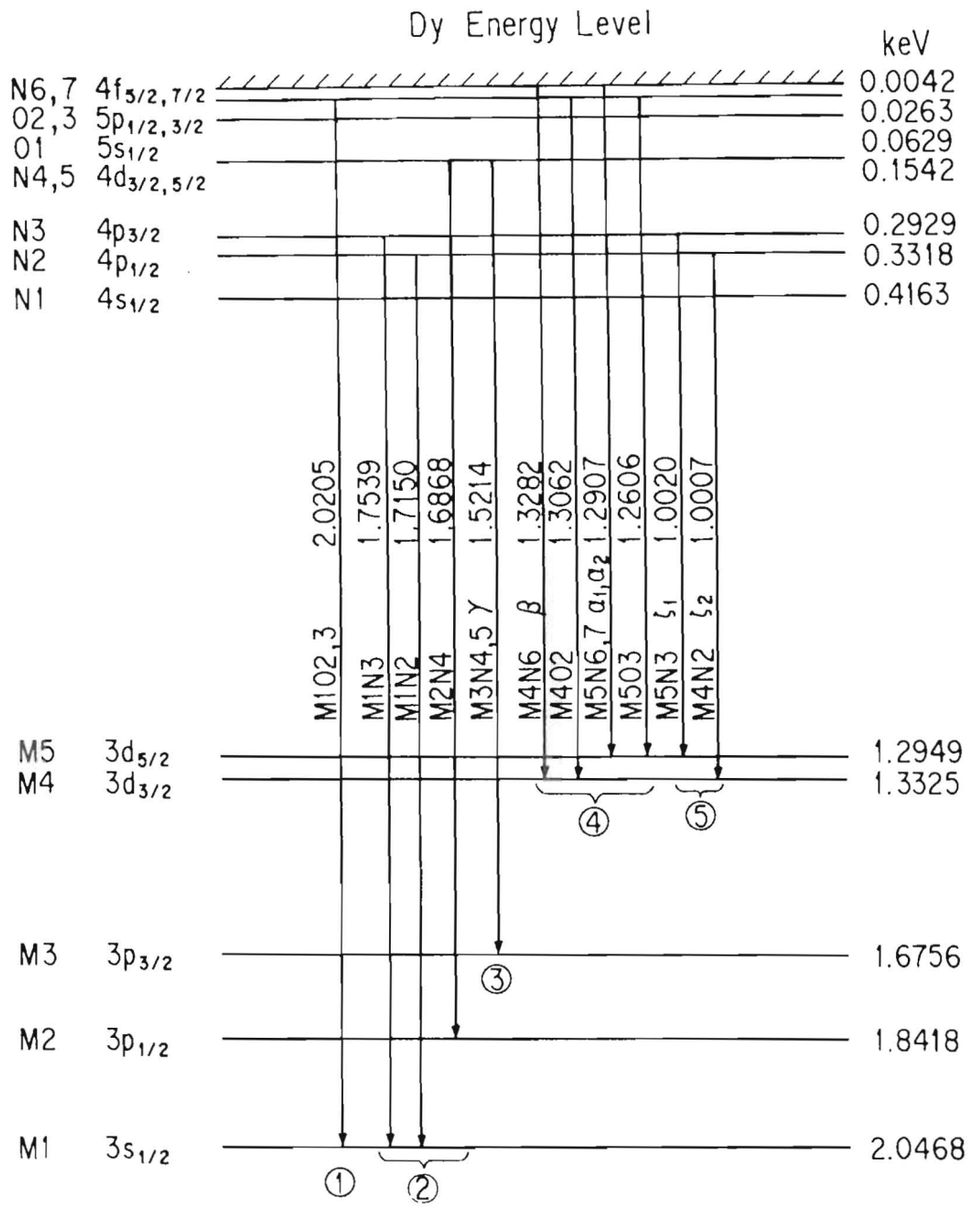

Fig. 1 Level scheme of the M shell and higher shells of Dy atom and X-rays due to the electron transition between these subshells. ①~⑤ stand for names of peaks in a spectrum from a ^{163}Ho source measured with a Si(Li) detector, where peak ① corresponds to the highest peak.

The relation between these five peaks and the level scheme of Dy atom is shown in Fig. 1. For each peak we evaluated the detection efficiency of the Si(Li)-detector and the self-absorption of the source itself for emitted X-rays.After correcting for the detection efficiency and the self-absorption together with the solid angle of the Si(Li) detector, intensities of M X-rays emitted from the source No. 3 were deduced for each peak. Using the total number of ^{163}Ho atoms in the source, we can get the M X-ray intensity per second per atom per 4π steradians for each peak.

Summing up these intensities, we get the total intensity of M X-rays from the ^{163}Ho source No. 3 of $(4.7 \pm 1.5) \times 10^{-15}$ photons per second per atom per 4π steradians.

If we assume that the average M-fluorescence yield for the dysprosium atom is 0.98 %[3], the partial M-capture half-life of ^{163}Ho was obtained to be

$T_{1/2}^{M} = (4.5 \pm 1.5) \times 10^{4}$ yr. [1]

Following the CERN group [4] we adopted the log *ft* value of 5.12 for the nuclear matrix element relevant to the transition ^{163}Ho (E.C.) ^{163}Dy

From the value of $T_{1/2}^{M}$ and the log *ft* value a relation between the Q-value and the electron neutrino mass ($m_{\nu e}$) was obtained. In this deduction, the electronic wave functions at the position of a nucleus calculated by Mann and Waber[5] and the exchange and overlap correction factors tabulated by Bambynek et al[2] were used.

Using this relation we get $Q = 2.45 \pm 0.08$ keV for $m_{\nu e} = 0$ eV. If we use an upper limit for the Q-value of 3.3 keV directly measured by the CERN group[6], we get an upper limit for the mass of the electron neutrino of 1.25 keV[1].

If we adopt 2.45 keV for the Q-value of ^{163}Ho, the half-life of ^{163}Ho is estimated to be $(6 \pm 2) \times 10^{3}$ yr. [1]

At the Neutrino '82 Conference held at Balatonfüred, Hungary, June 1982, a talk on $m_{\nu e}$ was given by S. Y. In this talk the Q-value of (2.3 ± 0.15) keV and the half-life of $(9^{+5}_{-2}) \times 10^{2}$ yr were reported. However, in deriving these values, the spin-isospin polarization effect on the nuclear matrix element was overlooked in the analysis.

Based on these values, the figure of merit[8),9] of the internal bremsstrahlung at electron capture in ^{163}Ho for measuring the electron neutrino mass was estimated to be 1.8×10^{-11} for O-capture. Comparing this value with the value of $\sim 10^{-8}$ for the case of the electron anti neutrino mass measurement using the tritium β-spectrum, the IBEC approach** to measure the electron neutrino mass seems rather difficult.

** For the IBEC approach, we constructed a crystal X-ray spectrometer combined with two-dimensional multiwire proportional chamber as the position detector[10].

Therefore we began to seek other means to determine the electron neutrino mass.

In a talk presented by S. Y. at the International Europhysics Conference on High Energy Physics, Brighton, UK, July 20-27, 1983 [2),11)], the following description of a different new approach was given:

"We are going to do an experiment which hopefully can reduce the atomic physics uncertainties of the dysprosium atom using a monochromatic photon beam from 2.5 GeV Electron Storage Ring in our "Photon Factory" (Synchrotron Radiation Facility in KEK).

The experimental setup is schematically shown in Fig. 1 of Chapter 6. Photon beams from the storage ring are monochromated through a double crystal monochromator and impinge upon a Dy target. Incident photon beams are monitored with some photon detector. We will use beams with three different energies, E_a, E_b and E_c where $E_a > E_{M1} > E_b > E_{M2} > E_c$ and E_{M1} and E_{M2} stand for the binding energies of the M_1 and M_2 subshells, respectively. The energy widths of these photon beams are a few eV and sharp enough to remain distinct from the M_1 and M_2 levels. M X-rays emitted by dysprosium atoms excited by the incident photon beams, are measured with a Si(Li) detector.

If one subtracts E_b spectrum from E_a spectrum, appropriately scaling by the incident energy and properly normalizing, one can obtain an M_1 spectrum which corresponds to the M X-ray spectrum in the case where there are vacancies in M_1 subshell only. A similar subtraction of E_c spectrum from E_b spectrum yields the corresponding spectrum for the M_2 subshell.

Using these two spectra (M_1 and M_2), λ_{M1} and λ_{M2} can be separately reduced from the ^{163}Ho atom spectrum, where λ_{M1} and λ_{M2} are the decay constants due to M_1 capture and M_2 capture, respectively. These results can then be used to determine $m_{\nu e}$."

It is very interesting to compare the above sentence with Equations (15) and (16) in Chap. 13.

References

1) S. Yasumi et al., Phys. Lett. **122**B (1983) 461.
2) S. Yasumi, Proc. Intern. Europhys Conf. High Energy Physics Brighton, UK, July 1983, p.391.
3) W. Bambynek et al., Rev. Med. Phys. **49** (1977) 77.
4) B. Jonson et al., Nucl. Phys. A**396** (1983) 479c.
5) J. B. Mann and J. T. Waber, Atomic Data **5** (1973) 201.
6) J. U. Andersen et al., Phys. Lett., **113**B (1982) 72.
7) S. Yasumi et al., Proc. 1982 Intern. Neutrino Conference, Balatonfüred, Hungary, June 1982, Vol. 1, p. 59.
8) A. De Rújula, Nucl. Phys. B**188** (1981) 414.
9) K. Rüsager et al., Physica Scripta **31** (1985) 321.
10) Y. Inagaki, Proc. 7th Workshop on $m_{\nu e}$, KEK Report 83-15, 1983, E, P. 51. (in Japanese)
11) S. Yasumi et al., KEK Preprint 83-17, 1983, E.

Chapter 6

Study in the period from 1984 to 1986

S. Yasumi and Y. Inagaki*

Teikyo University/KEK
**Tokyo Kasei University*

On December 10th of 1982, a Letter of Intent [1] in which we proposed an experiment aiming at the electron neutrino mass measurement using synchrotron radiation X-rays from the KEK・PF storage ring, was presented to the Photon Factory, KEK.

In May of 1983, a seminar on "Studies on the M-shell of the dysprosium atom using monochromatic X-rays for a measurement of $m_{\nu e}$" (hereafter, this title is abbreviated as $m_{\nu e}$-PF experiment) was given by S.Y. in the Photon Factory. In this seminar there were a lot of encouraging discussions and the undulator beam line (BL-2) of a 2.5 GeV electron storage ring at KEK・PF was recommended as photon beams to be used.

In December of 1983, a proposal on the $m_{\nu e}$-PF experiment was presented to the Photon Factory and in the next January this proposal was approved by PF・PAC of KEK [Proposal No. 83-111].

At the 9th Workshop on $m_{\nu e}$ we again discussed a method to determine $m_{\nu e}$ and finally reached to the following one: [2], [3], [4]

If Sp^{163Ho} stands for a photon spectrum from ^{163}Ho, where the number of photons per atom per second is plotted as a function of the energy of photons, we then have

$$Sp^{163Ho}(k) = \frac{1}{N_0}\frac{d}{dt}\left[N_{M1}\cdot S_{M1}(k) + N_{M2}\cdot S_{M2}(k)\right]$$

$$= \frac{d}{dt}\left[n_{M1}\cdot S_{M1}(k) + n_{M2}\cdot S_{M2}(k)\right]$$

$$= \frac{dn_{M1}}{dt}\cdot S_{M1}(k) + \frac{dn_{M2}}{dt}\cdot S_{M2}(k),$$

therefore we get the following equation

$$Sp^{163Ho}(k) = \lambda_{M1} \cdot S_{M1}(k) + \lambda_{M2} \cdot S_{M2}(k), \quad (1)$$

where

$S_{Mi}(k)$ $(i=1,2)$	:	M X-ray spectrum from a Dy atom in the case where there is one vacancy in the Mi subshell (i =1,2) only,
k	:	energy of emitted photons
$N_{Mi}(k)$ $(i=1,2)$	:	number of vacancies produced in the Mi subshell in the decay ^{163}Ho (E.C.) ^{163}Dy,
n_{Mi}	:	$\equiv N_{Mi}/N_o$,
N_o	:	total number of ^{163}Ho atoms in a ^{163}Ho source,
λ_{Mi} $(i=1,2)$	:	partial Mi-capture decay constant.

Equation (1) tells us that when we reconstruct $Sp^{163Ho}(k)$ spectrum using spectra $S_{M1}(k)$ and $S_{M2}(k)$, the coefficients of $S_{M1}(k)$ and $S_{M2}(k)$ correspond to λ_{M1} and λ_{M2}, respectively.

Next, the $S_{M1}(k)$ and $S_{M2}(k)$ spectra of dysprosium atom can be obtained using the following "photon subtraction method" from fluorescence spectrum measurements in the photoionization of dysprosium atoms with monochromatic photons, whose energies have an appropriate relation with the binding energies of M_i subshells as follows.

If $S_E(k)$ denotes an M X-ray fluorescence spectrum from Dy atoms excited by monochromatic photons having an energy E, $S_E(k)$ is represented by the following equation:

$$S_E(k) = N \cdot m \cdot \sum_{i=1}^{5} \sigma_i(E) \cdot S_{Mi}(k), \quad (2)$$

$$(i = 1 \sim 5)$$

where

N	:	total number of incident photons having an energy E,
m	:	number of dysprosium atoms in a target per cm^2,
$\sigma_i(E)$	:	photoionization cross section of the Mi subshell for an incident photons of an energy E,
$S_{Mi}(k)$ (i = 1 - 5):		M X-ray spectrum from a Dy atom in the case where there is one vacancy in the Mi (i = 1- 5) subshell only.

S_{Mi} (k) in equations (1) and (2) comprises the Auger and Coster-Kronig transition probabilities and the X-ray transition probabilities.

For E, we take five energies; E_a, E_b, E_c, E_d and E_e, where E_a $E_{M1}>E_b>E_{M2}>E_c>E_{M3}>E_d>E_{M4}>E_e>E_{M5}$, and E_{Mi} (i =1 - 5) stands for the binding energy of the Mi (i = 1- 5) subshell of the dysprosium atom. If the energy widths of these photon beams are a few eV and sharp enough to remain distinct from each subshell level, then equation (2) becomes

$$
\begin{aligned}
S_{Ea}(k) &= Nm\{\sigma_1(E_a)\cdot S_{M1}(k)+\sigma_2(E_a)\cdot S_{M2}(k)+\sigma_3(E_a)\cdot S_{M3}(k)+\sigma_4(E_a)\cdot S_{M4}(k)+\sigma_5(E_a)\cdot S_{M5}(k)\},\\
S_{Eb}(k) &= Nm\{\sigma_2(E_b)\cdot S_{M2}(k)+\sigma_3(E_b)\cdot S_{M3}(k)+\sigma_4(E_b)\cdot S_{M4}(k)+\sigma_5(E_b)\cdot S_{M5}(k)\},\\
S_{Ec}(k) &= Nm\{\sigma_3(E_c)\cdot S_{M3}(k)+\sigma_4(E_c)\cdot S_{M4}(k)+\sigma_5(E_c)\cdot S_{M5}(k)\},\\
S_{Ed}(k) &= Nm\{\sigma_4(E_d)\cdot S_{M4}(k)+\sigma_5(E_d)\cdot S_{M5}(k)\},\\
S_{Ee}(k) &= Nm\{\sigma_5(E_e)\cdot S_{M5}(k)\}.
\end{aligned}
\tag{3}
$$

where N is assumed to be normalized for all cases.

If N, m and $\sigma_i(E)$ are known , one can obtain the S_{Mi} (i = 1- 5) in turn by using the above five equations (3). Spectra $S_{M1}(k)$ and $S_{M2}(k)$ thus obtained, can be used to reconstruct the $Sp^{163Ho}(k)$ spectrum for determining λ_{M1} and λ_{M2}.

If we assume some value for the nuclear matrix element (or log *ft* value) of the decay ^{163}Ho (E.C) ^{163}Dy, the mass of the electron neutrino, $m_{\nu e}$, and the Q-value can be deduced, using λ_{M1} and λ_{M2} as two constraints for the formula of the electron capture decay rate.

The $m_{\nu e}$-PF experiment [No. 83-111] was performed in the period from February of 1984 to May of 1985 using a setup shown in Fig. 1. M X-rays emitted by dysprosium atoms excited with incident monochromatic photon beams were measured with two Si(Li) detectors, one of which is set in the direction of the polarization of the photon beams (horizontal) and another is set at an angle of 90° to the direction of the polarization of the photon beams (vertical), as shown in Fig. 1. The former was used for fluorescence spectrum measurements and the latter was used for overall monitoring. At first we used a double reflection crystal monochromator made of beryl, and later a double reflection monochromator made of InSb was successfully used for obtaining monochromatic photons of higher energies.

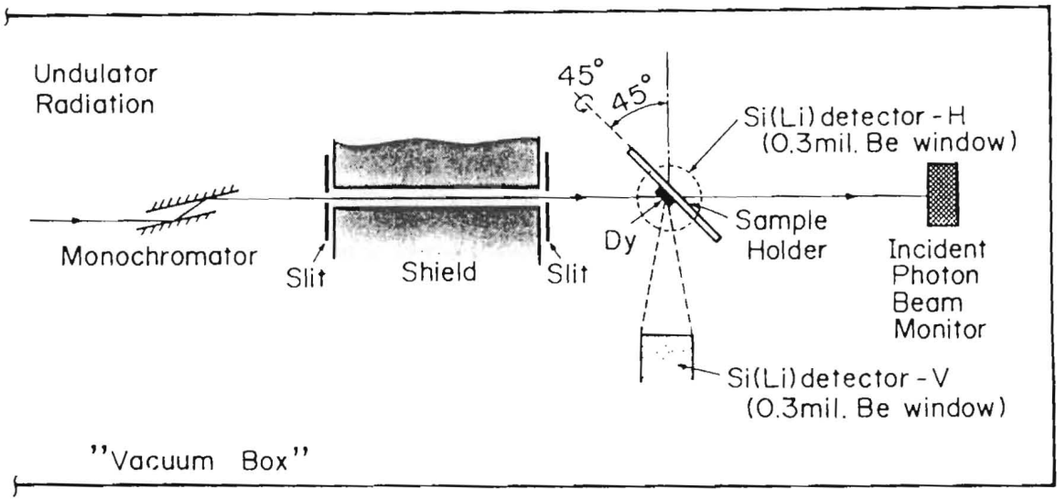

Fig. 1 Experimental setup of the fluorescence spectrum measurement of the dysprosium atom.

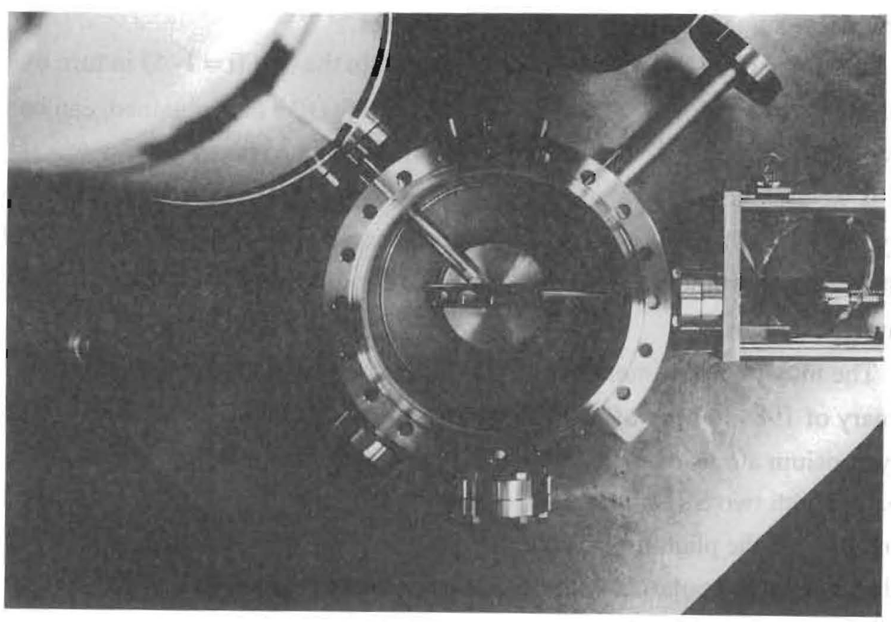

Inside view of the taraget chamber. The Si(Li) detector and the target system having a linear feed through are seen.

Generally speaking, however, experiment No. 83-111 was only a preliminary experiment for measuring $m_{\nu e}$. Since the direction of photon beams after passing through the monochromator was not fixed when rotating its Bragg angle in order to change the energy of photons, the alignment of the setup required for each photon energy took us a rather long time. Also the quality of photon beams was not so good. Photoioniztion cross sections $\sigma_i(E)$ were not very well known. Furthermore, the total number of incident photons during the measurement could not be measured very accurately (At that time we used a photodiode for the photon intensity monitor). Preliminary results by the experiment No. 83-111 were described in references 3) and 5).

But it should be noted that in the experiment [No. 83-111] very important data were taken on the response functions of a Si(Li) detector for monochromatic photons in the energy range 1.3 - 4.0 keV. Readers are invited to read reference 6) and Chapter 7 for this subject.

Since we could not determine the $S_{M1}(k)$ and $S_{M2}(k)$ spectra from fluorescence spectrum measurements on Dy atoms, we took the following approach to estimate those two spectra [7].

The number of photons included in the S_{M1} and S_{M2} is represented by

$$\begin{aligned} S_{M1} : \ & \omega_1 + f_{12}\omega_2 + (f_{13} + f_{12}f_{23})\,\omega_3 \\ & + (f_{14} + f_{12}f_{24} + f_{13}f_{34} + f_{12}f_{23}\,f_{34})\,\omega_4 \\ & + (f_{15} + f_{12}f_{25} + f_{13}f_{35} + f_{14}f_{45} + f_{12}f_{23}f_{35} \\ & + f_{12}f_{24}f_{45} + f_{13}f_{34}f_{45} + f_{12}f_{23}f_{34}f_{45})\,\omega_5, \end{aligned} \tag{4}$$

$$\begin{aligned} S_{M2} : \ & \omega_2 + f_{23}\omega_3 + (f_{24} + f_{23}f_{34})\,\omega_4 \\ & + (f_{25} + f_{23}f_{35} + f_{24}f_{45} + f_{23}f_{34}\,f_{45})\,\omega_5, \end{aligned} \tag{5}$$

where ω_i $(i = 1 - 5)$: Mi subshell fluorescence yield,

f_{ij} : Coster-Kronig coefficient for the vacancy transition from Mi subshell to Mj subshell.

When Γ_i denotes the total level width of the Mi subshell, the fluorescence yield for this subshell is defined as

$$\omega_i = \sum_j \gamma_{ij}/\Gamma_i \qquad (i = 1 - 5)$$

where γ_{ij} : partial radiative width corresponding to the electron transition from X_j subshell to M_i subshell, and X denotes shells higher than the M shell.

Since no relativistic calculation of non-radiative transition probability for dysprosium atoms has been reported so far, we estimated the values of fij and Γ_i from the non-relativistic values of McGuire[8] and the relativistic values of Chen et al.[9] for holmium and ytterbium. The results are shown in Table 1 [7]. The partial radiative width γ_{ij} was taken from the relativistic calculations by Mukoyama and Adachi [10].

Table 1

M-shell Coster-Kronig coefficients f_{ij} and level widths Γ_i for dysprosium

f_{ij}	value	Γ_i	value (eV)
f_{12}	0.307	Γ_1	14.94
f_{13}	0.599	Γ_2	9.04
f_{14}	0.085	Γ_3	9.27
f_{15}	0.116	Γ_4	1.81
		Γ_5	1.24
f_{23}	0.091		
f_{24}	0.665		
f_{25}	0.141		
f_{34}	0.149		
f_{35}	0.747		
f_{45}	0.348		

The $S_{M1}(k)$ and $S_{M2}(k)$ spectra were constructed from various characteristic X-ray lines corresponding to γ_{ij} included in ω_i of expressions (4) and (5), using response functions of the Si(Li) detector used in the measurement of the photon spectrum from the ^{163}Ho source No. 3. In this construction, the self-absorption correction due to

the ^{163}Ho source itself and the detection efficiency of the Si(Li) detector were also taken into account.

When we tried to reconstruct the $Sp^{163Ho}(k)$ spectrum using the $S_{M1}(k)$ and $S_{M2}(k)$ thus obtained, it was found that there were some discrepancies around peak ④ and peak ①. Peak④ (~1.3 keV) includes γ_{M5N7} and γ_{M4N6} transitions and peak ① (~2.0 keV) includes $\gamma_{M1\ O2,3}$ transition.

Therefore the non-linear least-squares method was applied to minimize the χ^2-value for fitting equation (1), taking three radiative widths, γ_{M5N7} and γ_{M4N6} and $\gamma_{M1\ O2,3}$, as unknowns in addition to λ_{M1} and λ_{M2}, as shown in Fig. 2.[11)]

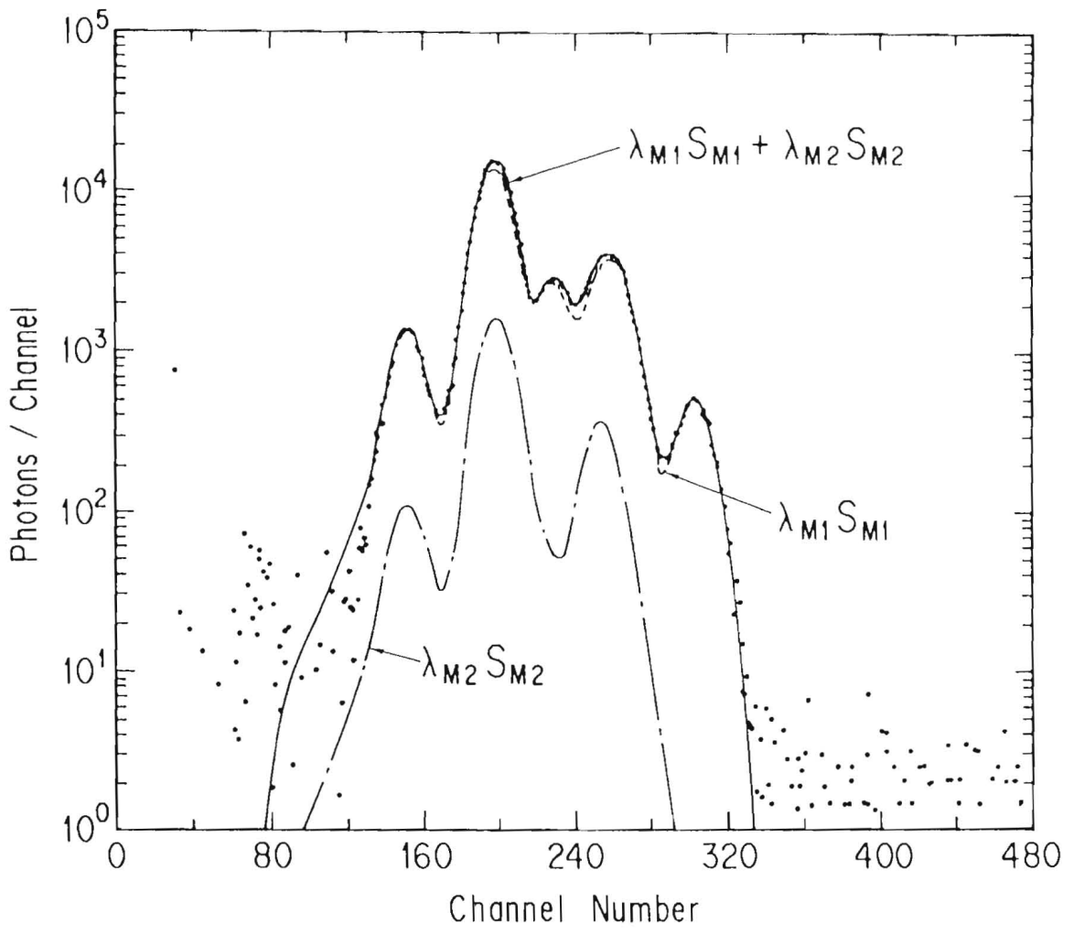

Fig.2 Reconstruction of the Sp^{163Ho} spectrum using the S_{M1} and S_{M2} spectra. The solid curve, the broken curve and the dot-dashed curve represent $\lambda_{M1}S_{M1} + \lambda_{M2}S_{M2}$, $\lambda_{M1}S_{M1}$ and $\lambda_{M2}S_{M2}$, respectively. Closed circles represent experimental data of Sp^{163Ho}.

The results[7] are

$$\lambda_{M1} = (0.9740 \pm 0.0041) \times 10^{-12}\ s^{-1},$$

$$\lambda_{M2} = (0.08170 \pm 0.0035) \times 10^{-12}\ s^{-1},$$

with

$$\gamma_{M5N7} = 1.749 \times 10^{-3}\ eV,$$

$$\gamma_{M4N6} = 1.340 \times 10^{-3}\ eV,$$

$$\gamma_{M1\,O2,3} = 2.159 \times 10^{-3}\ eV.$$

In Table 2, these values of γ_{M5N7}, γ_{M4N6} and $\gamma_{M1\,O2,3}$ are compared with radiative widths calculated by Mukoyama and Adachi[10] and the reduction factors are also indicated.

Table 2

	Radiative width by Mukoyama and Adachi (eV)	Reduction factor
γ_{M5N7}	6.389×10^{-3}	0.274
γ_{M4N6}	1.373×10^{-3}	0.976
$\gamma_{M1O2,3}$	1.687×10^{-3}	1.280

In June of 1985 the half-life of ^{163}Ho was measured by O. Kawakami and A. Masuda of University of Tokyo[12]. They determined this quantity by measuring the production rate of ^{163}Dy due to electron capture in ^{163}Ho with isotope-dilution mass spectrometry as initially done by Baisden et al.[13].

Their value is

$$T_{1/2} = 4569 \pm 27\ yr \qquad (68\%\ CL)$$

which is in excellent agreement with the value of Baisen et al.[13]. This corresponds to

$$\lambda_t = (4.807 \pm 0.028) \times 10^{-12}\ s^{-1}\ .$$

Using the values of λ_{M1}, λ_{M2}, and λ_t, as three constraints*, $m_{\nu e}$, the Q-value and the nuclear matrix element, $|m_N|^2$, for the decay of ^{163}Ho, were at one effort determined from the formula of the electron capture rate as follows:

$$m_{\nu e} = 205^{+345}_{-205}\ \text{eV}, \qquad Q = 2.70^{+0.13}_{-0.02}\ \text{keV},$$

$$|m_N|^2 = 0.0409^{-0.0033}_{+0.0016} \quad \text{or} \quad \log ft = 4.98^{+0.04}_{-0.02}\ .$$

It should be noted that the $\log ft$ value for the decay ^{163}Ho (E.C.) ^{163}Dy was firstly measured in the present experiment.

A summary of final results for $m_{\nu e}$ and the Q-value is shown in Fig. 3.

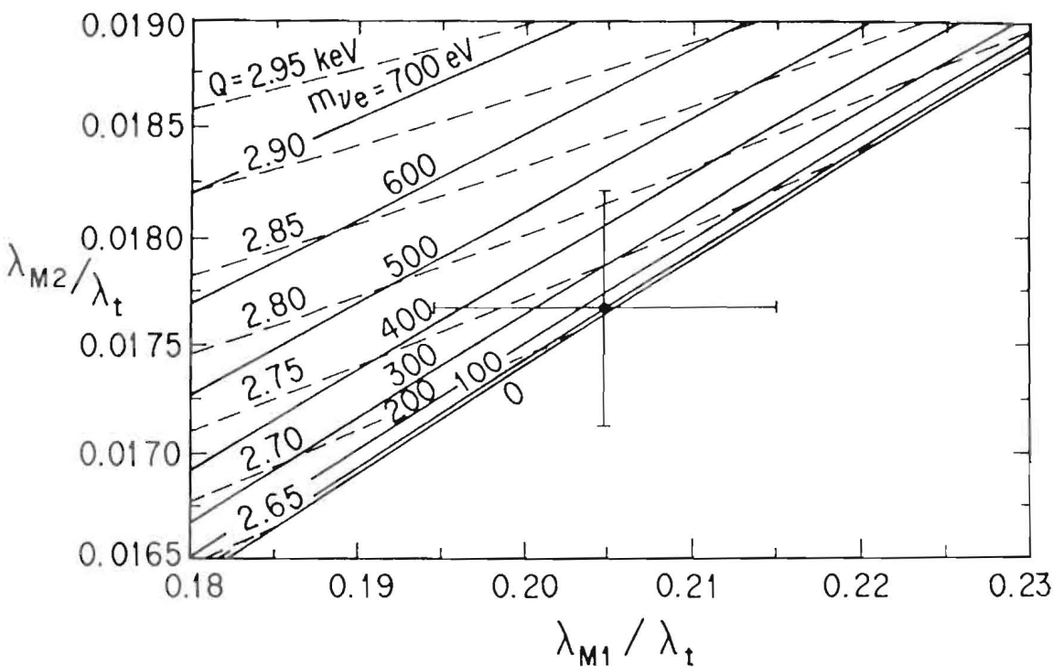

Fig. 3 Summary of the final results for $m_{\nu e}$ and the Q-value.

---

* It should be noted that three constaints enables us not to assume some value for the nuclear matrix element for the decay of ^{163}Ho [14].

References

1) S. Yasumi, KEK Report 83-15, 1983, p.67.

2) S. Yasumi, KEK Report 83-24, 1984, p.32.

3) S. Yasumi et al., Proc. Neutrino'84, Nordkirchen near Dortmund, June 11-16, 1984 p.202; KEK Report 84-9, 1984.

4) S. Yasumi et al., Neutrino 'Mass and Low Energy Weak Interactions, Telemark, 1984 edited by V. Barger and D. Cline, p.398.

5) Y. Inagaki, KEK Report 84-19, 1985, p.15.

6) Y. Inagaki, K. Shima and H. Maezawa, Nucl. Instrum. Meth. B**27** (1987) 353.

7) S. Yasumi et al., Phys. Lett. B**181** (1986) 169.

8) E. J. McGuire, Phys. Rev. A**5** (1972) 1043.

9) M. H. Chen, B. Crasemann and H. Mark, Phys. Rev. A**27** (1983) 2989. Phys. Rev. A**21** (1980) 449.

10) T. Mukoyama and H. Adachi, J. Phys. Soc. Japan **53** (1984) 984.

11) S. Yasumi et al., Proc. Intern. Symposium on Weak and Electromagnetic Interactions in Nuclei, Heidelberg, July 1-5, 1986 p. 786.

12) O. Kawakami et al., Proc. XVI INS Symposium Neutrino Mass and Related Topics, Tokyo, 16-18 March 1988 p.274.

13) P. A. Baisden et al., Phys. Rev C**28** (1983) 337.

14) S. Yasumi et al., Proc. Intern. Europhys. Conf. High Energy Physics, Bari (Italy), 18-24, 1985, p. 442.

Chapter 7

Response Functions of a Si(Li) Detector for Low Energy X-rays

Yosuke INAGAKI
Tokyo Kasei University, Tokyo 173, Japan

The response functions of a Si(Li) detector were measured for low energy monochromatic X-rays using synchrotron radiation from a 2.5 GeV electron storage ring at KEK[1]. The monochromatic photons in the energy range 1.3 - 4.0 keV were detected by the planar Si(Li) detector (Ortec) of 4.23 mm × 10.8 mm^2 effective volume. The energy resolution was 125 keV(fwhm) at 2.0 keV. The manufacturer's specification lists the thickness of the Be window as 8 μm, the gold contact as ≈200 A and the Si dead layer as ≈ 0.1 μm, respectively.

As shown typically in fig. 1 for an incident photon energy just above the Si-K absorption edge (1.839 keV), the response function $R(i)$ of a Si(Li) detector can be decomposed into four components of a dominating Gausian full-energy photopeak $G(i)$, a low energy tail $T(i)$, a step-like function $S(i)$ and a background $BG(i)$, i.e.,

$$R(i) = G(i) + T(i) + S(i) + BG(i), \tag{1}$$

where i is the channel number equivalent to the photon energy. The basic configuration of a p-i-n^+ type planar Si(Li) detector is illustrated schematically in fig. 2a.

The Gausian term is physically well understood. The full-energy peak corresponds to the state where the number of electron-hole pairs are completely collected in the intrinsic region of a Si(Li) detector. The width of the Gausian peak is determined by the statistical fluctuation of the electron-hole pairs and by the random electronic noise of the detector system. The Gaussian shape with a standard deviation σ and a peak position i_0 is given by

$$G(i) = H_g \exp\left[-(i-i_0)^2/2\sigma^2\right], \tag{2}$$

and the standard deviation expressed as

$$\sigma^2 = \varepsilon \mathrm{FE} + \sigma_e^{\,2}, \tag{3}$$

where ε is the energy to create one electron-hole pair for Si (3.76 eV at 77 K), F is the Fano factor, E is the incident photon energy and σ_e is the electronic noise.

A number of analytical functions have been proposed in order to represent the low -eneregy tail and the step-like functions. The origin of the low-energy tail and the step-like function has been explained only qualitatively by the imcomplete charge collection and the trapping -detrapping effect in the surface dead layer. We introduced a simple geometrical model in order to describe the strucure and behavior of the low-energy tail. As shown in fig. 2a, it is assumed that the charge-collection efficiency $\eta = 1$ for the intrinsic region and $\eta = 0$ for the p-type Si region so-called Si dead layer. The photoelectric absorption process is dominant for photon energy below ≈ 10 keV. When the incident photon is absorbed by a Si atom at a depth of x from the front surface, the atom ejects a photoelectron with an average range of R ; a number of electron-hole pairs are created through the successive ionization process. Assuming that the angular distribution of photoelectrons is isotropic, the density of charge carriers is almost uniform within a sphere of radius R. The patial volume of the sphere penetrating into the intrinsic region is given by

$$V(x) = \frac{\pi}{3} R^3 \left(1 - \frac{t_0 - x}{R}\right)^2 \left(2 + \frac{t_0 - x}{R}\right), \tag{4}$$

where t_0 is thickness of the Si dead layer. Since the partially collected charge is proportional to the volume $V(x)$, its ratio to the fully collcted charge, i.e. charge ratio, is given by

$r(x) = (1-X)^2(2+X)/4$ for $x < t_0 + R$ (5)

where $X = (t_0 - x)/R$. Therefor, the probability distribution of collectable charge as a function of the depth x can be written as

$$p(x) = r(x)\ e^{-\mu x}, \tag{6}$$

where μ is the linear absorption coefficient of Si. As shown in fig. 2c, the number densities of the low-energy tail and the Gaussian peak area are given respectively, as

$$N_t = \int_{\max(0,t_0-R)}^{t_0+R} p(x)dx, \tag{7}$$

and

$$N_p = \int_{t_0+R}^{d} p(x)dx, \tag{8}$$

where d is total depth of the Si dead layer and the intrinsic region. From the probabilty distribution function $p(x)$, the probabilty between x and x+dx can be rewritten as

$$p(x)\,\mathrm{d}x = q(x)\,\mathrm{d}r, \tag{9}$$

where

$$q(x) = \frac{1}{3}R\frac{(1-X)(2+X)}{1+X}e^{-\mu x}. \tag{10}$$

From eqs. (5) and (10), the probability distribution function can be obtained as a parametric representation of the depth x. It can be seen from the raw data of the response functions that there exists a threshold for the low-energy tail around half the energy of the Gaussian peak caused by the photoelectrons emitted from the gold contact on the Si dead layer. We modified the charge ratio of eq. (5) as

$$r'(x) = (1-r_0)r(x) + r_0, \tag{11}$$

where r_0 is the "threshold ratio" which shifs up the endpoint energy of the low-energy tail. Replacing the argument of $q(r)$ from r to i using $i = i_0\ r'(x)$, where i is the channnel number corresponding to the pulse height, we can finally obtained the probability distribution function $q(i)$ as a parametric representation. Thus the low-energy tail function can be obtained by making a convolution of $q(i)$ with a Gaussian of σ as

$$T(i) = H_t \int_{-\infty}^{i_0} q(t)\exp\left[-(t-i)^2/2\sigma^2\right]dt \tag{12}$$

Many analytical functions have been proposed to represent the step-like continuum, but a clear physical mechanism to produce the feature is not known yet. Maybe the electron-hole pairs created in the Si dead layer produce the step-like continuum Since the electric field strength in the dead layer is almost zero as shown in fig. 2c, the drift velocity of charge carriers is very slow. Therefore, the step-like continuum may be produced by the slow pulses from a Si(Li) detector. We adopted the widely used complementary error function as a step-like function, which is the convolution of the step function with a Gaussian of the detector resolution σ, i.e.

$$\frac{1}{\sqrt{2\pi}\sigma}\int_{-\infty}^{i_0} \theta(t)\exp\left[-(t-i)^2/2\sigma^2\right]dt = \frac{1}{2}erfc\left[(i-i_0)/\sqrt{2}\sigma\right]. \tag{13}$$

Here, the step function is given by

$$\theta(i) = \begin{cases} 1 & \text{for } i \le i_0 \\ 0 & \text{for } i > i_0 \end{cases} \tag{14}$$

Thus, the step-like function is given by

$$S(i) = H_s\ erfc\left[(i-i_0)/\sqrt{2}\sigma\right]. \tag{15}$$

The background term arises from the external backgroud radiations, such as cosmic-rays, high-energy γ-rays and electronic white noises. We tested various functions for

representing the background by the nonlinear least-squares method. The simplest and best function was the exponential type given by

$$BG(i) = a \exp(-bi) + c, \tag{16}$$

where a, b and c are the fitting parameters. We used the slope parameter b as a common value to fit all response function data.

The result of a fit based on this model were excellent for the experimental data over a wide energy range.

References

[1] Y.Inagaki, K.Shima and H.Maezawa, Nucl. Instr. and Meth B27(1987)353.

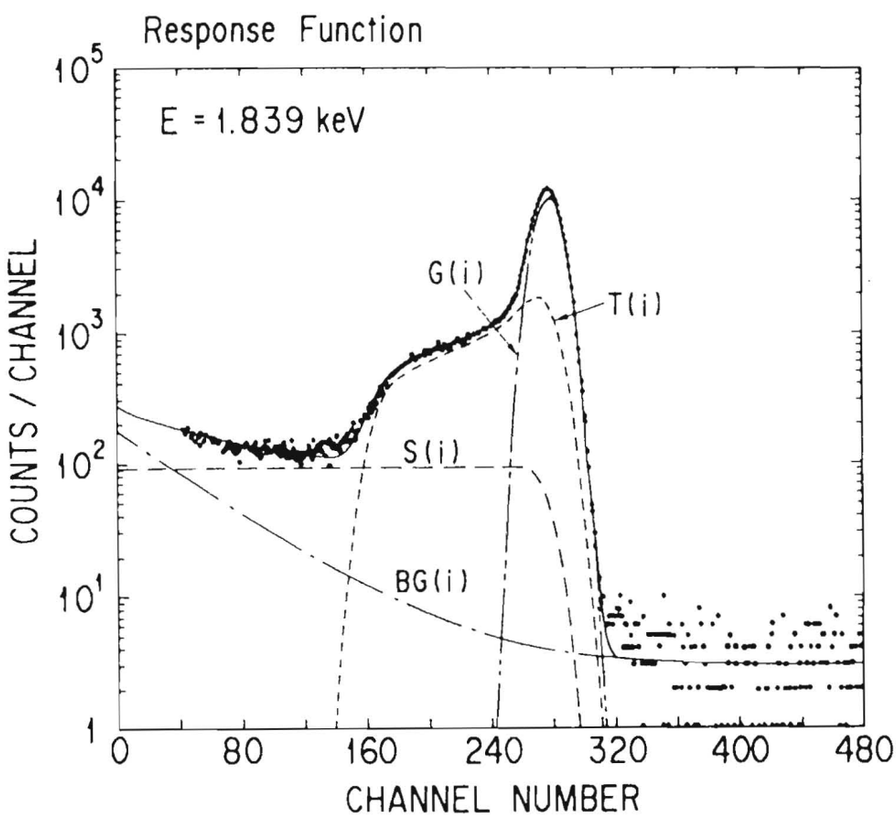

Fig. 1. Components of the response function.

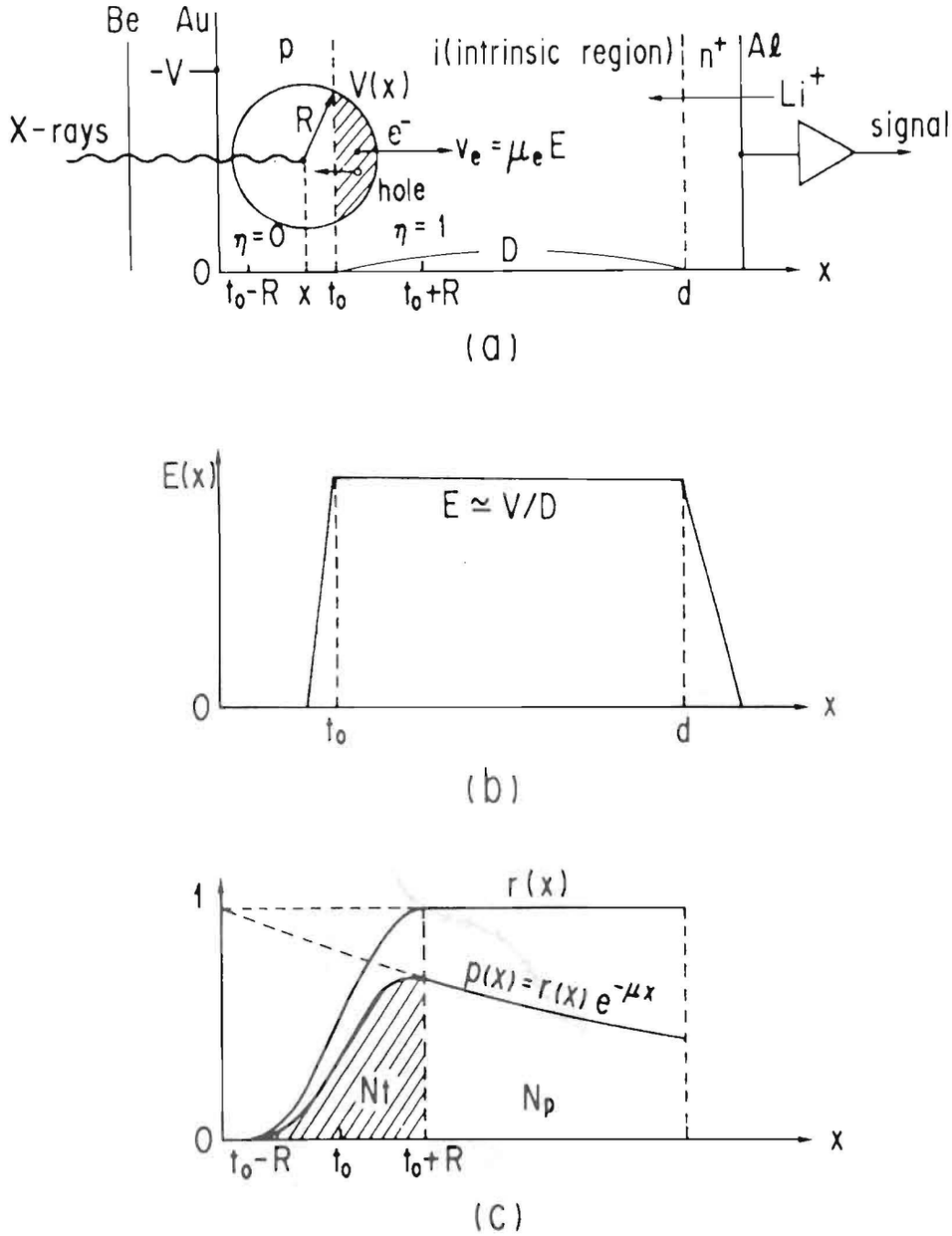

Fig. 2. a) Basic configuration of a p–i–n$^+$ type planar Si(Li) detector. b) Schematic electric field strength. c) The charge ratio $r(x)$ and the probability distribution function $p(x)$ for the low-energy tail as a function of the depth x.

Chapter 8

Influence of the Window Effect of Si(Li) X-ray Detector on the Response Function and Detection Efficiency

K.Shima, Y.Inagaki, H.Maezawa and S.Yasumi

1. Introduction

It is generally accepted that the surface of a Si(Li) x-ray detector is composed of a gold-electrode layer, a Si dead layer and an intrinsic volume of Li-drifted Si[1]. Here, the dead layer is meant to be the Si region where the charge collection efficiency, η , is zero (this layer is hereafter referred to as NCCL i.e., no charge collection layer). concerning the dead layer, little is known for its geometrical and physical property. Firstly, even the presence of the dead layer has not been directly confirmed. And hence, the reports on its thickness d_{Si} are rare, and their results are rough. Since the knowledge on the precise value of d_{Si} is essential for the understanding of response function and determination of detection efficiency, the establishment of method to confirm the value d_{Si} is strongly requested. Secondly, it is suggested that the appearance of the tail spectrum extending to the lower energy side of the Gaussian photo-peak in a Si(Li) detector spectrum is closely related to the Si layer where charge collection is incomplete ($0<\eta<1$) (this layer is hereafter referred to as ICCL i.e., incomplete charge collection layer). However, not only the thickness of ICCL but also the relationship between ICCL and response function has not been clarified yet.

Considering above features, this paper is intended to search NCCL and ICCL of Si(Li) detectors. Our interest is focused on the thickness of these layers. Furthermore, discussion is done on the influence of the presence of detector window such as gold electrode, NCH and ICICLE on the response function and detection efficiency.

The transmission of x-rays passing through the Is dead layer jumps at the Is-K absorption edge energy 1.84 keg. Noticing this property, the jump ratio of the detection efficiency was precisely measured by changing the incident energies of mono-energetic photons at around 1.84 keV. Based on this jump ratio value and response function, NCCL and ICCL have been searched and investigated. Mono-energetic photons were supplied by SOR (synchrotron orbit radiation).

2. Relationship between detection efficiency and dead layer

Fig.1 shows the typical x-ray spectra of a Si(Li) x-ray detector irradiated by mono-energetic x-rays of energies above 1.84 keV and below 1.84 keV. Each spectrum is composed of a main peak, a low energy tail, an escape peak and a plateau spectrum extending from zero to incident energy. Remarkable difference in these two spectra of above and below 1.84 keV is in the intensity ratio of the tail to main peak. Under the simple model that the Si(Li) detector is composed of a Au electrode, a Si dead layer, and an intrinsic region as is shown in Fig.2a, the detection efficiency ε for the detection of the counts N of the area under Gaussian distribution of the main peak can be written as

$$\varepsilon_{Si(Li)} = T(Be)\,T(Au)\,T(Si)\,C_{cap}(Si)\,C_{esc}\,C, \qquad (1)$$

where T(Be), T(Au) and T(Si) describe the transmission of x-rays through Be window, Au contact and Si dead layer (NCCL), respectively. $C_{cap}(Si)$ is the efficiency for x-rays photoabsorbed in the effective volume, C_{esc} is the correction for the production of an escape peak, and the last term C includes all other corrections such as the effects of the nonuniformity of the detection sensitivity[4] and of the dead time for counting. The factors T(Be), T(Au), T(Si) and C_{esc} are described as

$$T(Be) = \exp(-\mu_{Be} d_{Be}), \qquad (2)$$

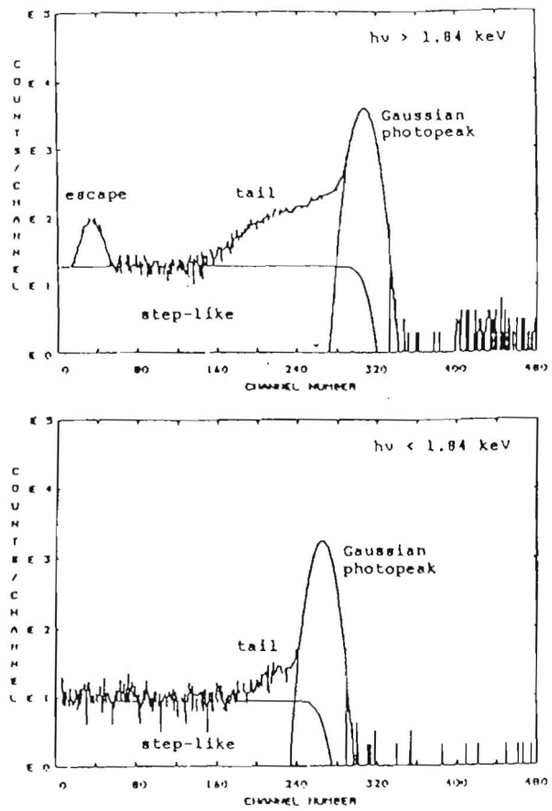

Fig.1 Typical x-ray spectra of a Si(Li) x-ray detector irradiated with monoenergetic x-rays of energies (a) above 1.84 keV, and (b) below 1.84 keV.

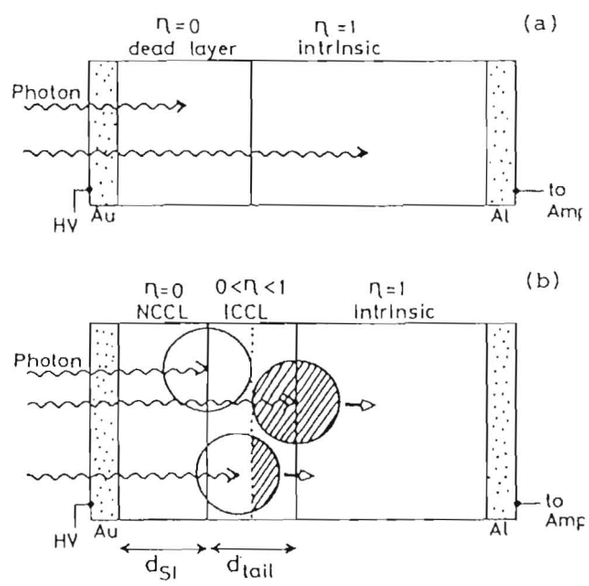

Fig.2 Schematic diagram of window of a Si(Li) detector. (a) The detector is assumed to be composed of two Si regions ; η=0 (dead layer) and η=1 (intrinsic region). (b) The detector is assumed to be composed of three Si regions ; η=0 (NCCL), 0<η<1 (ICCL) and η=1 (intrinsic region).

$$T(Au) = \exp(-\mu_{Au} d_{Au}), \quad (3)$$
$$T(Si) = \exp(-\mu_{Si} d_{Si}), \quad (4)$$
$$C_{esc} = 1/(1+N_{esc}/N), \quad (5)$$

where μ_i and d_i respectively denote the absorption coefficient and the thickness for material i, and N_{esc} is the x-ray counts of escape peak.

As was pointed out by Llacer[2] and Shima et al.[3], the area of low energy tail spectrum, N_{tail}, is a fractional product from incident x-rays and it should be regarded to be the loss count from the main peak count N. In eq.(1), the consideration for this loss count is missing. Since the tail spectrum is considered to originate at the boundary between the intrinsic region and the dead layer in Fig.2a, we restart from the model as is drawn in Fig.2b in which the detector is composed of NCCL ($\eta = 0$), ICCL ($0<\eta<1$) producing the tail spectrum, and an intrinsic region ($\eta=1$). In this case, the expression for ε can be described by

$$\varepsilon_{Si(Li)} = T(Be)\, T(Au)\, T(Si)\, C_{cap}(Si)\, C_{esc}\, C_{tail}\, C, \quad (6)$$

where C_{tail} is the correction for the production of the tail spectrum, i.e., the ratio of photons passing through ICCL and being photoabsorbed in the intrinsic region to the photons absorbed in the ICCL, given by

$$C_{tail} = 1/(1 + N_{tail}/N)\,. \quad (7)$$

The detection efficiency given in eq.(6) is not a smooth function of x-ray energy, but changes rapidly at Si-K absorption edge energy, because , the factors T(Si), C_{esc} and C_{tail} change rapidly at 1.84 keV. Therefore, if the jump ratio, $\varepsilon_H/\varepsilon_L$, of $\varepsilon_{Si(Li)}$ in eq.(6) at 1.84 keV given by

$$\varepsilon_H/\varepsilon_L = \{C_{esc}C_{tail}T(Si)\}_H/\{C_{esc}C_{tail}T(Si)\}_L\,, \quad (8)$$

is experimentally measured, and the ratios $\{C_{esc}\}_H/\{C_{esc}\}_L$, $\{C_{tail}\}_H/\{C_{tail}\}_L$ are also measured, then the ratio $\{T(Si)\}_H/\{T(Si)\}_L$ is inevitably obtainable. Here, H and L respectively indicate the limits for values $\varepsilon_{Si(Li)}$, C_{esc} , C_{tail} , or T(Si) approaching from higher side and lower side of x-ray energies to 1.84 keV. Thus the thickness of NCCL, d_{Si}, can be estimated from the ratio $\{T(Si)\}_H/\{T(Si)\}_L$ and eq.(4).

3. Experimental procedure

The experiment was done at the Photon Factory of National Laboratory for High Energy Physics, KEK, where the synchrotron radiation from 2.5 GeV electron storage ring is available. The monoenergetic photon beam was obtained from undulator radiation coupled with a channel-cut monochrometer, made of InSb for photons above 1.74 keV. The energy spread of incident photons was less than 1 eV and the contamination of the higher order photons was less than 0.02 %.

In order to obtain the values $\varepsilon_H/\varepsilon_L$, $\{C_{esc}\}_H/\{C_{esc}\}_L$ and $\{C_{tail}\}_H/\{C_{tail}\}_L$ in eq.(8) experimentally, the limits of $\varepsilon_{Si(Li)}$, C_{esc} (or N_{esc}/N in eq.(5)) , and C_{tail} (or N_{tail}/N in eq.(7)) approaching from lower energy side of 1.84 keV and and from higher energy side of 1.84 keV were deduced by scanning the incident photon energy at around 1.84 keV. A schematic of the apparatus is illustrated in fig.3.

A high purity Lucite plate was irradiated with a photon beam of 2mm x 1mm in spot size. The elastically scattered photons were detected simultaneously with a Si(Li) detector and a proportional counter installed at ±135º to the beam direction.

In the present geometry displayed in fig.3, the ratio of the main peak count of the Si(Li) detector, N , to the peak count of the proportional counter, N_{pc} , is written as

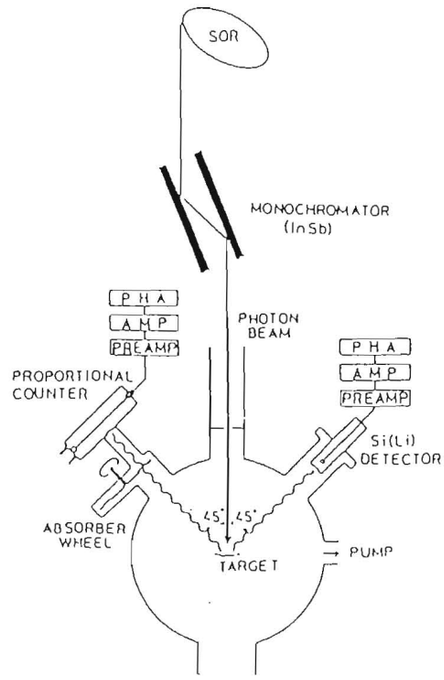

Fig.3 Schematic diagram of experimental apparatus. A high purity lucite target is irradiated with monoenergetic photons, and elastically scattered photons are simultaneously detected with a Si(Li) detector and a proportional counter.

$$N/N_{pc} = \varepsilon_{Si(Li)}\Omega_{Si(Li)}/(\varepsilon_{pc}\Omega_{pc}) , \qquad (9)$$

where ε_{pc} means the detection efficiency of the proportional counter, $\Omega_{Si(Li)}$= 2.27×10^{-4} sr and Ω_{pc} = 6.75×10^{-5} sr are respectively the solid angles subtending the effective area of Si(Li) detector (10.8 mm^2) and proportional counter (7.06 mm^2). The endcap of the Si(Li) detector was placed inside the vacuum. Its energy resolution was 160 eV at 5.9 keV and the manufacturer's specification lists the thickness of Be window as 8 μm, the gold contact as 200 Å and the Si dead layer as 0.1 μm. On the other hand, the proportional counter was composed of 6 μm aluminized Mylar window, and the flow-mode PR gas region whose effective diameter was 34 mm. The ε_{pc} value, defined as the product of (a) the transmission of x-rays through a Mylar window and (b) the x-ray absorption efficiency for x-rays inside the PR gas counter, was obtained as follows. The x-ray counts of a Si(Li) detector normalized by the counts of a proportional counter were compared between the case with a 6 μm Mylar sheet inserted in front of the Si(Li) detector and the case free from the Mylar sheet (see fig.3), which leads to the value (a). On the other hand, the value (b) was evaluated through calculation by using the effective PR gas thickness and photoabsorption cross sections. The raw spectra obtained with a Si(Li) detector were already shown in fig.1. As for the deduction of x-ray counts of the main peak N, the tail area N_{tail} . and the escape peak N_{esc}, firstly, the plateau component (drawn with hatched lines) was subtracted from the original spectrum using a step-like function[5]. Secondly, the counts N and N_{esc} were determined using a Gaussian distribution. Finally, the remaining x-ray counts were regarded as N_{tail}. All the present Si(Li) spectra were obtained under the background free condition for the detection of monoenergetic photons. Nevertheless, as is seen in fig.1, the spectrum is inherently accompanied by the plateau component extending to the incident energy.

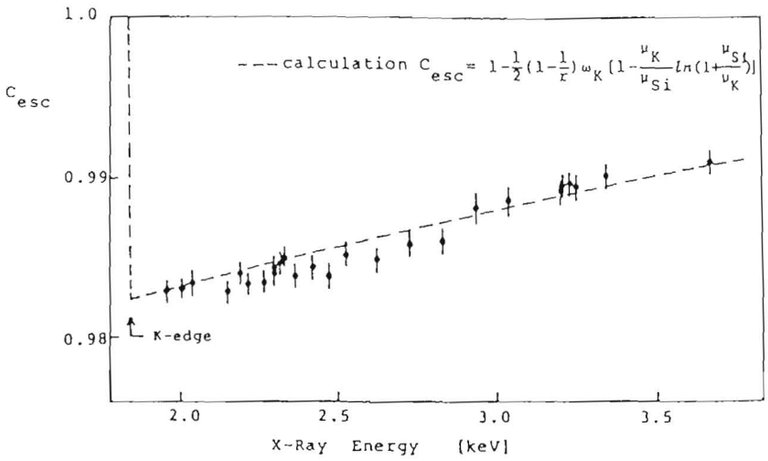

Fig.4 Observed C_{esc} values defined by eq.(5) along with calculated values..

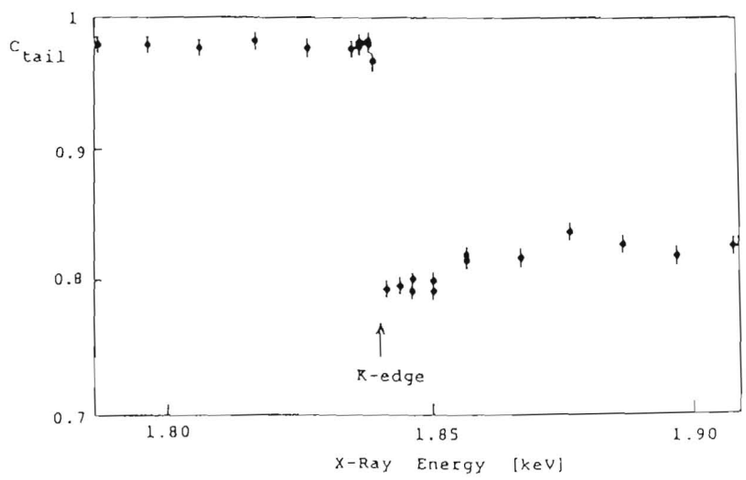

Fig.5 Observed values of C_{tail} defined by eq.(7).

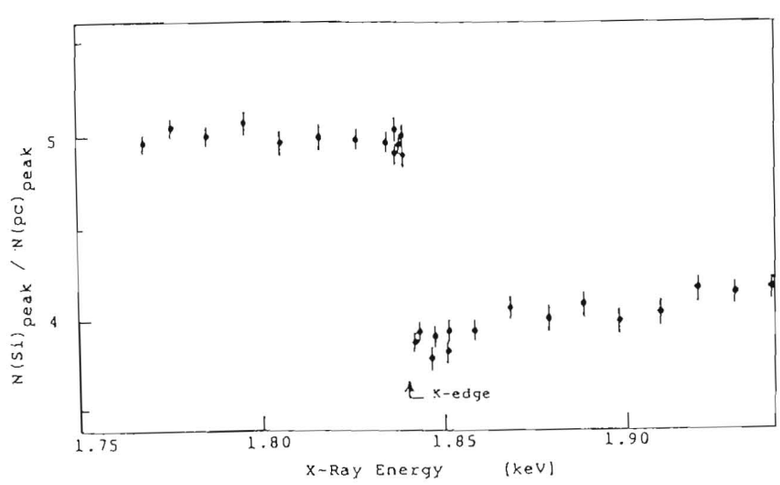

Fig.6 Ratio of Gaussian main peak count detected with a Si(Li) detector to that detected with a proportional counter, $N(Si)_{peak}/N(pc)_{peak}$.

This component is to be discussed in a separate paper[6], and it is sufficient to mention here that this component is irrespective of the detection efficiency.

4. Results

Fig.4 shows the observed C_{esc} values along with the calculation by Reed et al.[7] (originally, it is presented with the ratio N_{esc}/N in eq.(5)) given by,

$$C_{esc} = 1 - 0.5(1 - 1/r)\ \omega_K\{1-(\mu_K/\mu_{Si})\ln(1+\mu_{Si}/\mu_K)\}, \qquad (10)$$

where r is the jump ratio of absorption coefficient at the Si-K absorption edge energy, ω_K is the Si-K shell fluorescence yield, and μ_K is the absorption coefficient for Si-K x-rays in Si. Concerning the value C_{esc} , observed values are known to be reproduced by eq.(10), which has been reconfirmed at present by obtaining much more data points. Extrapolating the observed values to 1.84 keV in fig.4, we obtain the ratio of C_{esc} in eq.(5) as

$$\{C_{esc}\}_H/\{C_{esc}\}_L = 0.9818 \pm 0.0004, \qquad (11)$$

where the value $\{C_{tail}\}_L = 1$, as is easily estimated from similar formula to eq.(10) for the escape of Si-L x-rays.

Production of the tail spectrum is caused by the incomplete charge collection near the detector surface[2,3,8]. Hence, the N_{tail}/N values of x-rays below 1.84 keV, which are absorbed in relatively deeper portion of the detector surface, are much smaller than those of x-rays just above 1.84 keV. Fig.5 shows the C_{tail} values of eq.(7) based on the data of N_{tail}/N . The limit of C_{tail} values approaching 1.84 keV becomes as

$$\{C_{tail}\}_H/\{C_{tail}\}_L = 0.807\ (1 \pm 0.025). \qquad (12)$$

In order to deduce the ratio of detection efficiency $\varepsilon_H/\varepsilon_L$ in eq.(8), the x-ray count of the main peak, N , was divided by the corresponding peak count of the proportional counter, N_{pc} (see eq.(8)). Results are shown in Fig.6 as a function of x-ray energy. In order to obtain the ratio $\varepsilon_H/\varepsilon_L = \{N/N_{pc}\}_H/\{N/N_{pc}\}_L$, the limits of $\{N/N_{pc}\}_H$ and $\{N/N_{pc}\}_L$ at 1.84 keV are to be evaluated from fig.6. Using the parameterized functions for each set of N/N_{pc} curve determined through least squared fitting, the ratio of limits of two curves at 1.84 keV is given as

$$\varepsilon_H / \varepsilon_L = 0.790\ (1 \pm 0.007). \qquad (13)$$

The value of d_{Si} can be evaluated from eqs.(4) (6) (9) (10) and (11). Taking into account the experimental errors and using the tabulated absorption coefficient[9] for , we obtain

$$d_{Si} = 0.005 \pm 0.036\ \mu m \qquad (14)$$

5. Discussion

5.1. NCCL and OCCL

Present result of d_{Si} in eq.(14) indicates that the dead layer which does not produce output signal , NCCL , is extremely thin, and may be regarded to be absent within the experimental uncertainty. This is an amazing fact, because it has long been considered that there exists such a layer as $\eta = 0$.

On the other hand, if we compare eqs.(12) and (13), it is understood that the discontinuity of $\varepsilon_{Si(Li)}$ at 1.84 keV is dominantly caused by the factor C_{tail} apart from the small fraction of the escape peak. This fact means that the photons absorbed in the vicinity of the detector surface are mostly detected as a tail spectrum. Under the model given in Fig.2b, the effective thickness for the production of tail spectrum, d_{tail} , can be estimated through the relation,

$$C_{tail} = 1/(1+ N_{tail}/N) = \exp(-\ \mu_{Si}\, d_{tail}\ ), \text{ and} \qquad (15)$$

$$\{C_{tail}\}_H/\{C_{tail}\}_L = \exp(\{-\ (\mu_{Si})_H + (\mu_{Si})_L\ \}\ d_{tail}\ ), \qquad (16)$$

where $(\mu_{Si})_H$ and $(\mu_{Si})_L$ indicate the absorption coefficient at the limits of higher and lower energy sides of 1.84 keV, respectively. From eqs.(12) and (16) , we obtain,

$$d_{tail} = 0.26\ \mu m\ . \qquad (17)$$

Some manufacturers of Si(Li) detectors list the thickness of "Si dead layer" in the specification for each detector —— it is typically 0.1 or 0.2 μm. Within the framework of the author's knowledge, the basis for the derivation of this thickness is not clear. In addition, it is not certain if this "dead layer" means NCCL or ICCL. For the investigated detector at present, it can be said that only ICCL is present in the "dead layer".

5.2. Detection efficiency

At present, so-called "dead layer" has been divided into two layers, and each layer of NCCL and ICCL has been individually confirmed to be present or not. The concept for the dead layer being composed of two layers is correlated to the estimation of detection efficiency, $\varepsilon_{Si(Li)}$. Because, currently accepted expression of $\varepsilon_{Si(Li)}$ given by eq.(1) becomes to be replaced to a new expression of eq.(6), where a new term $T(Si)xC_{tail}$ is introduced in stead of the term T(Si) in eq.(1).

Values of $\varepsilon_{Si(Li)}$ at photon energies less than about 3 keV are dominated by the transmission of photons through Be window, gold-electrode layer, NCCL and ICCL. In the determination of $\varepsilon_{Si(Li)}$ in this energy region, particular caution is needed in the adoption of the thicknesses of above mentioned layers. Because they differ detector by detector. With respect to the thickness of gold layer, it is reported to range from 140 to 260 Å for investigated 5 detectors[10], meanwhile the indicated value in this detector's specification is 200 Å.

Since there are no suitable standard radioisotopes available for the determination of $\varepsilon_{Si(Li)}$ in low energy region, present procedure of using a proportional counter as a monitor counter and detecting monoenergetic x-rays both by a Si(Li) detector and a proportional counter has shown to be a powerful method.

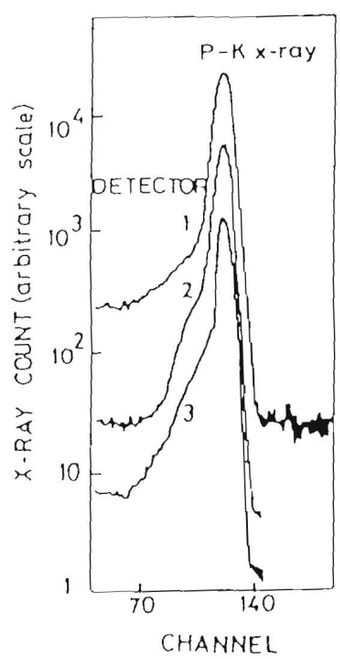

Fig.7 P-K x-ray spectra detected with three different Si(Li) detectors. Notice that the line shapes of tail spectra differ by detectors.

5.3. Response function

As was shown in Fig.1, a response function of low energy x-rays detected with a Si(Li) detector can be decomposed into four components of a main Gaussian photopeak, a low energy tail, an escape peak and a step-like function. The production of an escape peak is clear. Its line shape is Gaussian, and observed peak area is known to agree with the calculation by Reed[7]. Present experiment also supports this fact (see Fig.4).

Concerning the tail spectrum production, its origin is not definite. Firstly, as was described in section 4, the thickness of ICCL differs detector by detector, and hence, the area of tail spectrum relative to that of main Gaussian peak differs detector by detector. Secondly, as was mentioned in our previous paper[3], the line shape of the tail spectrum differs detector by detector. This is a future problem to be clarified.

As was mentioned in the text, the tail spectrum rapidly changes in magnitudes and line shapes at an incident photon energy of 1.84 keV. Furthermore, the line shape of tail spectrum differs detector by detector. In the derivation of x-ray peak counts from a complicated x-ray spectrum, particularly when the area of a small peak adjacent to a large peak is evaluated, one must be careful in the identification of x-rays and in the treatment of the line shape of tail spectrum.

References

1. A.H.Muggleton, Nucl. Instrum. Methods 101 (1972) 113.
2. J.Llacer, E.E.Huller and R.C.Cordi, IEEE Trans. Nucl. Sci. NS-24 (1977) 53.
3. K.Shima, S.Nagai, T.Mikumo and S.Yasumi, Nucl. Instrum. Methods 217 (1983) 515.
4. J.S.Hansen, J.C.McGeorge, D.Nix, W.D.Schmidt-Otto, I.Unus and R.W.Fink, Nucl. Instrum. Methods 106 (1973) 365.
5. Y.Inagaki, K.Shima and H.Maezawa, Nucl. Instrum. Methods B27 (1987) 353.
6. Y.Inagaki, to be published.
7. S.J.B.Reed and N.G.Ware, J. Phys. E: Sci. Instr. 5 (1972) 582.
8. F.S.Goulding, Nucl. Instrum. Methods 142 (1977) 213.
9. Wm.J.Veigele, At. Data & Nucl. Data Tables 5 (1973) 51.
10. K.Shima, K.Umetani and T.Mikumo, J. Appl. Phys. 51 (1980) 846.

Chapter 9

N_0 & $T_{1/2}$ of ^{163}Ho source

Osamu Kawakami* and Akimasa Masuda**

The University of Tokyo, Tokyo 113, Japan

Abstract

The total number of ^{163}Ho atoms in the ^{163}Ho source was precisely measured by mass spectrometric isotope-dilution method. The total number of ^{163}Ho atoms in the ^{163}Ho sdource has been observed to be $(6.481\pm0.012)X10^{15}$ atoms. The half-life of ^{163}Ho was investigated by mass spectrometric determination of the quqntity of ^{163}Dy formed by the electron capture decay of ^{163}Ho. The half-life of ^{163}Ho has been measured to be 4569 ± 27 yr (68% confidence level). The result of the present work is in excellent agreement with the value previously obtained by Baisden et al.

Introduction

The precise determination of the total number of ^{163}Ho atoms(N_0) in the ^{163}Ho source and half-life of $^{163}Ho(T_{1/2})$ are very important for measuring the mass of the electron neutrino. Particle induce X-ray emission (PIXE) method was first applied to the analysis of the number of Ho in the sources[1], but large errors were unavoidable. On the other hand, isotope-dilution mass spectrometry (IDMS) is one of the most precise method for the analysis of trace element. Therefore IDMS was applied to the measurement of ^{163}Ho stoms in the source.

The previous values of the half-life of ^{163}reported ranged

---

* Present address : Metal Mining agency of Japan, 1-24-14, Toranomon, Minato-ku, Tokyo 105, Japan

** Present address : The University of Electro-Communications, 1-5-1 Chofugaoka, Chofu-shi, Tokyo 182, Japan

widely from 33 to 7000 yr[2-5]. Baisden et al.[6] investigated the half-life of ^{163}Ho by measuring the production rate of ^{163}Dy due to the electron capture in ^{163}Ho with isotope-dilution mass spectrometry (IDMS), and obtained the result of 4570±50 yr. Since IDMS is an absolute measurement, we reinvestigated the half-life of ^{163}Ho with IDMS.[7]

Baisden et al. used about 0.7 mg of ^{163}Ho for the parent fraction and measured the isotope ratios of Dy over a period of about 0.6 yr. In the present work, employing as little as 0.0016 mg of ^{163}Ho, the number of ^{163}Dy growing from ^{163}Ho over a period of about 1.3 yr was determined with a high accuracy. In our mass spectrometric measurements, observation of mono-oxide ion beams of Dy made it possible to avoid the interferences of NdO^+ and SmO^+, whose mass numbers are equal to those of Dy^+ ions.

Section 1

Holmium-163 nuclide was produced with the $^{164}Dy(p,2n)$ reaction by the use of an enriched ^{164}Dy metal target.[8] The ^{163}Ho and the target ^{164}Dy were chemically separated[4], and ^{163}Ho was electroplated onto a nickel foil. The ^{163}Ho was used as a source of the X-ray measurement. After the measurement of X-rays from ^{163}Ho, we destructed the source and further isolated Ho to attain a more complete separation from Dy coming from the target with an ion exchange method. The deposition of ^{163}Ho in the source was leached with 3M hydrochloric acid, at the same time Ni foil was slightly dissolved, and the solution was diluted with water until total weight was about 100 g. A part of this solution was used for the determination of the total number of ^{163}Ho atoms in the source. Known quantity of natural standard solution of ^{165}Ho was added to a part of leached solution as a spike for ^{163}Ho. Preliminary mass spectrometry of leached solution indicated that the source included ^{165}Ho and the target Dy which atomic numbers were from 160 to 164 other than ^{163}Ho. Since a separation of ^{163}Ho and ^{163}Dy in the mass spectrometry was difficult, it was require that Ho and Dy should be chemicaly separated before IDMS.

The resin was AG50W-X8, 100-200 mesh, cation exchanger and a quartz tube of 2.4 mm diameter used as a column with quartz wool at the bottom. The column was loaded to a length of 10 cm with the resin. The α-hydroxyisobutyric acid(α-HIB), 0.15 M with pH=3.8, was used as an eluant. The calibration of the elution was carried out in advance with 100 ng of Ho and 50 ng of Dy, and the elution curves for Ho and Dy were checked by ICP mass spectromter (VG Isotope LTD, England).

Isotopic ratio $^{163}Ho/^{165}Ho$ of the chemically separated Ho fraction was measured by a mass spectrometer. The surface ionization mass spectrometer used in this work was a JMS-05RB type of JEOL LTD., Japan (ion beam radius 30 cm, 90 sector, maximum acceleration voltage 10 kV). Because an electron multiplier was used as a detector system for ion beams, a correction factor of root mass ($(m_1/m_2)^{1/2}$, where m_1 and m_2 are the mass numbers of the isotopes 1 and 2, respectively) was applied to the gain. A YHP345A digital voltmeter and a HP9835A desktop computer were used for the reading of the ion beam intensity. The reading program was a modification of the program made by K. Fujii et al.[9] The number of ^{163}Ho atoms in ^{163}source was calculated by the observed isotopic ratio of $^{163o}Ho/^{165}Ho$. The total number of ^{163}Ho in the ^{163}Ho source(N_0) has been calculated to be $(6.481\pm0.012)X10^{15}$ atoms.

Section 2

For the investigation of $T_{1/2}$, a large portion of the leached solution from the source was used. Holmium was chemicaly separated in a same manner as described previously. The Ho fraction thus obtained is hereafter called the parent ^{163}Ho fraction. Using the holmium standard as references in IDMS, we determined the quantity of ^{163}Ho in the parent fraction to be $1.5608\pm0.0027\mu g$. We also determined the quantity of enriched ^{160}Dy, which was used for a "spike" solution to measure

the quantity of ^{163}Dy generated in the ^{163}Ho parent fraction.

A known amount of enriched ^{160}Dy spike solution, containing 1.6020±0.0023 ng of Dy, was added to the parent ^{163}Ho fraction. After the period of 1.3231±0.0014 yr, Dy was recovered from the half aliquot of the parent solution with a duplicate ion exchange. The α-HIB in this Dy fraction was decomposed by low temperature oxygen plasma (IBC 1000, International Plasma LTD., USA). This Dy fraction is hereafter called the daughter Dy fraction.

In our mass spectrometry, the sample was dissolved in a drop of nitric acid and loaded onto a rhenium single filament of the ion source of the mass spectrometer. Mono-oxide ion beams of Dy or Ho were produced and measured under controlled small leakage of oxygen gas into the ionization chamber, where a correction for oxygen isotopes were made using the isotope ratios of $^{18}O/^{16}O=0.00211$ and $^{17}O/^{16}O=0.000387$ observed by Wasserberg et al.[10]

The measured isotope ratios of Ho of the parent ^{163}Ho fraction and the isotope abundances of target Dy are listed in Tables I and II,respectively. The measured isotope abundances for natural Dy and enriched ^{160}Dy, which was used as a spike, are also listed in Table II. Observed isotope abundances for natural dysprosium were consistent with the value reported by Holliger and Devillers.[11]

In the measurement of isotope ratios of the daughter Dy fraction, the filament current was changed stepwise from 2.49 to 3.12 A with 31 steps (m=31). In each step the isotopic measurement of $^{161}Dy/^{164}Dy$, $^{162}Dy/^{164}Dy$ and $^{163}Dy/^{164}Dy$ were repeated 9 times. The daughter Dy fraction consisted of four components, i.e., spike ^{160}Dy, radiogenic ^{163}Dy, target ^{164}Dy and natural Dy. The natural (or blank) Dy is asssumed to be come from reagent and chemical processes.

Since the quantity of spike Dy is known, solving these ratios gives the number of radiogenic ^{163}Dy atoms.[7] In the estimation of errors of the

Table I. Isotope ratios of $^{165}Ho/^{163}Ho$

Run	m	$^{165}Ho/^{163}Ho$
run 1	12	0.02808+0.00007[a]
run 2	11	0.02812+0.00015
run 3	15	0.02836+0.00010
run 4	12	0.02831+0.00020
run 5	10	0.02828+0.00016
simple mean		0.02823+0.00005[b]

[a] Standard error of the mean x of m values (x_1, x_2, x_m) measured at m filament currents in a run, defined as $s/\sqrt{m}$, where s is calculated from

$$s^2 = \sum_{i=1}^{m}(x_i-x)^2/(m-1), \text{ and } x = \sum_{i=1}^{m}x_i/m.$$

The value of x_i itself was a simple mean of 9 measurements for a given filament current.

[b] Since the scattering of the results of the different runs (y_1, y_2, $\cdots$, y_n) was larger than the combined error of the weighted average of the runs, we estimate and adopted the standard error of the simple mean (y) of the runs externally as s/n with n=5, where s is calculated from

$$s^2 = \sum_{j=1}^{n}(y_i-y)^2/(n-1) \text{ and } y = \sum_{j=1}^{n}y_i/n.$$

Table II. Isotope abundances(%) of Dy for each component.

	natural		spike	target
isotope	this work	ref.1	enriched ^{160}Dy	enriched ^{164}Dy
156	0.0541+0.0004	0.056+0.001	0.0118+0.0006	*
158	0.0943+0.0004	0.096+0.002	0.0482+0.0006	*
160	2.3377+0.0019	2.34 +0.02	63.213 +0.035	0.1154+0.0009
161	18.862 +0.014	18.91 +0.05	21.598 +0.034	0.9344+0.0023
162	25.453 +0.013	25.51 +0.07	7.442 +0.019	1.4514+0.0017
163	24.902 +0.010	24.90 +0.07	4.375 +0.024	3.6565+0.0034
164	28.298 +0.0073	28.19 +0.08	3.312 +0.016	93.842 +0.043

Errors were estimated in the same way as in Table I, where m = 10 20 and n = 4 6.

* not detected.

Table III. Analytical results of Dy atoms for the four components in the daughter Dy fraction.

component	total number of Dy atoms in each component ($x10^{10}$)	total weight of Dy atoms ($x10^{-12}$ g)	proportion of ^{163}Dy nuclide[a] (%)
spike (S)	600.9+0.9	1602.0+2.3	17.7
natural (N)	22.4+1.1	60.4+1.1	3.8
target (T)	8.25+0.23	22.45+0.30	0.2
radiogenic (R)	115.77+0.62	313.3+1.7	78.3

[a] The proportion of ^{163}Dy in each component to the total ^{163}Dy in the daughter Dy fraction.

solution for all terms, i.e. observed isotope ratios were taken into account. In this calculation the propagation of errors were properly considered by a numerical method. Results are listed in Table III.

In spite of our very careful purification of ^{163}Ho, a small amount of the target Dy (22.45 pg) has been found to exist in the final daughter Dy fraction. Also there was 60 pg of natural Dy in the dauter Dy fraction as the blank of chemical separations. In the above process of calculation the separated daughter Dy fraction was considerd to be free from ^{163}Ho. If ^{163}Ho is remaining in the daughter Dy fraction, the isotope ratios of $^{163}Dy/^{164}Dy$ should change systematically with increase of the filament current or temperature. But the isotope ratio $^{163}Dy/^{164}Dy$ did not change for a wide range of filament current from 2.49 to 3.12 A.

The half life of ^{163}Ho was calculated from equation (1).

$$T_{1/2} = \frac{t \ln 2}{\ln(1 - n^{163}Dy/n^{163}Ho)} \qquad (1)$$

where t is the standing period of the parent ^{163}Ho, 1.321±0.0014 yr, $n^{163}Dy$ is the number of radiogenic ^{163}Dy atoms and $n^{163}Ho$ is the number of parent ^{163}Ho atoms, $n^{163}Ho=(5.769\pm0.010)\times10^{15}$.

The calculation led to the value of $T_{1/2}$=4569±27 yr (68 % confidence level) for the half-life of ^{163}Ho.

IV. Section 3

Our result of $T_{1/2}$ is in close agreement with the value of 4570±50 yr obtaioned by Baisden et al.[6] They resolved their mass spectrometric results into 6 components, i.e. radiogenic Dy, spike Dy, blank Dy, tracer Dy, ^{165}Ho and NdO. On the other hand we resolved the daughter Dy fraction into 4 components, i.e. radiogenic, spike, blank and target Dy. Since the mono-oxide ion beams were measured in this study, it was not required to subtract the interference of NdO. Besides, as mentioned above, we need not take into

account the presence of any Ho in the Dy fraction. Thus, we succeeded in obtaining a highly reliable half-life of ^{163}Ho, employing a very small amount of ^{163}Ho corresponding to 1/400 of the amount used by Baisden et al. On the bases of the good agreement between the two results obtained under rather different conditions of analysis for the half life of ^{163}Ho, we can take a weighted mean of the two values as $T_{1/2}=4569\pm38$ yr (95 % confidence level).

Acknowledgements

The authors are greatly thankful to Dr. K. Yoshida and Dr. H. Shimizu, the University of Tokyo, for their useful discussions and Drs. T. Shinozuka, K. Sera, G. Izawa, M. Yagi and K. Masumoto, Tohoku University, for their preparation of ^{163}Ho nuclide.

References

[1] M.Fujioka K.Ishii T.Shinozuka K.Sera K.Katube T.Omori G.Izawa M.Yagi K.Masumoto and S.Yasumi. Proceedings of the 4 the Workshop on the Mass of the Electron Neutrino. KEK 82-2 19 (1982).

[2] R.A.Nauman M.C.Michel and J.L.Power. J. Inorg. Nucl. Chem. **15** 194 (1960).

[3] P.K.Hopke, J.S.Evans and R.A.Naumann. Phys. Rev. **171**. 171 (1968).

[4] J.U.Andersen, G.J.Beyer, G.Charpak, A.De.Rujala, B.Elbek, H.A.Gustafsson, P.G.Hansen, B.Jonson, P.Kunudsen, E.Laegsgaard, J.Pedersen and H.L.Ravn. Phys. Lett. **113B** 72 (1983).

[5] S. Yasumi, G. Rajasekaran, M. Ando, F. Ochiai, H. Ikeda, T. Ohta, P. M. Stefan, M. Murayama, N. Hasimoto, M. Fujioka, K. Ishii, T. Shinozuka, K. Sera, T. Omori, G. Izawa, M. Yagi, K. Masumoto and K. Shima. Phys. Lett. **122B**, 461 (1983).

[6] P. A. Baisden, D. H. Sisson, S. Niemeyer, B. Hudson, C. L. Bennett and R. A. Naumann. Phys. Rev. **C28**, 37 (1983).

[7] O. Kawakami and A. Masuda. Physical Review C38, 1857 (1988).

[8] K. Ishii, M. Fujioka, K. Sera, T. Shinozuka and K. Katsube. Nucl. Instrum. Methods Phys. Res. **205**, 563 (1983).

[9] K.Fujii, Y.Hirao and H.Mabuchi, Hozonkagaku, **18**, 94 (1979).

[10] G.J. Wasserburg, S.B.Jacobsen, D.J.Depaolo, M.T.McCulloch and T.Wen. Geochim. Cosmochim. Acta **45**, 2311 (1981).

[11] P.Holliger and C.Devillers. Earth Planet. Sci. Lett. **52**, 76 (1981).

Chapter 10

Description of the Soft X-ray Undulator Beamline

H. Maezawa and S. Kishimoto

Photon Factory, National Laboratory for High Energy Physics

1. Introduction.

Purpose of the experiment at the Photon Factory, a synchrotron radiation light source facility, made as a part of the study on the mass of the electron neutrino was (1) to analyze the M X-ray fluorescence spectra of Dy atom excited by monochromatic X-ray beam with some different photon energies and then (2) to deduce the fluorescence spectra each of which was due only to a single M subshell vacancy in Dy atom. To obtain the monochromatic X-ray beam with photon energies covering the M_1 and M_2 subshell excitation region of Dy which ranged from 1.7 keV to 2.1 keV, we used a beamline BL-2A of the facility which was composed of a soft x-ray undulator and an InSb double crystal monochromator. The following gives description of the beamline in brevity as far as the experiment is concerned. Detailed descriptions on the arrangement of beamline and its performance will be found in Refs. [1] - [4].

2. Undulator radiation - the light source.

The soft X-ray undulator was chosen as the light source because not only of its capability of energy coverage but also of its high brilliance in the source character. The fifth-order harmonic of the undulator radiation was able to be tuned finely as a quasi-monochromatic light source to cover the photon energy region, although the BL-2 undulator was originally optimized in such that its most intense first order harmonic covered the K-shell absorption region of the light elements C, N, and O ranged from 300 eV to 600 eV. Since the Dy target must be optically as thinner as possible to minimize the effect of self-absorption that is essential to the experiment, the target must be irradiated instead as intensely as possible with sufficiently narrow bandwidth. The requirements for the source properties were best satisfied by the many-period undulator which could emit the harmonic synchrotron radiation spatially into sufficiently narrow cone with the quasi-monochromaticity.

Wavelength of the n-th harmonic of undulator radiation is given on axis by

$$\lambda_n = \frac{\lambda_u}{2n\gamma^2}\left(1+\frac{K^2}{2}\right), \tag{1}$$

where, λ_n is the wavelength of the n-th harmonic, λ_u the period length of undulation, n the odd harmonic number, γ the kinetic energy of electron/positron circulating the storage ring in the rest mass unit given numerically by,

$$\gamma = 1957 \cdot E(\mathrm{GeV}), \tag{2}$$

and K the deflection parameter given numerically by

$$K = 93.4 \cdot \lambda_u(\mathrm{m}) \cdot B(\mathrm{T}). \tag{3}$$

Here, E is the kinetic energy in GeV and B is the magnetic flux density generated by the undulator magnets. The harmonic radiation is emitted within a cone of half angular width of $\Delta\theta_n$ which is given by

$$\Delta\theta_n = \frac{1}{\gamma}\sqrt{\frac{1+K^2/2}{2nN}}, \tag{4}$$

where, N is the number of the undulator periods. As for the quasi-monochromaticity, the full fractional bandwidth of the n-th harmonic is approximately given by

$$\frac{\Delta\lambda_n}{\lambda_n} \approx \sqrt{\left(\frac{1}{nN}\right)^2 + \left(\frac{\gamma^2 \cdot \psi^2}{1+K^2/2}\right)^2}, \tag{5}$$

where, ψ is effective half angular aperture in observation which is convolution of angles, the one defined by any diaphragm or slit inserted into the beamline and the other by effective source size. The peak brightness of the n-th harmonic is given numerically in unit of photons per sec·mA·mrad^2·0.1% bandwidth by

$$I_n = 1.74 \times 10^{11} \cdot E^2 \cdot N^2 \cdot F_n(K), \tag{6}$$

ideally for zero beam emittance and infinitesimal aperture, although it degrades practically by some orders of magnitude depending on the real emittance of circulating electron/positron beam. The function $F_n(K)$ is given by

$$F_n(K) = \frac{n^2 \cdot K^2}{(1 + K^2/2)^2} [J_{(n+1)/2}(\xi) - J_{(n-1)/2}(\xi)]^2 , \qquad (7)$$

where, J is the Bessel function and the argument $\xi = n^2 \cdot K^2/(4 + 2K^2)$.

In our experiment, $E = 2.5$ GeV, i.e., $\gamma = 4893$, $\lambda_u = 0.06$ m and $N = 60$. The magnetic flux density of the undulator B was tuned from 0.02 to 0.4 T, i.e., the deflection parameter was tuned from 0.11 to 2.24. The stored beam current of the storage ring was ranged from 360 to 200 mA.

3. InSb - the crystal monochromator.

A pair of synthetic InSb crystal ($2d = 7.481$Å for (111) plane) was used as the element of monochromator which was capable to provide the beam of photon energies above 1.7 keV with the resolving power of about 10^3 which was sufficiently high to the experiment. The InSb was chosen as the monochromator crystal because not only of its capability of the photon energy coverage but also it does not have Si as the constituent that makes greatly easier the data analyses in the vicinity of Si-K absorption edge. As has been described in chapters 7 and 8 of this monograph, the efficiency and response function of the Si(Li) detector are appreciably influenced by the existence of Si-K absorption edge. Therefore, the combination of InSb crystal with the soft X-ray undulator was best fit to this experiment.

From consideration of peak width of the diffraction function, resolving power of the crystal monochromator in this low energy soft X-ray region is roughly estimated by number of crystal planes contained within the optical depth.

$$\frac{\lambda}{2 \cdot \Delta\lambda} \approx \frac{D \cdot \sin\theta}{2d} = \frac{D \cdot \lambda}{4d^2} \qquad (8)$$

where, D is the optical depth, d the spacing of the crystal planes and θ the glancing angle of incidence of X-ray beam onto the crystal plane. The absorption cross section in unit of cm^2/g is given by Henke et. al. [5] to be 1.51×10^3 for In and 1.66×10^3 for Sb at $h\nu = 2.042$ keV. The weight density of these metals in unit of g/cm^3 is 7.3 and 6.7, respectively. Therefore, we could estimate for InSb that $D \approx 9000$Å and $D/2d \approx 1200$. Thus, the resolving power of the monochromator ranged around 10^3.

4. Solutions for some problems.

The undulator radiation beam is inevitably accompanied by intense Brems strahlung γ-rays which originate in collision of the circulating electron/positron beam with residual gas atoms in the storage ring and is emitted into the cone as narrow as $1/\gamma$. To make the experiment free from the background γ-rays, the exit beam axis of the monochromator was constantly off-set from the incident beam through the double reflection. Then the γ-rays are stopped by lead blocks placed on axis downstream of the first crystal.

The higher order diffraction was suppressed in some extent by finely detuning the parallelism of the two crystal planes. Since the cross section for generation of M_1 subshell vacancy in Dy is exceedingly small, the effect due to the higher order diffraction must be minimized as far as possible even though the cross section by the higher order diffraction is far smaller than that by the first order diffraction.

An adjustable slit system placed upstream of the first crystal was indispensable to avoid possible degradation of the crystal by heat load due to the intense undulator radiation. The first crystal was always kept cooled during operation of the beamline with a cooling system which was composed of a heat pipe and some radiating fans [4].

Since there was no detection system which could measure directly the high soft X-ray flux such as 10^8 - 10^{12} photons/sec., we devised a combination of a proportional gas counter and some Be absorbers. Attenuation by each absorber was measured directly using the same beamline as will be described in chapter 13 in detail.

References .

[1] H. Maezawa et.al., SPIE Proceedings Vol. **733**, pp. 96-100, 1986.

[2] H. Maezawa et.al., Appl. Opt. **25**(1986)3260-3268.

[3] H. Maezawa et.al., Rev. Sci. Instrum. **60**(1989)1889-1892.

[4] Y. Kitajima et.al., Rev. Sci. Instrum. **63**(1992)886-889.

[5] B. L. Henke et.al., Atomic Data and Nucl. Data tables **27**(1982)1-144.

Chapter 11

Study in the period from 1987 to 1990

S. Yasumi and S. Kishimoto*

Teikyo University/KEK
**Photon Factory, KEK*

$m_{\nu e}$-PF Experiment No. 87-175 was approved in September of 1987.

From February 18th to July 15th of 1989 the experiment was performed. At the BL-2A beam line with a double reflection crystal monochromator made of InSb, fluorescence spectrum measurements for incident monochromatic photons of an energy $E_a = 2.250$ keV, $E_b = 1.944$ keV and $E_c = 1.758$ keV were done with a Si(Li) detector.

Monochromatic photon beams were very intense and its exit beam axis was fixed when rotating the Bragg angle of the crystal monochromator. Therefore we succeeded gathering data of sufficient statistics for a dysprosium target 10 $\mu g/cm^2$ thick.

The intensity of incident photon beams was measured with a photon counter[1)] which consists of proportional counter and a beryllium absorber array as shown in Fig. 3 and 4 of Chap. 13. The proportional counter was filled with Xe or Kr gas admixed with 10 % iso-butane at about 380 Torr. The counter can absorb the total energy of incident photons used in the experiment.

Adjusting the width of the slits and the thickness of the Be absorber array to reduce the intensity of photon beams incident upon the photon counter, we could measure the intensity of incident monochromatic photons by the photon counter simultaneously with measurements of the intensity of fluorescence photons by the Si(Li) detector. That means we could successfully measure the intensity of incident monochromatic photon beams absolutely, using the intensity of fluorescence photons measured with the Si(Li) detector as a reference.

Our method of determining the mass of the electron neutrino using electron capture in ^{163}Ho is based on the assumption that two spectra S_{M1} and S_{M2}, the M X-ray spectra of dysprosium when there is one vacancy in the M_1 and M_2 subshell respectively, are the same for the following two cases*; electron capture in ^{163}Ho and photoionization of Dy atom.

---

* Peak ④ in these spectra should be excluded in the reconstruction of $Sp^{163Ho}(k)$ spectrum.

In order to check the validity of this assumption, the energy of the 5p-3s line was measured for both cases .

The results[2] are

$$E^{EC}_{5p-3s} = 2.005 \pm 0.001 \text{ keV}, \qquad \text{and}$$

$$E^{PI}_{5p-3s} = 2.002 \pm 0.003 \text{ keV}.$$

Thus the energy difference between two cases was found to be less than a few eV, indicating a partial evidence on the validity of the method to measure $m_{\nu e}$.

This result seems to contradict Livermore's result[3], although they used an electron bombardment on Dy atoms.

Next, we tried to do fluorescence spectrum measurements for monochromatic photons of an energy $E_d = 1.504$ keV, $E_e = 1.314$ keV, using the BL-2B beamline with a grazing angle incidence grating monochromator. However, we found that there were unwanted photons of an energy of around 1.6 keV. Therefore we could not perform these experiments.

In September of 1989, Experiment No. 89-200 was approved.

We continued to try to get photon beams having a good quality in the energy range of E_d and E_e. We examined the quality of photon beams passing through a double reflection beryl-crystal monochromator at the BL-2A line. It was found that the quality of these photon beams was far from a good one.

Then we tried again to use the BL-2B line to get monochromatic photons of an energy E_d and E_e. Finally we found* there were some possibilities to suppress unwanted photons around 1.6 keV by adjusting parameters of the undulator device and the monochromator at the BL-2B.

References

1) S. Kishimoto, KEK Report 90-22, 1991, p.19

2) S. Yasumi et al., Nucl. Phys. B (Proc. Suppl.) **16** (1990) 499

3) P. T. Springer et al., Phys. Rev. A**31** (1985) 1965

---

* We appreciate much effort done by A. Yagishita.

Chapter 12

Estimation of Atomic Parameters for Electron Capture Decay of ^{163}Ho

Takeshi Mukoyama
Institute for Chemical Research, Kyoto University,
Uji, Kyoto, 611 Japan

Abstract

The atomic parameters necessary for determination of the rest mass of electron neutrino by electron capture decay of ^{163}Ho have been estimated relativistically with the Dirac-Fock and Dirac-Fock-Slater methods. The obtained results are used for analysis of the measured M-x-ray spectra to estimate the rest mass of electron neutrino.

1 Introduction

The radioactive nuclide, ^{163}Ho, has been considered as the most promising candidate to measure the rest mass of electron neutrino by electron-capture decay. The Q value of capture decay in this nuclide is known to be $2.710^{+0.100}_{-0.005}$ keV.[1] Owing to the smallness of the Q value, the ground state of ^{163}Ho can decay to the ground state of ^{163}Dy only through M- and higher-shell electron capture.

There have been proposed several methods to measure the rest mass of electron neutrino using electron capture decay. The most favorable method among them is to measure the decay rate of electron capture, which depends on the neutrino rest mass, by observing the M-x-ray spectrum. In order to analyze experimental x-ray spectra and to determine the rest mass of electron neutrino, various atomic parameters for Ho and its daughter atom are necessary. The experimental principle for determination of the neutrino rest mass is described elsewhere.[1]

In the case of ^{163}Ho, the decay process predominantly takes place through M_1 capture, but the contributions from the M_2 and higher shells should also been taken into consideration. It is generally accepted that the probability for electron capture decay can be described within the framework of single-electron picture and is proportional to the density of the electron to be captured at the position of the nucleus. In electron capture decay, the nuclear charge decreases

by one and an inner-shell vacancy is produced in the final state. This means that the central potential for atomic electrons in the initial state is different from the potential in the final state and the electron wave functions in the parent atom are no longer orthogonal to those in the daughter atom. Because of the lack of orthogonality of atomic wave functions, the existence of other electrons in atoms should be taken into account in the complete description of electron capture decay of the nucleus. This is known as the exchange and overlap effects in electron capture decay. The correction factors for the exchange and overlap effects in electron capture decay have been studied using various atomic wave functions and compiled in the review article.[2] However, for M and higher shells of Ho no theoretical calculation has been reported, except for only one case for M_1 shell.

When an M-shell vacancy is produced by electron capture of ^{163}Ho, M x rays of the daughter atom, Dy, are emitted. Although M capture takes place only for M_1 and M_2 shells, the vacancy can transfer to other M subshells due to Coster-Kronig transition and practically distribute all over M subshells before x-ray emission. For K- and L-shell vacancy, extensive theoretical calculations for x-ray emission rates have been made, but the calculations for M-subshell vacancy are rather scarce. In the case of Dy, no relativistic calculation has been performed.

The x-ray spectrum with an initial vacancy in M_1 and M_2 shell can be estimated from the vacancy distribution for M_i subshells ($i = 1, \ldots, 5$) and the x-ray fluorescence yield for each M_i subshell. The former is obtained from the Coster-Kronig coefficients and the latter is calculated from the x-ray emission rates and the total level widths for M_i subshells.

The present report is the summary of theoretical estimation for these atomic parameters for Ho and Dy. The exchange and overlap correction factors for Ho[3] and the M_i-shell x-ray emission rates for Dy[4] have been calculated relativistically with the Dirac-Fock-Slater (DFS) method[5] and the Dirac-Fock (DF) method.[6] On the other hand, the Coster-Kronig coefficients and the total level widths for M_i subshells in Dy have been obtained from the tabulated nonrelativistic values by applying the relativistic correction.

2 Exchange and Overlap Correction for Electron Capture

According to the usual theory for orbital electron capture decay, the probability that an electron is captured by the nucleus can be written by[2]

$$\lambda = \frac{G^2 \xi}{2\pi} \sum_i q_i^2 B_i |\psi_i(0)|^2 , \tag{1}$$

where G is the β-decay coupling constant, ξ the appropriate combination of nuclear matrix element, q_i the energy of the neutrino emitted during the i-shell capture, B_i the exchange and overlap correction factor for the i-shell capture, and $|\psi_i(0)|$ the i-shell electron wave function in the parent atom at the nuclear surface. Here the rest mass of the electron neutrino is assumed to be negligibly small.

The exchange and overlap correction factor in Eq. (1) is given by

$$B_i = |f_i/\psi_i(0)|^2 \ , \tag{2}$$

where f_i is called the capture amplitude. Bahcall[7] introduced the simplifying assumptions to calculate f_i that the contributions from other shells are neglected and the existence of the inner-shell hole is not taken into account. His capture amplitude, for example, of $3s$ capture is expressed as

$$\begin{aligned} f_{3s} =& < 1s'|1s >< 2s'|2s > \psi_{3s}(0) \ - \ < 1s'|3s >< 2s'|2s > \psi_{1s}(0) \\ & - \ < 2s'|3s >< 1s'|1s > \psi_{2s}(0) \ , \end{aligned} \tag{3}$$

where $|1s >$ means the $1s$-shell electron wave function in the parent atom and the primed quantity corresponds to the daughter atom. The f_i values for other shells can be defined in the similar manner. In the present work, we modified the Bahcall theory to include all the atomic shells up to $n = 5$, where n is the principal quantum number. Furthermore, the presence of the M-shell vacancy in the daughter atom was taken into consideration.

On the other hand, Vatai[8] used the many-electron wave functions and developed the correction factor including the presence of the vacancy in the daughter atom. He retained only the exchange integral in the form of $< \psi_{\beta'}|\psi_i >$ and neglected all other exchange integrals, $< \psi_{\beta'}|\psi_\beta >$ for $\beta' \neq \beta$. The capture amplitude for $3s$ electron in the Vatai correction is

$$\begin{aligned} f_{3s} \ &= \ \psi_{3s}(0) < 1s'|1s >< 2s'|2s >< 2p'|2p > \cdots \\ &- \ \psi_{1s}(0) < 1s'|3s >< 2s'|2s >< 2p'|2p > \cdots \\ &- \ \psi_{2s}(0) < 1s'|1s >< 2s'|3s >< 2p'|2p > \cdots \\ &- \ \cdots\cdots \ . \end{aligned} \tag{4}$$

We have calculated the exchange and overlap correction factor with the DFS[5] and DF[6] wave functions. The initial state is the ground state of Ho atom, while the final state corresponds to the Dy atom with an M-shell vacancy. The effect of finite nuclear size was taken into consideration by assuming that the proton charge distribution inside the nucleus is given by the Fermi distribution. In the DFS method, the statistical scaling parameter α is taken to be unity.

The calculated results are shown in Table 1. The DFS values are in agreement with the DF ones. This fact suggests that the wave-function effect is not so important. In general, the Vatai correction gives slightly smaller values than the Bahcall correction, but both results are in good agreement with each other.

Table 1: Exchange and overlap correction factors for electron capture decay of Ho atom.

Shell	MB[a]	Bennet[b]	DFS		DF	
			B[c]	V[d]	B	V
K	0.992		0.993	0.993	0.990	0.989
L_1	1.026		1.033	1.031	1.031	1.030
L_2	0.989		0.989	0.986	0.981	0.979
M_1	1.063	1.065	1.089	1.081	1.086	1.083
M_2		0.935	1.039	1.030	1.035	1.031
N_1		1.12	1.166	1.152	1.159	1.151
N_2		0.88	1.121	1.107	1.116	1.108
O_1		1.18	1.225	1.217	1.265	1.248
O_2		0.82	1.257	1.225	1.247	1.224

a) Martin and Blichert-Toft (Ref. 9).
b) Bennet (Ref. 10).
c) Bahcall correction.
d) Vatai correction.

For comparison, other theoretical results are also listed in Table 1. Only one theoretical calculation for Ho atom was made by Martin and Blichert-Toft[9] in the Vatai correction using the DFS wave functions. Their values for K, L_1, $L_{2,3}$, and M_1 shells agree with the present calculations.

Bennett[10] obtained the correction factors for M_1, N_1, and O_1 shells by interpolation and extrapolation from the tabulated values of Bambynek *et al.*[2] Then he assumed that the average of ns and $np_{1/2}$ factors is unity and estimated the values for the M_2, N_2, and O_2 shells. His values for ns shells are in agreement with the present results. However, for $np_{1/2}$ shells the values of Bennett are smaller than unity, while the present values are larger than unity. This indicates that the assumption made by Bennett is invalid.

3 X-Ray Emission Rates

In the first-order perturbation theory, the radiative rate for an electron from a state i to a state f can be written by[11]

$$\Gamma = 2\,\alpha\,k^2 \sum_L \left[f_L(m) + f_L(e)\right] \ . \tag{5}$$

Here $f_L(m)$ and $f_L(e)$ are the oscillator strengths for the L-th magnetic and electric multipoles,

$$f_L(m) = B(-\kappa_i, \kappa_f, L)\, R_L^2(m)/k \ , \tag{6}$$

and

$$f_L(e) = B(\kappa_i, \kappa_f, L)\, R_L^2(e)/k \ , \tag{7}$$

where $B(\kappa_i, \kappa_f, L)$ is the angular coupling coefficient, k is the energy of the photon, κ is the relativistic quantum number, and $R_L(m)$ and $R_L(e)$ are the radial matrix elements. The expressions for angular coupling coefficients and radial matrix elements are given in Ref. 11. All possible multipoles as well as the retardation effect are included in Eq. (5) and relativistic units ($\hbar = m_e = c = 1$) are used.

The radial matrix elements were calculated with the DFS[5] and DF[6] wave functions. The effect of the finite nuclear size was taken into account by assuming the nucleus as a uniformly charged sphere.

There has been used either of two kinds of approximations in the theoretical calculations for x-ray emission rates. The first one is the so-called *frozen-orbital* approximation, where the same atomic potential is used both for the initial and final states. The wave functions for the ground state without any vacancy have been usually employed. All the wave functions are orthogonal with each other, but no allowance for core relaxation due to the existence of a vacancy is taken into account. Based on this approximation, we calculated the M-shell x-ray emission rates for rare earth elements using the DFS wave functions.[12]

After M capture decay, there exists an M_i-shell vacancy in the initial state and it moves to an outer shell after M x rays are emitted. It is more realistic to take into account the presence of the vacancy and to use different atomic potentials for initial and final states. This approximation is called *relaxed-orbital* approximation. Since the atomic potentials should be calculated for different electron configurations in this case, the computation of x-ray emission rates is tedious and time-consuming.

Using these two approximations, we have calculated the M-x-ray emission rates for Dy with the DF wave functions. The obtained results for M_i subshells are listed in Tables 2–6 together with the DFS calculations in the frozen-orbital approximation.[12] It is clear from the table that in the case of allowed (dipole) transitions the DF results in two approximations as well as the DFS values agree with each other. There is more than factor-of-two difference in the following cases; the transitions from N_1 and O_1 shells for M_1-shell x rays, from N_2, N_7, and O_2 shells for M_2-shell x rays, from O_1 and P_1 shells for M_4-shell x rays, and from O_1, O_2, and P_1 shells for M_5-shell x rays. In all these transitions, the contributions from magnetic multipoles are significant.[12] However, these transitions are weak and it can be said that for strong components of M x rays the difference among three methods is small.

Table 2: M_1-shell x-ray emission rates in Dy ($eV/\hbar$).

Shell	DFS[a)]	DF(F)[b)]	DF(R)[c)]
M_2	7.807(-5)[d)]	8.783(-5)	8.537(-5)
M_3	1.150(-3)	1.185(-3)	1.170(-3)
M_4	4.383(-7)	5.054(-7)	4.836(-7)
M_5	8.914(-7)	1.005(-6)	9.651(-7)
N_1	1.029(-9)	1.003(-9)	2.828(-9)
N_2	5.366(-3)	4.971(-3)	4.826(-3)
N_3	6.043(-3)	5.611(-3)	5.372(-3)
N_4	3.253(-5)	3.138(-5)	3.175(-5)
N_5	4.539(-5)	4.400(-5)	4.446(-5)
N_6	9.846(-8)	1.017(-7)	1.249(-7)
N_7	6.543(-8)	6.520(-8)	7.803(-8)
O_1	2.797(-10)	2.549(-10)	4.996(-10)
O_2	7.923(-4)	6.865(-4)	6.663(-4)
O_3	8.944(-4)	7.534(-4)	7.048(-4)
P_1	2.264(-11)	1.799(-11)	2.407(-11)

a) Dirac-Fock-Slater model in frozen-orbital approximation (Ref. 12).
b) Dirac-Fock model in frozen-orbital approximation.
c) Dirac-Fock model in relaxed-orbital approximation.
d) 7.807(-5) means 7.807×10^{-5}.

Table 3: M_2-shell x-ray emission rates in Dy (eV/$\hbar$).

Shell	DFS[a)]	DF(F)[b)]	DF(R)[c)]
M_3	3.008(-8)[d)]	3.073(-8)	3.507(-8)
M_4	2.371(-3)	2.372(-3)	2.293(-3)
M_5	2.670(-10)	3.293(-10)	3.264(-10)
N_1	2.007(-3)	1.935(-3)	1.800(-3)
N_2	3.330(-10)	3.274(-10)	7.084(-10)
N_3	8.471(-6)	8.201(-6)	7.746(-6)
N_4	1.001(-2)	9.124(-3)	8.957(-3)
N_5	2.997(-8)	3.083(-8)	3.303(-8)
N_6	6.125(-5)	5.849(-5)	6.423(-5)
N_7	6.622(-11)	7.401(-11)	1.052(-10)
O_1	3.351(-4)	3.031(-4)	2.840(-4)
O_2	6.853(-11)	6.354(-11)	1.597(-10)
O_3	1.266(-6)	1.194(-6)	7.141(-7)
P_1	2.657(-5)	1.874(-5)	2.593(-5)

a) Dirac-Fock-Slater model in frozen-orbital approximation (Ref. 12).
b) Dirac-Fock model in frozen-orbital approximation.
c) Dirac-Fock model in relaxed-orbital approximation.
d) 3.008(-8) means 3.008×10^{-8}.

Table 4: M_3-shell x-ray emission rates in Dy ($eV/\hbar$).

Shell	DFS[a)]	DF(F)[b)]	DF(R)[c)]
M_4	6.873(-5)[d)]	7.114(-5)	6.757(-5)
M_5	8.823(-4)	8.889(-4)	8.486(-4)
N_1	2.626(-3)	2.524(-3)	2.394(-3)
N_2	4.524(-6)	4.395(-6)	4.227(-6)
N_3	3.941(-6)	3.836(-6)	3.653(-6)
N_4	1.233(-3)	1.132(-3)	1.119(-3)
N_5	9.903(-3)	9.103(-3)	8.965(-3)
N_6	7.375(-6)	7.106(-6)	7.711(-6)
N_7	2.201(-5)	2.039(-5)	2.234(-5)
O_1	4.309(-4)	3.861(-4)	3.813(-4)
O_2	6.638(-7)	6.494(-7)	5.033(-7)
O_3	5.729(-7)	5.400(-7)	3.866(-7)
P_1	3.410(-5)	2.386(-5)	3.360(-5)

a) Dirac-Fock-Slater model in frozen-orbital approximation (Ref. 12).
b) Dirac-Fock model in frozen-orbital approximation.
c) Dirac-Fock model in relaxed-orbital approximation.
d) 6.873(-5) means 6.873×10^{-5}.

Table 5: M_4-shell x-ray emission rates in Dy (eV/$\hbar$).

Shell	DFS[a)]	DF(F)[b)]	DF(R)[c)]
M_5	2.868(-10)[d)]	3.135(-10)	3.501(-10)
N_1	4.678(-7)	4.300(-7)	3.583(-7)
N_2	8.751(-4)	8.194(-4)	7.206(-4)
N_3	1.177(-4)	1.109(-4)	9.251(-5)
N_4	1.499(-6)	1.402(-6)	1.232(-6)
N_5	6.141(-7)	5.766(-7)	4.984(-7)
N_6	1.373(-2)	1.236(-2)	1.267(-2)
N_7	4.103(-9)	4.258(-9)	5.381(-9)
O_1	9.082(-8)	9.647(-8)	2.009(-7)
O_2	1.120(-4)	1.024(-4)	1.319(-4)
O_3	1.452(-5)	1.306(-5)	1.689(-5)
P_1	7.359(-9)	5.747(-9)	1.281(-8)

a) Dirac-Fock-Slater model in frozen-orbital approximation (Ref. 12).
b) Dirac-Fock model in frozen-orbital approximation.
c) Dirac-Fock model in relaxed-orbital approximation.
d) 2.868(-10) means 2.868×10^{-10}.

Table 6: M_5-shell x-ray emission rates in Dy (eV/$\hbar$).

Shell	DFS[a)]	DF(F)[b)]	DF(R)[c)]
N_1	4.342(-7)[d)]	4.107(-7)	3.492(-7)
N_2	4.196(-10)	4.129(-10)	4.199(-10)
N_3	7.634(-4)	7.342(-4)	6.270(-5)
N_4	4.140(-7)	3.954(-7)	3.524(-7)
N_5	1.584(-6)	1.521(-6)	1.340(-6)
N_6	6.441(-4)	5.841(-4)	6.003(-4)
N_7	6.389(-3)	5.557(-3)	5.747(-3)
O_1	8.389(-8)	8.447(-8)	1.815(-7)
O_2	6.525(-11)	7.471(-11)	2.283(-10)
O_3	9.410(-5)	8.345(-5)	1.083(-4)
P_1	6.790(-9)	5.219(-9)	1.176(-8)

a) Dirac-Fock-Slater model in frozen-orbital approximation (Ref. 12).
b) Dirac-Fock model in frozen-orbital approximation.
c) Dirac-Fock model in relaxed-orbital approximation.
d) 4.342(-7) means 4.342×10^{-7}.

4 Fluorescence Yields and Level Widths

When a vacancy is produced in the M_1 shell of Dy by electron capture decay, the intensity of M x rays is given by

$$\begin{aligned} I_1 &= \omega_1 + f_{12}\,\omega_2 + (f_{13} + f_{12}f_{23})\,\omega_3 \\ &+ (f_{14} + f_{12}f_{24} + f_{13}f_{34} + f_{12}f_{23}f_{34})\,\omega_4 \\ &+ (f_{15} + f_{12}f_{25} + f_{13}f_{35} + f_{14}f_{45} + f_{12}f_{23}f_{35} \\ &+ f_{12}f_{24}f_{45} + f_{13}f_{34}f_{45} + f_{12}f_{23}f_{34}f_{45})\,\omega_5 \ , \end{aligned} \tag{8}$$

where ω_i $(i = 1, \ldots, 5)$ is the M_i-subshell fluorescence yield and f_{ij} is the Coster-Kronig coefficient for vacancy transfer from the M_i subshell to the M_j subshell. The subshell fluorescence yield is written by

$$\omega_i = \sum_j \gamma_{ij}/\Gamma_i \ , \tag{9}$$

where Γ_i is the total level width for the M_i subshell, γ_{ij} is the partial radiative width corresponding to the electron transition from the X_j shell to the M_i subshell, and X denotes the shells higher than the M_i subshell.

The M-x-ray intensity for the M_2-subshell vacancy can be written in the similar expression:

$$\begin{aligned} I_2 &= \omega_2 + f_{23}\,\omega_3 + (f_{24} + f_{23}f_{34})\,\omega_4 \\ &+ (f_{25} + f_{23}f_{35} + f_{24}f_{45} + f_{23}f_{34}f_{45})\,\omega_5 \ . \end{aligned} \tag{10}$$

For the M_i subshells in Dy atom, no theoretical calculation of the total level widths and fluorescence yields has been reported. Here we have estimated the f_{ij} and Γ_i values from the nonrelativistic values of McGuire[13] and the relativistic values of Chen *et al.*[14,15] for other elements. First, the nonrelativistic values for Dy were obtained by interpolation from the values of McGuire for $Z = 63$, 67, and 70. Then the relativistic correction factor was obtained as the ratio of the relativistic value of Chen *et al.* to the nonrelativistic value of McGuire for $Z = 67$ in the case of the $M_{1,2,3}$ shells and for $Z = 70$ in the case of the $M_{4,5}$ shells. The correction factor thus obtained was multiplied to the nonrelativistic value of Dy. The Coster-Kronig coefficients and the total level widths of M subshells estimated in the present work are listed in Table 7. For γ_{ij} values, we use the x-ray emission rates calculated in the previous section.

5 Conclusion

We have calculated the atomic parameters necessary for determination of the rest mass of electron neutrino by electron capture decay of ^{163}Ho. These parameters are used to analyze the experimental M-x-ray spectra from the decay of ^{163}Ho and fluorescence spectra of Dy atom excited by synchrotron radiation.

Table 7: M-shell Coster-Kronig coefficients, f_{ij} and level widths, Γ_i for Dy

Coefficient	f_{ij}	Level width	Γ_i (eV)
f_{12}	0.307	Γ_1	14.94
f_{13}	0.599	Γ_2	9.04
f_{14}	0.085	Γ_3	9.27
f_{15}	0.116	Γ_4	1.81
		Γ_5	1.24
f_{23}	0.091		
f_{24}	0.665		
f_{25}	0.141		
f_{34}	0.149		
f_{35}	0.747		
f_{45}	0.348		

In the present work, we have used the relaxed-orbital approximation for x-ray emission rates. In this case, the atomic wave functions in the initial states are not orthogonal to those in the final state. This fact suggests that the exchange and overlap effects similar to the case of the electron capture decay be appreciable. The importance of these effects in K- and L-x-ray emission rates has already been pointed out by Scofield.[16,17] More elaborate calculations for M-x-ray emission rates including these effects would be very useful.

There has been reported no theoretical calculation for the Coster-Kronig coefficients and total level widths for M subshells in Dy. It is hoped that the relativistic calculations of the Auger transition probabilities (including the Coster-Kronig transitions) for M subshells be performed in near future.

References

1. S. Yasumi, H. Maezawa, K. Shima, Y. Inagaki, T. Mukoyama, T. Mizogawa, K. Sera, S. Kishimoto, M. Fujioka, K. Ishii, T. Omori, G. Izawa, and O. Kawakami, Phys. Letters B **334**, 229 (1994).

2. W. Bambynek, H. Behrens, M. H. Chen, B. Crasemann, M. L. Fitzpatrick, K. W. D. Ledingham, H. Genz, M. Mutterer, and R. L. Intemann, Rev. Mod. Phys. **49**, 78 (1977).

3. T. Mukoyama, Bull. Inst. Chem. Res., Kyoto Univ. **65**, 17 (1987).

4. T. Mukoyama, Bull. Inst. Chem. Res., Kyoto Univ. **66**, 624 (1989).

5. D. Liberman, J. T. Waber, and D. T. Cromer, Phys. Rev. **A137**, 27 (1970).

6. J. P. Desclaux, Comp. Phys. Commun. **9**, 31 (1975).

7. I. N. Bahcall, Phys. Rev. **129**, 2683 (1963).

8. E. Vatai, Nucl. Phys. **A165**, 541 (1970).

9. M. J. Martin and P. H. Blichert-Toft, Nucl. Data **8**, 1 (1970).

10. C. L. Bennett, in *Neutrino Mass and Low Energy Weak Interactions, Telemark, 1984*, ed. by V. Barger and D. Cline (World Scientific, Singapore, 1985), p. 128.

11. J. H. Scofield, Phys. Rev. **179**, 9 (1969).

12. T. Mukoyama and H. Adachi, J. Phys. Soc. Jpn **53**, 984 (1984).

13. E. J. McGuire, Phys. Rev. A **5**, 1043 (1972).

14. M. H. Chen, B. Crasemann, and H. Mark, Phys. Rev. A **21**, 449 (1980).

15. M. H. Chen, B. Crasemann, and H. Mark, Phys. Rev. A **27**, 2989 (1983).

16. J. H. Scofield, Phys. Rev. A **9**, 1041 (1974).

17. J. H. Scofield, Phys. Rev. A **10**, 1507 (1974).

Chapter 13

Study in the period from 1991 to 1995

S. Yasumi and H. Maezawa*

Teikyo University/KEK
**Photon Factory, KEK*

$m_{\nu e}$-PF Experiment No. 91-272 was approved in October of 1991.

The method to derive the S_{M1} and S_{M2} spectra using equation (3) in Chapter 6, does not include any approximation, but is rather complicated. If we use undulator photon beams for the incident photons, the spectra S_{M3}, S_{M4} and S_{M5} might have some angular distributions[1], because the incident photon beam is almost completely polarized in the horizontal plane. Furthermore, for the time being, there is no way of producing a monochromatic photon beam of good enough quality whose energy lies in the energy range between ~1.2 and ~1.6keV. In fact the latter has been a main bottleneck for our $m_{\nu e}$-study.

Therefore we began to seek a new method to determine the S_{M1} and S_{M2} spectra of Dy without using incident photons of an energy below 1.6 keV.

After a lot of discussions we found the following method[2].

Let us take $E_{M1}+\Gamma_1/2$ for Ea and $E_{M1}-\Gamma_1/2$ and $E_{M1}-3\Gamma_1/2$ in equation (3) of Chapter 6, then the equation becomes

$$\begin{aligned} S_{E_{M1}+\Gamma_1/2} = c\{&\sigma_1(E_{M1}+\Gamma_1/2)\cdot S_{M1}+\sigma_2(E_{M1}+\Gamma_1/2)\cdot S_{M2} \\ &+\sigma_3(E_{M1}+\Gamma_1/2)\cdot S_{M3}+\sigma_4(E_{M1}+\Gamma_1/2)\cdot S_{M4} \\ &+\sigma_5(E_{M1}+\Gamma_1/2)\cdot S_{M5}\}, \end{aligned} \tag{1}$$

$$\begin{aligned} S_{E_{M1}-\Gamma_1/2} = c\{&\sigma_2(E_{M1}-\Gamma_1/2)\cdot S_{M2} \\ &+\sigma_3(E_{M1}-\Gamma_1/2)\cdot S_{M3}+\sigma_4(E_{M1}-\Gamma_1/2)\cdot S_{M4} \\ &+\sigma_5(E_{M1}-\Gamma_1/2)\cdot S_{M5}\}, \end{aligned} \tag{2}$$

$$
\begin{aligned}
S_{E_{M1}-3\Gamma_1/2} = c\{ & \sigma_2(E_{M1}-3\Gamma_1/2)\cdot S_{M2} \\
& +\sigma_3(E_{M1}-3\Gamma_1/2)\cdot S_{M3}+\sigma_4(E_{M1}-3\Gamma_1/2)\cdot S_{M4} \\
& +\sigma_5(E_{M1}-3\Gamma_1/2)\cdot S_{M5}\}
\end{aligned} \tag{3}
$$

where c ≡ Nm and N is assumed to be normalized.

Subtracting equation (2) from equation (1), we have

$$
\begin{aligned}
& S_{E_{M1}+\Gamma_1/2} - S_{E_{M1}-\Gamma_1/2} \\
& = c\left\{\sigma_1(E_{M1}+\Gamma_1/2)\cdot S_{M1} + \left[\sigma_2(E_{M1}+\Gamma_1/2)-\sigma_2(E_{M1}-\Gamma_1/2)\right]\cdot S_{M2}+\cdots\right\} \\
& = c\left\{\sigma_1(E_{M1}+\Gamma_1/2)\cdot S_{M1} + \left[\left.\frac{d\sigma_2}{dE}\right|_{E=E_{M1}} \times \Gamma_1\right]\cdot S_{M2}+\cdots\right\}
\end{aligned} \tag{4}
$$

Next, subtracting equation (3) from equation (2), we have

$$
\begin{aligned}
& S_{E_{M1}-\Gamma_1/2} - S_{E_{M1}-3\Gamma_1/2} \\
& = c\left\{\left[\sigma_2(E_{M1}-\Gamma_1/2)-\sigma_2(E_{M1}-3\Gamma_1/2)\right]\cdot S_{M2}+\cdots\right\} \\
& = c\left\{\left[\left.\frac{d\sigma_2}{dE}\right|_{E=E_{M1-\Gamma_1}} \times \Gamma_1\right]\cdot S_{M2}+\cdots\right\}
\end{aligned} \tag{5}
$$

Finally we subtract equation (5) from equation (4),

$$
\begin{aligned}
& S_{E_{M1}+\Gamma_1/2} - S_{E_{M1}-\Gamma_1/2} - \left(S_{E_{M1}-\Gamma_1/2} - S_{E_{M1}-3\Gamma_1/2}\right) \\
& = c\left\{\sigma_1(E_{M1}+\Gamma_1/2)\cdot S_{M1} + \left[\left(\left.\frac{d\sigma_2}{dE}\right|_{E=E_{M1}} \times \Gamma_1\right) - \left(\left.\frac{d\sigma_2}{dE}\right|_{E=E_{M1-\Gamma_1}} \times \Gamma_1\right)\right]\cdot S_{M2}+\cdots\right\}
\end{aligned}
$$

$$= c\left\{\sigma_1\left(E_{M1}+\Gamma_1/2\right)\cdot S_{M1}+\left(\left.\frac{d^2\sigma_2}{dE^2}\right|_{E=E_{M1}-\Gamma_1/2}\times\Gamma_1^{\,2}\right)\cdot S_{M2}+\cdots\right\}$$

$$= c\sigma_1\left(E_{M1}+\Gamma_1/2\right)\left\{S_{M1}+\frac{1}{\sigma_1\left(E_{M1}+\Gamma_1/2\right)}\sum_{i=2}^{5}\left(\left.\frac{d^2\sigma_i}{dE^2}\right|_{E=E_{M1}-\Gamma_1/2}\times\Gamma_1^{\,2}\right)\cdot S_{Mi}\right\} \tag{6}$$

Taking into account of the energy dependence of σ_i, it can be shown that all coefficients of S_{Mi} (i = 2 - 5) in equation (6) are negligibly small. Therefore, with good approximation, equation (6) becomes,

$$S_{E_{M1}+\Gamma_1/2}+S_{E_{M1}-3\Gamma_1/2}-2S_{E_{M1}-\Gamma_1/2}$$

$$= c\sigma_1\left(E_{M1}+\Gamma_1/2\right)\cdot S_{M1} \tag{7}$$

$$\therefore S_{M1}=\frac{S_{E_{M1}+\Gamma_1/2}+S_{E_{M1}-3\Gamma_1/2}-2S_{E_{M1}-\Gamma_1/2}}{c\sigma_1\left(E_{M1}+\Gamma_1/2\right)}$$

Similarly, using three fluorescence spectrum measurement with monochromatic photons whose energies are $E_{M2}+\Gamma_2/2$ $E_{M2}-\Gamma_2/2$, and $E_{M2}-3\Gamma_2/2$, we have

$$S_{M2}=\frac{S_{E_{M2}+\Gamma_2/2}+S_{E_{M2}-3\Gamma_2/2}-2S_{E_{M2}-\Gamma_2/2}}{c\sigma_2\left(E_{M2}+\Gamma_2/2\right)} \tag{8}$$

After the March-run of Experiment No., 91-272, based on this method, the last experiment of No. 91-272 was performed in December of 1992 and in February of 1993.

Experiments on ^{163}Ho

A photon spectrum from the ^{163}Ho source (No. 3) was measured in vacuum with a Si(Li) detector (ORTEC) having a Be window 0.3 mil thick (nominal)[3] as shown in Fig. 1. The production of ^{163}Ho using ^{164}Dy (p, 2n) ^{163}Ho reaction and the preparation of ^{163}Ho sources at Tohoku University are described in Chapters 2, 3 and 4 of this report.

The whole apparatus was shielded with lead 100 mm thick. The measuring time was 28.89 days (2.496 x 10^6s). The geometry of the Si(Li) detector, including

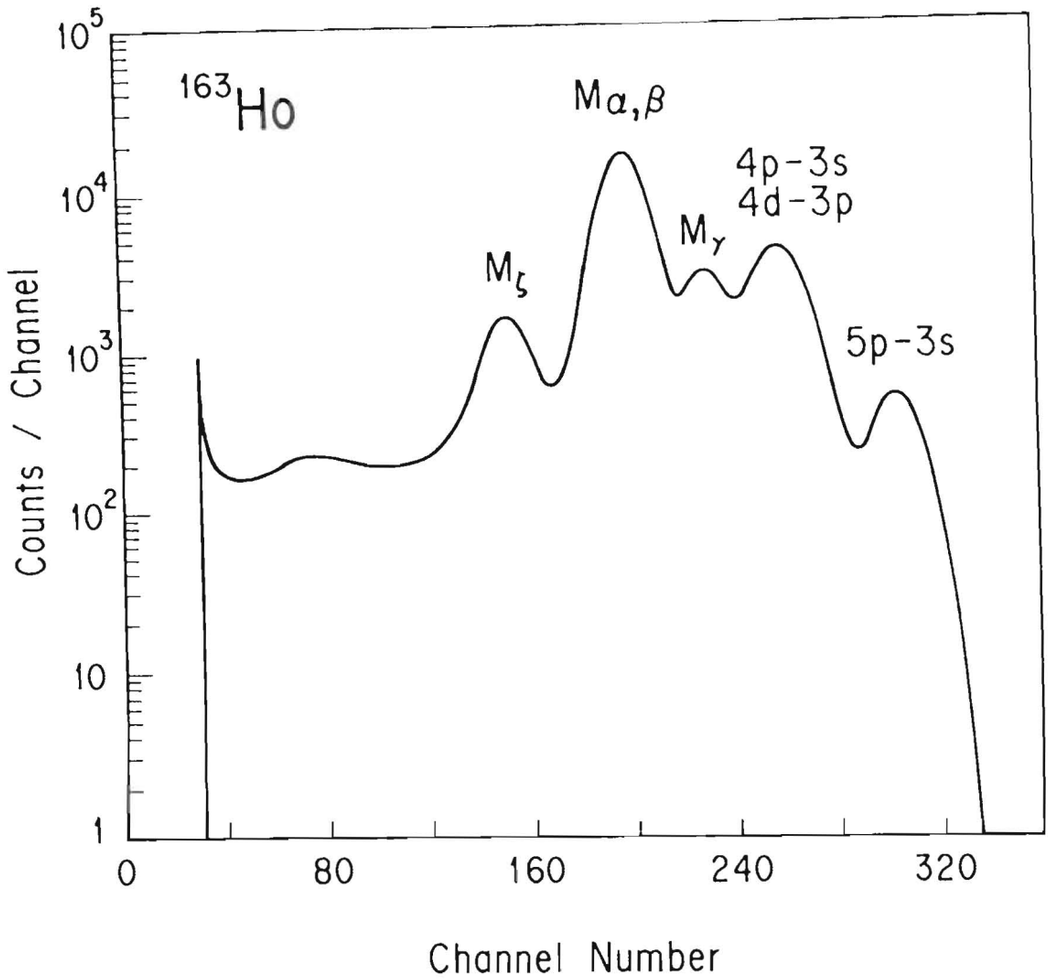

Fig.1 Photon spectrum from the ^{163}Ho source.

the effective area of a silicon crystal and the solid angle was carefully measured using several radioactive sources[4]. The solid angle thus estimated, was 0.09057 ± 0.00464 steradians.

The thickness of the Be window of the Si(Li) detector was also checked by comparing a photon spectrum measured using this detector with that measured using a windowless Si(Li) detector (HORIBA, Japan)[5].

The total number of ^{163}Ho atoms in the ^{163}Ho source, N_o, was measured at University of Tokyo with isotope-dilution mass spectrometry to be

$$N_o = (6.481 \pm 0.012) \times 10^{15} \text{ atoms}$$ [3],

which is in good agreement with the previous value determined by the PIXE method[7] within experimental uncertainties.

The Sp^{163Ho} spectrum in equation (1) of Chap. 6 is obtained from the ^{163}Ho spectrum, $^{163}Ho(k)$, as follows,

$$Sp^{163Ho}(k) = {}^{163}Ho(k) \times \frac{4\pi sr.}{0.09057 sr. \times 2.496 \times 10^{6} s \times 6.481 \times 10^{15} atoms}$$

$$= {}^{163}Ho(k) \times 8.577 \times 10^{-21} \quad [s^{-1} . atom^{-1}]. \qquad (9)$$

In the reconstruction of Sp^{163Ho} spectrum with the S_{M1} and S_{M2} spectra using equation (1) of Chap. 6, it is necessary that each peak in Sp^{163Ho} spectrum is corrected for the self-absorption due to the ^{163}Ho source itself.

Experiments on Dy

At first it is necessary to know the values of the binding energies of M_1 and M_2 sublevels of Dy atom and their total level widths, Γ_1 and Γ_2.

In order to observe M_1 and M_2 absorption edges, we measured the absorption curve of photons for dysprosium atom using a Dy-absorber 900 $\mu g/cm^2$ thick and an electron multiplier (Hamamatsu R 595) as a photon intensity monitor.

Then M_2 edge was clearly observed, but M_1 edge could not be observed.

T. Mizogawa proposed a method to observe M_1-edge, which utilizes the fact that the ratio of peak ② to peak ④ in a M-fluorescence spectrum of Dy changes almost in proportion to the excitation of M_1 sublevel, when changing the energy of incident photons in the energy range of about 100 eV around E_{M1} energy. Similarly, for M_2-edge, we can use the ratio of peak ② to peak ③.

Using Mizogawa's method, the binding energies of M_1 and M_2 sublevels and their total level widths were determined as follows:

$E_{M1} = 2.045$ keV, $\Gamma_1 = 50$ eV;

$E_{M2} = 1.843$ keV, $\Gamma_2 = 11$ eV.

From these data, we decided to take six energies [6] as indicated in Table 1 for energies of incident photons used for fluorescence spectrum measurements.

Table 1

$E_{M1} + \Gamma_1/2$	$E_{M1} - \Gamma_1/2$	$E_{M1} - 3\Gamma_1/2$
2.070 keV	2.020 keV	1.970 keV
$E_{M2} + \Gamma_2/2$	$E_{M2} - \Gamma_2/2$	$E_{M2} - 3\Gamma_2/2$
1.848 keV	1.837 keV	1.826 keV

An experimental setup of fluorescence spectrum measurements on dysprosium atoms is shown in Fig. 2 [6]. Undulator radiations from the BL-2A line of the 2.5 GeV Photon Factory Storage Ring at KEK were monochromated with a double reflection crystal (InSb) monochromator and directed onto a Dy target. The Dy target consists of Dy metal 10μg/cm^2 thick evaporated on a mylar sheet 0.1 mil thick. The target was set at an angle of 45 degrees to the direction of the incident photon beam as shown in Fig. 2.

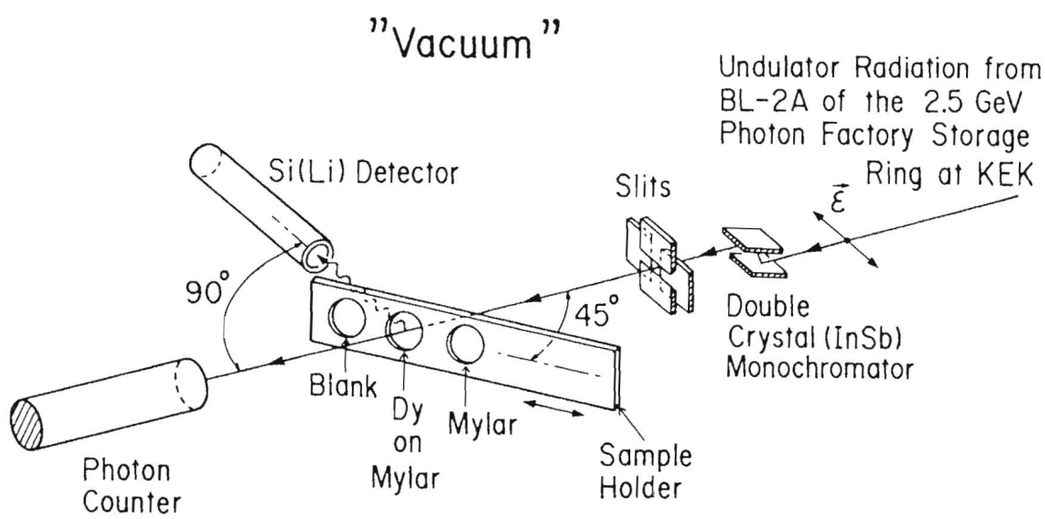

Fig.2 Experimental setup of the fluorescence spectrum measurement of the dysprosium atom.

The intensity of incident photon beams was measured with a photon counter which consists of a proportional counter and a Be-absorber array as shown in Fig. 3 [8] and Fig. 4 [8].

The proportional counter whose schematic diagram is shown in Fig. 4, was filled with Kr gas admixed with 10% iso-butane at about 380 Torr. Electrons liberated by incident photons migrate in the drift region by an electric field and enter

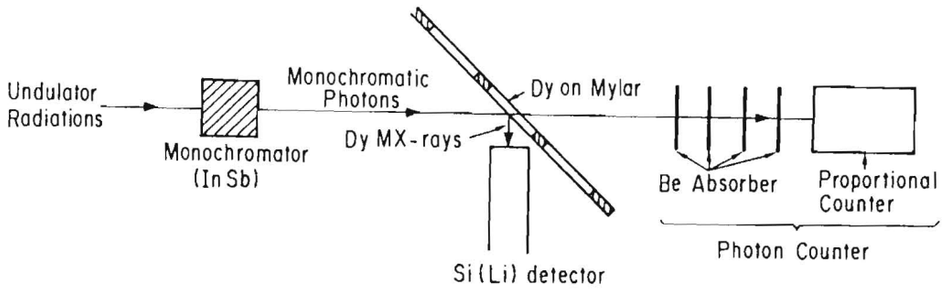

Fig. 3 Schematic diagram of the photon counter

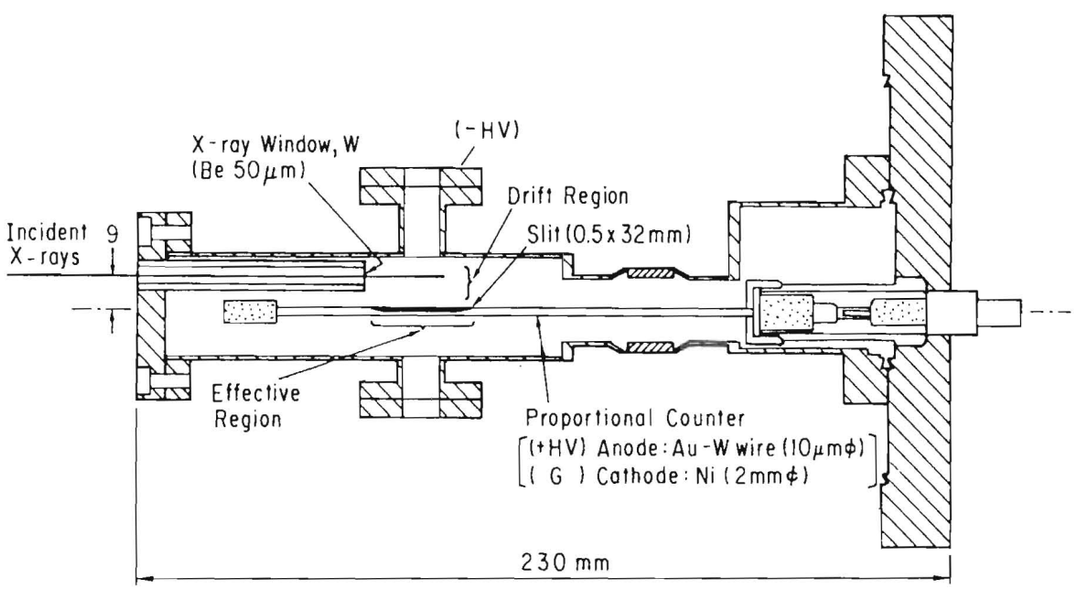

Fig. 4 Proportional counter.

into the proportional counter 2 mm in diameter passing through a slit located on the wall of the counter. The counter can absorb the total energy of incident photons in the energy region of the present experiment.

Fluorescence M X-rays emitted from the Dy target at 90° to the direction of the incident beam in a horizontal plane, were measured with the same Si(Li) detector* as what was used for measuring the photon spectrum from the ^{163}Ho source. It should be noted that elastic scattering could be largely suppressed in the direction of the Si(Li) detector, because the undulator photon beam is almost completely polarized in this direction as is shown in Fig. 2.

Fluorescence spectra of Dy were measured for incident photons of six energies indicated in Table 1. Some of these fluorescence spectra, S_E, are shown in Fig. 5 - Fig. 12, together with spectra subtracted their elastic parts, S_E^{-El}, using the response functions measured by our group [9].

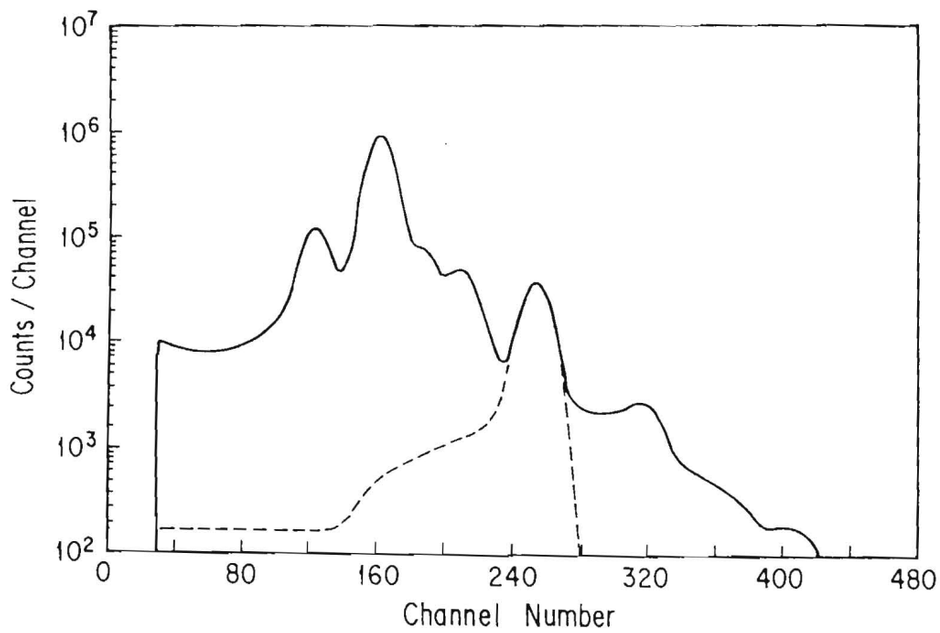

Fig. 5 Fluorescence spectrum of Dy for incident photons of an energy 2.070 keV, $S_{2.070}$. The broken curve shows the elastic part fitted by the response function.

* This fact gives a merit in the reconstruction of Sp^{163Ho} spectrum.

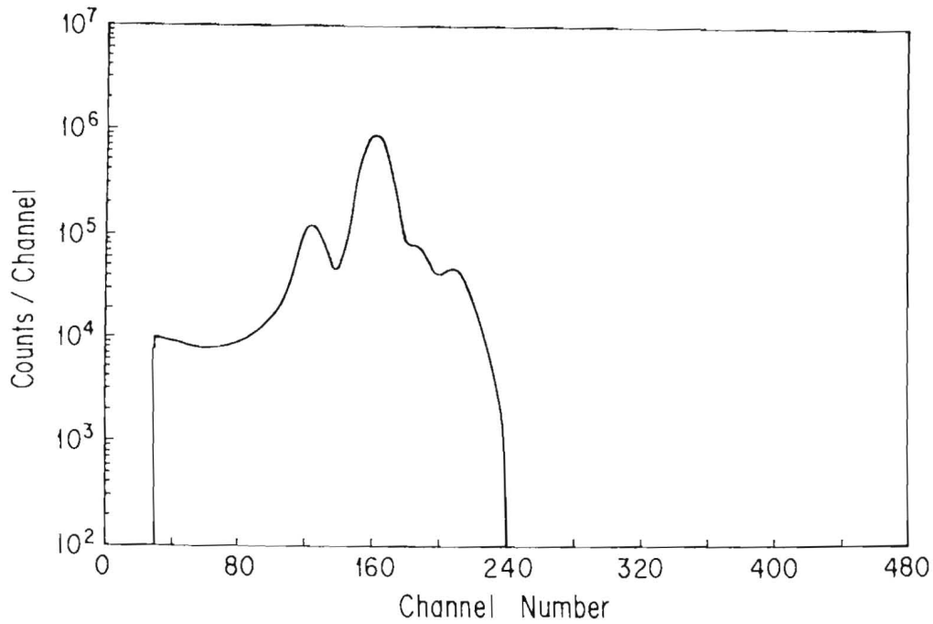

Fig. 6 Fluorescence spectrum of Dy for incident photons of an energy 2.070 keV subtracted its elastic part from $S_{2.070}$, $S_{2.070}^{-El}$.

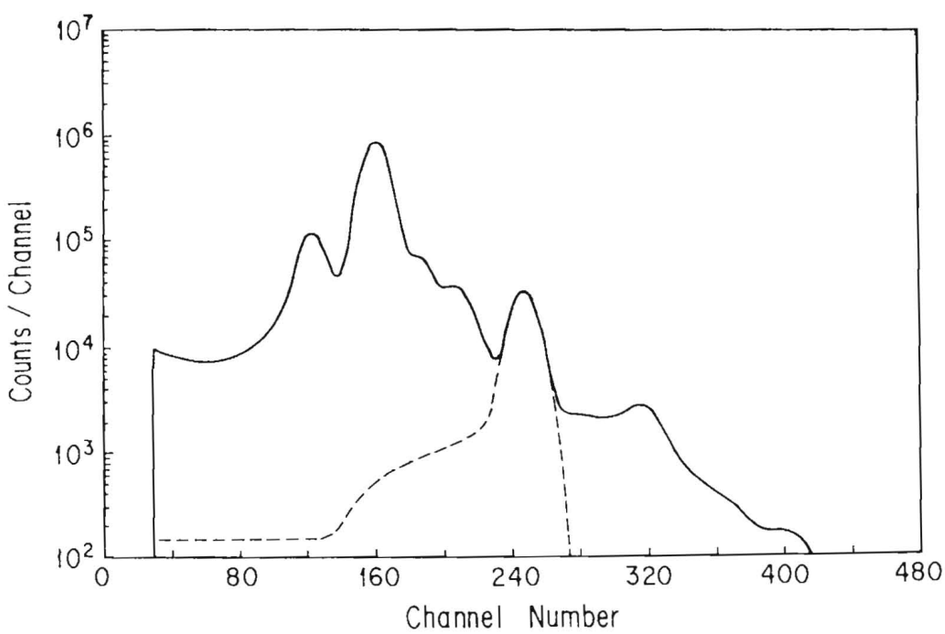

Fig. 7 Fluorescence spectrum of Dy for incident photons of an energy 2.020 keV, $S_{2.020}$. The broken curve shows the elastic part fitted by the response function.

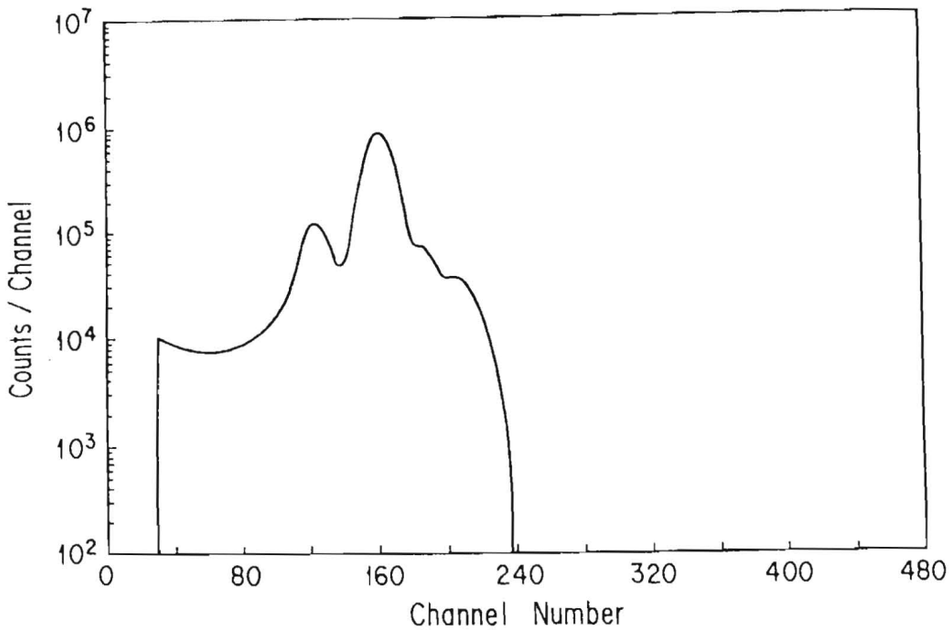

Fig. 8 Fluorescence spectrum of Dy for incident photons of an energy 2.020 keVsubtracted its elastic part from $S_{2.020}$, $S_{2.020}^{-El}$.

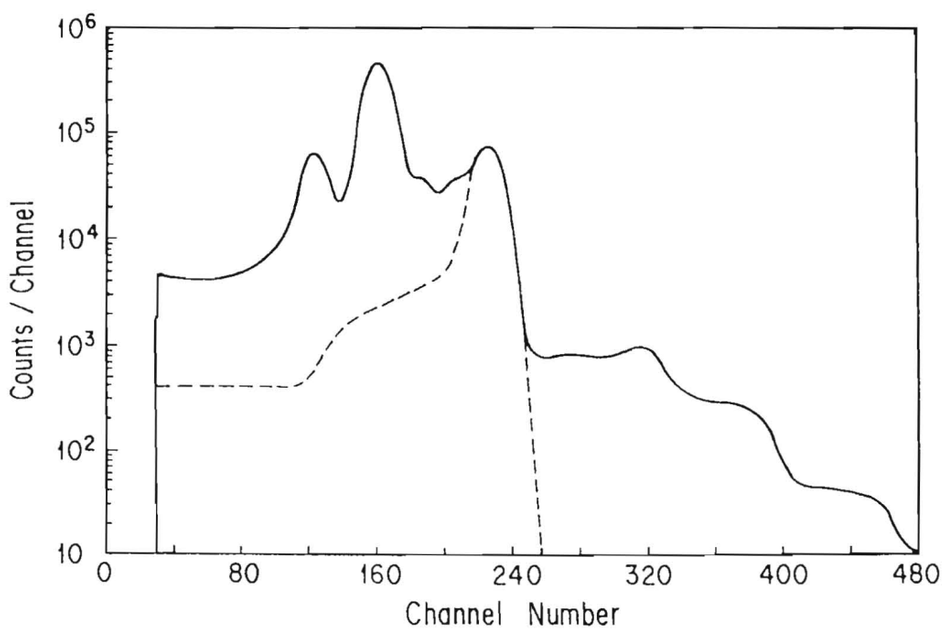

Fig. 9 Fluorescence spectrum of Dy for incident photons of an energy 1.848 keV, $S_{1.848}$. The broken curve shows the elastic part fitted by the response function.

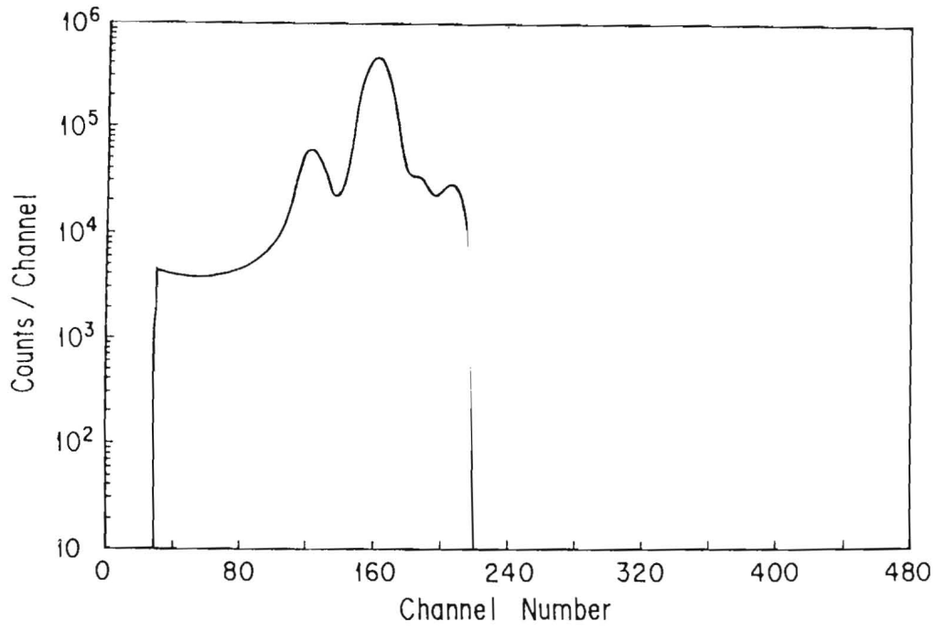

Fig. 10 Fluorescence spectrum of Dy for incident photons of an energy 1.848 keV subtracted its elastic part from $S_{1.848}$, $S_{1.848}^{-El}$.

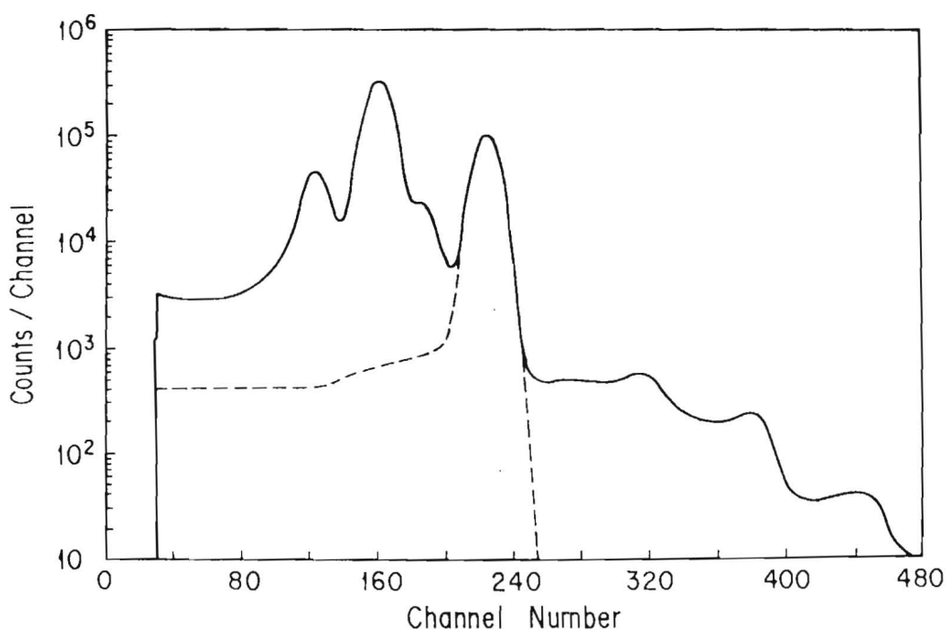

Fig. 11 Fluorescence spectrum of Dy for incident photons of an energy 1.826 keV, $S_{1.826}$. The broken curve shows the elastic part fitted by the response function.

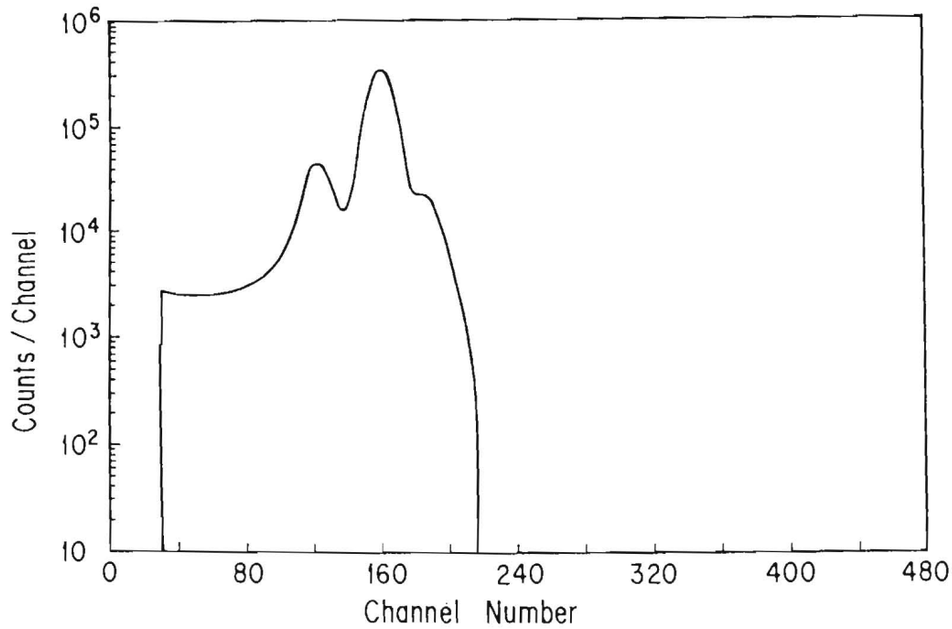

Fig. 12 Fluorescence spectrum of Dy for incident photons of an energy 1.826 keV subtracted its elastic part from $S_{1.826}$, $S_{1.826}^{-El}$.

Next, we move to a measurement of the total number of incident photons for each fluorescence measurement, N.

Adjusting the width of the slits in Fig. 2 and the thickness of the Be absorber array in Fig. 3 to reduce the intensity of photon beams incident upon the proportional counter, we could measure the intensity of incident monochromatic photons by the photon counter simultaneously with a measurement of the intensity of fluorescence photons by the Si(Li) detector. (Hereafter such a measurement is called "simultaneous measurement".) Typical photon spectra obtained with the photon counter are shown in Fig. 13 and Fig. 14.

This simultaneous measurement for incident photon beams of six energies gives us the number of incident photons counted with the photon counter divided by the number of corresponding fluorescence photons counted with the Si(Li) detector, $n^{p/s}$.

We also measured the attenuation or transmission due to each Be absorber used in the simultaneous measurements by comparing $n^{p/s}$ values for appropriate combination of Be absorbers as is shown in Table 2.

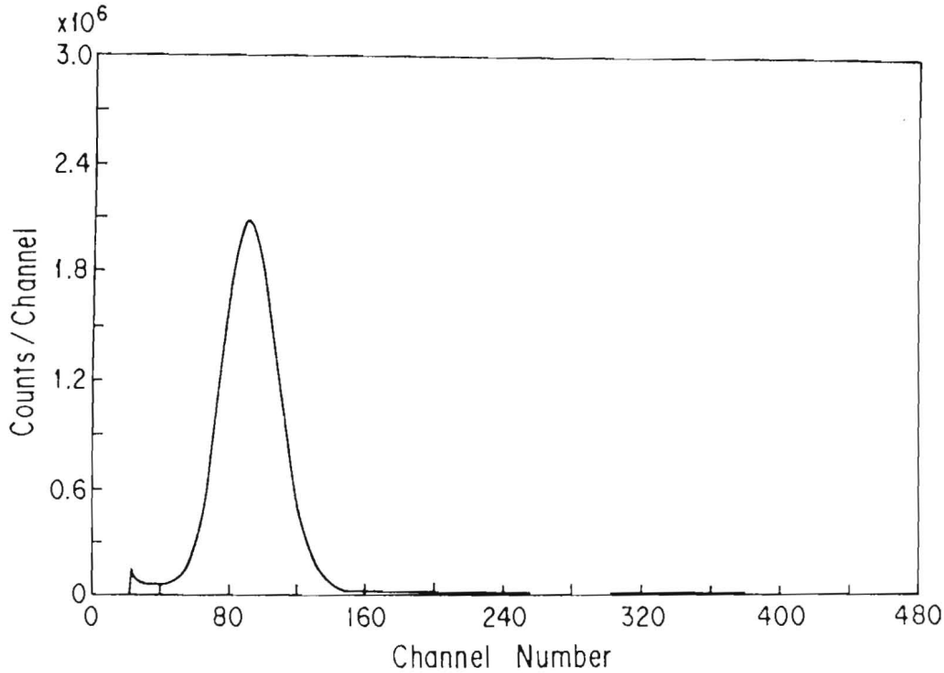

Fig. 13 Spectrum of incident photons of an energy 2.070 keV measured by the photon counter with a Be absorber 700 μm thick.

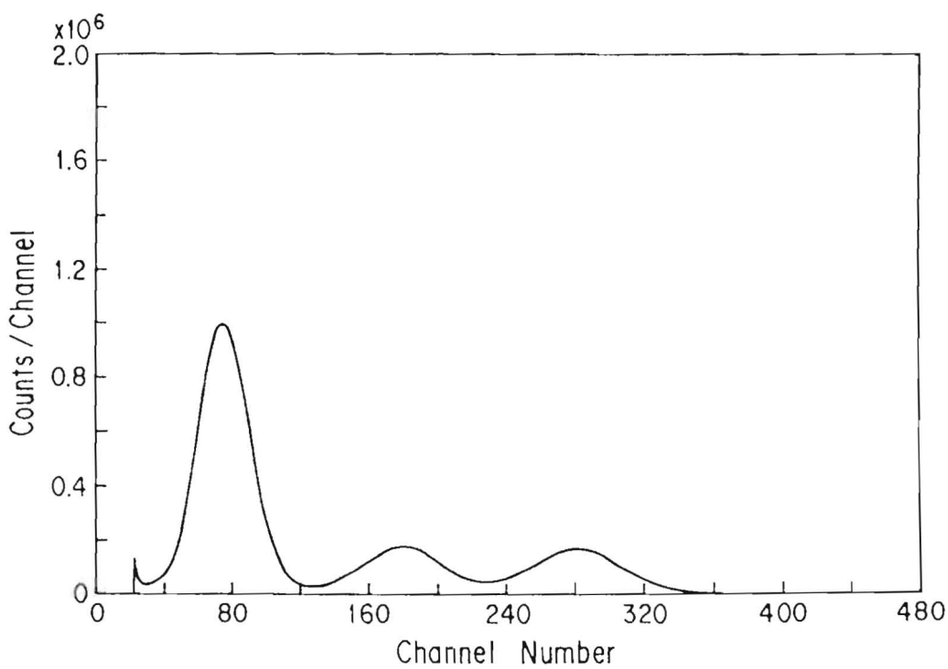

Fig. 14 Spectrum of incident photons of an energy 1.848 keV measured by the photon counter with a Be absorber 500 μm thick. Around Channel #180 and #280, photons from higher order diffractions are seen. However, taking account of the Be absorber, it is estimated that the intensity of these photons was negligibly low comparing with that of the photons of an energy 1.848 keV.

Table 2

Photon Energy keV	Absorber Au	bu	Bd	T_{Be} x 10^{-4}
2.070	0.127616	0.124797	0.0374495	5.96423
2.020	0.108517	0.105934	0.0289142	3.32388
1.970	0.0906923	0.0883611	0.0217157	1.74023
1.848	0.0535904	--	0.00938042	5.02700
1.837	0.0507395	--	0.00859694	4.36205
1.826	0.0479751	--	0.00786183	3.77172

In the Table, Au, bu and Bd are names of absorbers. For M_1, absorbers Au, bu and Bd were used, while absorbers Au and Bd were used for M_2. T_{Be} denotes the total attenuation due to the Be absorber array, namely

$$T_{Be} \text{ for } M_1 = T_{Au} \cdot T_{bu} \cdot T_{Bd},$$

and

$$T_{Be} \text{ for } M_2 = T_{Au} \cdot T_{Bd}.$$

Similarly the attenuation due to the X-ray window, W, in Fig. 4 and the Dy target were measured.

The total number of incident monochromatic photons which irradiated the Dy target during each fluorescent measurement, N, can be obtained by the equation

$$N = n^{p/s} \div (T_{Be} \times T_w \times T_T) \times [\text{ Integral counts with the Si(Li) detector}]$$

, where T_w and T_T stand for the attenuation due to the X-ray window of the photon counter and the Dy target, respectively.

The results are summarized in Table 3. In Table 3, normalization factors f_i^{Mi} are also indicated, where the number N for E = 2.070 keV and the number N for E = 1.848 keV are taken as a standard in the M_1 energy region and in the M_2 energy region, respectively.

Table 3 a)

	T				$n^{p/s}$	$n_o^{p/s}$ c)	Integral d) counts	N	f_i^{Mi}
	T_{Be}	T_w	T_T	T_{total} b)					
keV	x 10^{-4}			x 10^{-4}		x 10^7		x 10^{14}	
2.070	5.96423	0.565097	0.844964	2.84784	5881.62	2.06529	22,583,390	4.66412	1
2.020	3.32388	0.540262	0.837117	1.50327	3147.61	2.09385	21,756,187	4.55542	1.02386 (f_1^{M1})
1.970	1.74023	0.514043	0.826434	0.739289	1485.51	2.00937	15,020,389	3.01815	1.54536 (f_2^{M1})
1.848	5.02700	0.444278	0.796309	1.77759	3083.51	1.73465	10,586,405	1.83637	1
1.837	4.36205	0.437596	0.796011	1.51944	2904.45	1.91153	8,432,569	1.61191	1.13925 (f_1^{M2})
1.826	3.77172	0.430852	0.792950	1.28859	2619.42	2.03279	7,381,886	1.50058	1.22377 (f_2^{M2})

Remarks:

a) All figures are corrected for the dead time.

b) $T_{total} = T_{Be} \times T_w \times T_T$

c) $n_o^{p/s} = n^{p/s} \div T_{total}$

d) Integral counts for M_1 were taken for a channel interval between #100 and #227, and integral counts for M_2 were taken for a channel interval between #100 and #202.

During the data analysis we found the method to determine S_{M1} and S_{M2} spectra (equations (7) and (8)) did not work very well.

Investigating an origin of the above trouble, we finally reached the following method[6]. We take $E_{M1} + \Delta_1$ for E_a and $E_{M1} - \Delta_1'$ for E_b in equation (3) of Chap. 6, where Δ_1 and Δ_1' are assumed to be comparable with the level width of the M_1 subshell.

Then the above equation becomes,

$$\begin{aligned} S_{E_{M1}+\Delta_1} = c[&\sigma_1(E_{M1}+\Delta_1)\cdot S_{M1} + \sigma_2(E_{M1}+\Delta_1)\cdot S_{M2} \\ &+\sigma_3(E_{M1}+\Delta_1)\cdot S_{M3} + \sigma_4(E_{M1}+\Delta_1)\cdot S_{M4} \\ &+\sigma_5(E_{M1}+\Delta_1)\cdot S_{M5}] \end{aligned} \tag{10}$$

$$S_{E_{M1}-\Delta_1'} = c[\sigma_2\left(E_{M1}-\Delta_1'\right)\cdot S_{M2}$$

$$+\sigma_3\left(E_{M1}-\Delta_1'\right)\cdot S_{M3}+\sigma_4\left(E_{M1}-\Delta_1'\right)\cdot S_{M4} \qquad (11)$$

$$+\sigma_5\left(E_{M1}-\Delta_1'\right)\cdot S_{M5}]$$

where c ≡ Nm and N is normalized.

Photoionization cross sections for the Mi subshell, $\sigma_i(E)$, can be represented by the power law $\sigma i(E) = \alpha_i E^{-\beta i}$ (i = 1 - 5). We assume that all β_i in this equation are equal to two*. Then Equations (10) and (11) become

$$S_{E_{M1}+\Delta_1} = c\sigma_1\left(E_{M1}+\Delta_1\right)\cdot S_{M1}$$

$$+c\left(E_{M1}+\Delta_1\right)^{-2} \qquad (12)$$

$$\times[\alpha_2\cdot S_{M2}+\alpha_3\cdot S_{M3}+\alpha_4\cdot S_{M4}+\alpha_5\cdot S_{M5}],\cdots$$

and

$$S_{E_{M1}-\Delta_1'} = c\left(E_{M1}-\Delta_1'\right)^{-2}$$

$$\times[\alpha_2\cdot S_{M2}+\alpha_3\cdot S_{M3}+\alpha_4\cdot S_{M4}+\alpha_5\cdot S_{M5}],\cdots \qquad (13)$$

respectively. We multiply Eq (13) by $[(E_{M1} - \Delta_1')/(E_{M1} + \Delta_1)]^2$, then we have

$$\left(\frac{E_{M1}-\Delta_1'}{E_{M1}+\Delta_1}\right)^2\cdot S_{E_{M1}-\Delta_1'} = c\left(E_{M1}+\Delta_1\right)^{-2}$$

$$\times[\alpha_2\cdot S_{M2}+\alpha_3\cdot S_{M3}+\alpha_4\cdot S_{M4}+\alpha_5\cdot S_{M5}] \qquad (14)$$

---

* The power law-least squares fitting for partial photoionization cross sections showed that the exponents β_i are distributed in the range 1.58-2.85. Taking account that the Δ_i and Δ_i' are comparatively small, it can be estimated that this approximation introduces a systematic error of less than 1.5%.

Subtracting Eq(14) from Eq(13), we get

$$S_{E_{M1}+\Delta_1} - \left(\frac{E_{M1}-\Delta_1'}{E_{M1}+\Delta_1}\right)^2 \cdot S_{E_{M1}-\Delta_1'}$$

$$= c\sigma_1\left(E_{M1}+\Delta_1\right)\cdot S_{M1}$$

Finally we have

$$S_{M1}(k) = \frac{S_{E_{M1}+\Delta_1}(k) - \left(\frac{E_{M1}-\Delta_1'}{E_{M1}+\Delta_1}\right)^2 \cdot S_{E_{M1}-\Delta_1'}(k)}{c\sigma_1\left(E_{M1}+\Delta_1\right)} \tag{15}$$

Similarly, using two fluorescence spectrum measurements with monochromatic photons whose energies are $E_{M2} + \Delta_2$ and $E_{M2} - \Delta_2'$ where the energies Δ_2 and Δ_2' are assumed to be comparable with the level width of the M_2 subshell, we get

$$S_{M2}(k) = \frac{S_{E_{M2}+\Delta_2}(k) - \left(\frac{E_{M2}-\Delta_2'}{E_{M2}+\Delta_2}\right)^2 \cdot S_{E_{M2}-\Delta_2'}(k)}{c\sigma_2\left(E_{M2}+\Delta_2\right)} \tag{16}$$

We take 2.070 keV for $E_{M1} + \Delta_1$ and 2.020 keV for $E_{M1} - \Delta_1'$, then equation (15) become

$$S_{M1}(k) = \frac{S_{2.070}^{-E_l}(k) - \left(\frac{2.020}{2.070}\right)^2 \times f_1^{M1} \times S_{2.020}^{-E_l}(k)}{c\sigma_1\left(2.070\right)} \tag{17}$$

, were $f_1^{M1} = 1.024$ (from Table 3), and

$$c\sigma_1\left(2.070\right) = N_{2.070} \times m \times \sigma_1\left(2.070\right)$$

$$= 4.664\times10^{14} \times 5.24\times10^{16}\left[\frac{\text{atoms}}{\text{cm}^2}\right] \times 5.788\times10^{-20}\left[\frac{\text{cm}^2}{\text{atom}}\right]$$

$$= 141.46\times10^{10}$$

Similarly we take 1.848 keV for $E_{M2} + \Delta_2$ and 1.826 keV for $E_{M2} - \Delta_2'$, then (16) becomes

$$S_{M2}(k) = \frac{S_{1.848}^{-E_l}(k) - \left(\frac{1.826}{1.848}\right)^2 \times f_2^{M2} \times S_{1.826}^{-E_l}(k)}{c\sigma_2(1.848)} \tag{18}$$

, where $f_2^{M2} = 1.224$ (from Table 3), and

$$c\sigma_2(1.848) = N_{1.848} \times m \times \sigma_2(1.848)$$

$$= 1.836 \times 10^{14} \times 5.24 \times 10^{16}\left[\frac{\text{atoms}}{\text{cm}^2}\right] \times 6.547 \times 10^{-20}\left[\frac{\text{cm}^2}{\text{atom}}\right]$$

$$= 62.986 \times 10^{10}$$

The $S_{M1}(k)$ and $S_{M2}(k)$ spectra thus determined, should be corrected for the solid angle for the Si(Li)detector. This solid angle was estimated to be 0.003569 steradians. The M_1 and M_2 sublevels have a spin of 1/2, therefore the $S_{M1}(k)$ and $S_{M2}(k)$ have an isotropic angular distribution. Then, a factor for the correction of the solid angle of the Si(Li)detector is

$$0.003569 \text{ sr} \div 4\pi \text{ sr} = 2.840 \times 10^{-4}.$$

It is convenient to define c^{M1} and c^{M2} so as to include the correction factor for the solid angle of the Si(Li) detector just described, namely

c^{M1} = (c for M_1) x 2.840 x 10^{-4} = 401.7 x 10^6, and

c^{M2} = (c for M_2) x 2.840 x 10^{-4} = 178.9 x 10^6.

Therefore, c in equations (17) and (18) should be replaced by c^{M1} and c^{M2}, respectively. Using equations (17) and (18), we obtained $S_{M1}.c^{M1}.\sigma_1(2.070)$-spectrum and $S_{M2}.\ c^{M2}.\sigma_2(1.848)$-spectrum as shown in Fig. 15. [6)]

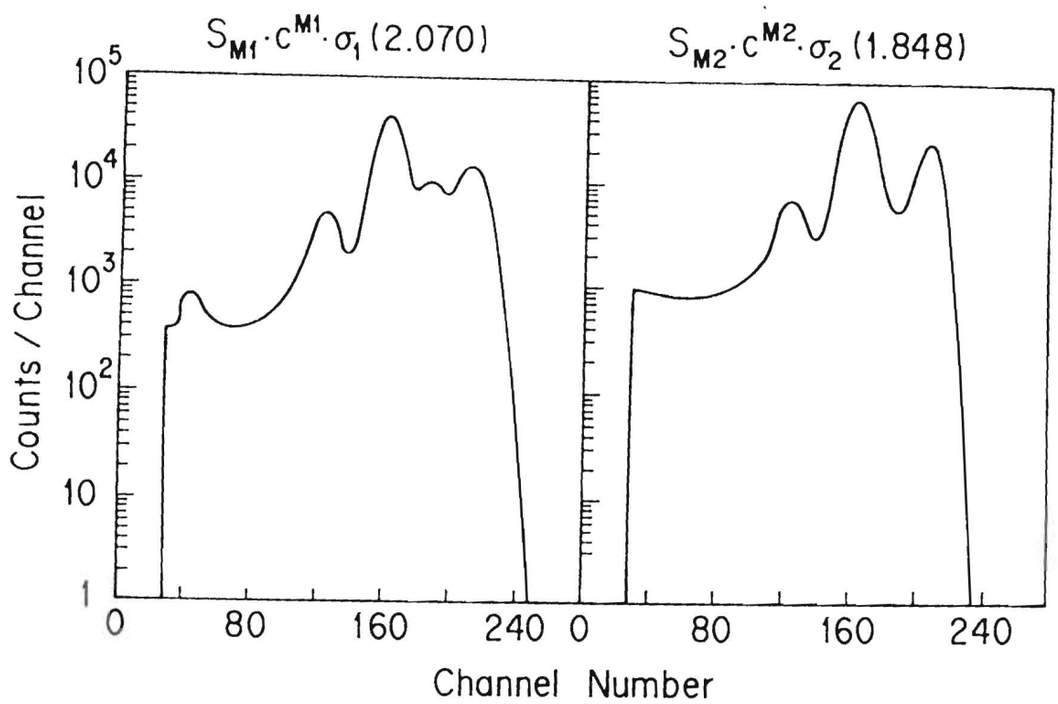

Fig. 15 Spectra of $S_{M1}(k) \cdot c^{M1} \cdot \sigma_1(2.070)$ and $S_{M2}(k) \cdot c^{M2} \cdot \sigma_2(1.848)$, where c^{M1} and c^{M2} stand for the normalized constants for M_1 and M_2, respectively.

In the reconstruction of the Sp^{163Ho} using S_{M1} and S_{M2}, it seems to be safer not to use the $M_{\alpha,\beta}$ peak in Fig. 1 and Fig. 15, because this peak includes X-ray transitions from the outermost shells of the Dy atom, namely M_5N_7 and M_4N_6. [3] Therefore we decided to reconstruct in an energy region* higher than the energy of $M\gamma$ by using integral counts of peaks. Furthermore, since the 5p-3s peak overlapped the elastic peak, it could not be used. Finally the reconstruction was done for peak ② and peak ③.

Here we write again equation (1) of Chap. 6,

$$Sp^{163Ho}(k) = \lambda_{M1} \cdot S_{M1}(k) + \lambda_{M2} \cdot S_{M2}(k) \tag{19}$$

Integral counts of each peak in $Sp^{163Ho}(k)$ on the left hand side were corrected for the self absorption in the ^{163}Ho source itself as follows;

---

* It was not easy to single out the $M\zeta$ peak without a large uncertainty.

$A_s^{Ho} = 0.9425$ for peak ② and

$A_s^{Ho} = 0.9237$ for peak ③,

where A_s^{Ho} denotes a correction factor for the self absorption.

Integral counts of each peak in S_{M2} and S_{M2} spectra on the right hand side were corrected for the absorption of incident photons and for the self-absorption of fluorescence photons due to the Dy target as follows;

$A_s^{Dy'} = 0.9463$ for peak ② in S_{M1},

$A_s^{Dy'} = 0.9405$ for peak ③ in S_{M1},

$A_s^{Dy'} = 0.9406$ for peak ② in S_{M2},

and

$A_s^{Dy'} = 0.9350$ for peak ③ in S_{M2},

where $A_s^{Dy'}$ denotes a correction factor for the absorption of incident photons due to the Dy target combined with the self-absorption of fluorescence photons due to the Dy target.

For peak ② in S_{M2} spectrum, the correction due to silicon impurities included in the mylar backing had to be taken into account, whose correction factor was estimated to be 0.901.

The correction for the detection efficiency of the Si(Li) detector is not necessary, because the same Si(Li) detector was used for a measurement of ^{163}Ho spectrum and Dy fluorescence spectra.

The reconstruction by Eq. (19) corresponds to solving the following two simultaneous equations of two variables, λ_{M1} and λ_{M2} ;

$$9.649 \times 10^{-16}\left[s^{-1} \cdot atom^{-1}\right] = 0.7808 \times 10^{-3}\left[atom^{-1}\right] \cdot \lambda_{M1} + 2.310 \times 10^{-3}\left[atom^{-1}\right] \cdot \lambda_{M2},$$

$$5.742 \times 10^{-16}\left[s^{-1} \cdot atom^{-1}\right] = 0.5297 \times 10^{-3}\left[atom^{-1}\right] \cdot \lambda_{M1} + 0.6204 \times 10^{-3}\left[atom^{-1}\right] \cdot \lambda_{M2}.$$

The solution 6) are

$\lambda_{M1} = (0.9846 \pm 0.0492) \times 10^{-12} s^{-1}$,

$\lambda_{M2} = (0.0850 \pm 0.0026) \times 10^{-12} s^{-1}$.

These results are in good agreement with the values obtained by our previous experiment (in the period form 1984 to 1986) within experimental uncertainties where theoretical S_{M1} and S_{M2} spectra modified by the experiment were used.

As we already described in Chapter 6, the half-life of ^{163}Ho nucleus was determined by measuring the production rate of ^{163}Dy due to electron capture in ^{163}Ho with isotope dilution mass spectrometry at University of Tokyo.

Our result [6] is

$$T_{1/2} = 4569 \pm 27\text{yr} \quad (68\%\ \text{CL})$$

or

$$\lambda t = (4.807 \pm 0.028) \times 10^{-12}\ s^{-1},$$

which is in excellent agreement with Baisden et al.'s value[10].

Using the values of λ_{M1} and λ_{M2} and λ_t as three constraints, $m_{\nu e}$ the Q-value and the log(*ft*) value for the decay of $^{163}Ho(E.C.)^{163}Dy$, were determined "at one effort" from the formula of the electron capture rate for the Gamow-Teller allowed transition[11]. The exchange and overlap correction factors were calculated by T. Mukoyama[12] by use of the Dirac-Fock wave functions. The radial wave functions at the holmium nucleus were taken from reference11). The results[6] are

$$m_{\nu e} = 110^{+350}_{-110}\text{eV},$$

$$Q = 2.710^{+0.100}_{-0.005}\text{keV}. \qquad \text{and}$$

$$\log ft = 4.993^{+0.030}_{-0.001} \qquad \text{or} \qquad |m_N|^2 = 0.04064^{+0.0001}_{-0.0027}$$

, where $|m_N|^2$ is the nuclear matrix element of the decay of ^{163}Ho.

Fig 16[6] shows a part of these results on a λ_{M1}/λ_t versus λ_{M2}/λ_t - diagram.

Therefore we conclude[6]

$$m_{\nu e} < 460\ \text{eV} \qquad (68\%\ \text{CL}).$$

According to "Review of Particle Properties" by PDG[13], the lowest upper limit for the mass of the electron neutrino is 225 eV by Springer et al.[14] However, taking account of Riisager's criticism (see Chap. 1), this value seems to be unreliable.

The next lowest upper limit for the mass of the electron neutrino is our 550 eV which was already described in Chap. 6.

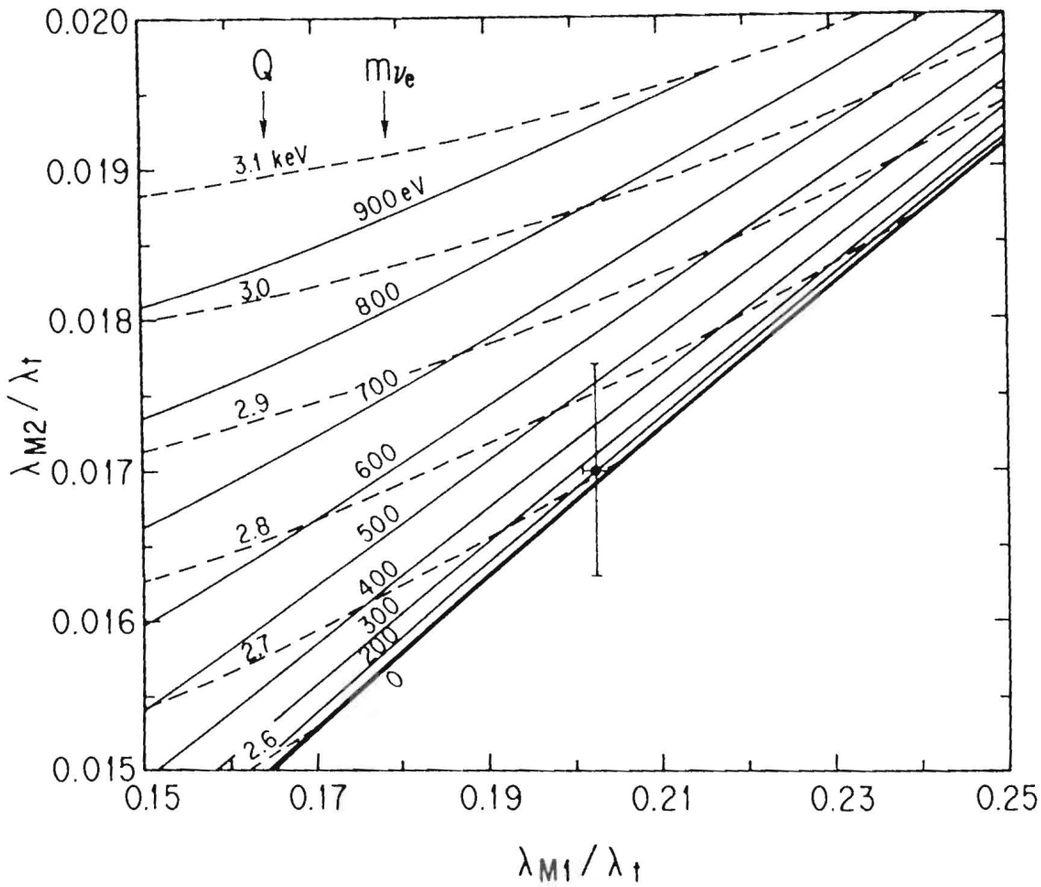

Fig. 16 Results of $m_{\nu e}$ and the Q-value shown on a λ_{M1}/λ_t versus λ_{M2}/λ_t -diagram.

In Experiment No. 91-272 an upper limit for the mass of the electron neutrino of 460 eV were obtained, **using the S_{M1} and S_{M2} spectra which were experimentally determined.**

Therefore we believe that our data on $m_{\nu e}$, the Q-value and log *ft* are most reliable values at present, though our upper limit for the mass of the electron neutrino is still very high, compared with the present upper limit for the mass of the electron antineutrino of 7.2 eV[15].

We are now measuring the ratio of N-Capture to M-Capture in ^{163}Ho using a heated proportional counter device[16]. If we succeed in determining the above ratio, this can serve as fourth constraint for three variables, $m_{\nu e}$, the Q-value and $|m_N|^2$.

We hope we will be able to reduce our present upper limit for $m_{\nu e}$ utilizing the above-mentioned over-constraint.

Finally we would like to point out that in this experiment we firstly succeeded in measuring log(*ft*) value for the decay of ^{163}Ho, and our value lies in between CERN's value (5.12)[17] and Princeton's value (4.9)[18].

References

1) T. Mukoyama, KEK 83-24, 1984, p. 19.
2) S. Yasumi et al., KEK Photon Factory Activity Report #10 (1992), p.28 in Contents of User's Reports.
3) S. Yasumi et al., Phys. Lett. B**181** (1986) 169.
4) K. Shima, Nucl. Instrum. Methods **165** (1979) 21.
5) S. Yasumi et al., Neutrino Mass and Low Energy Weak Interactions, eds. V. Barger and D. Cline (World Scientific, 1985) p. 398.
6) S. Yasumi et al., Phys. Lett. B**334** (1994) 229.
7) S. Yasumi et al., Phys. Lett. B**122** (1983) 461.
8) S. Kishimoto, KEK Report 90-22, 1991, p. 19.
9) Y. Inagaki, K. Shima and H. Maezawa, Nucl. Instrum. Methods B**27** (1987) 353.
10) P. A. Baisden et al., Phys. Rev. C**28** (1983) 337.
11) W. Bambynek et al., Rev. Modern Phys. **49** (1977) 77.
12) T. Mukoyama, Bull. Inst. Chem. Res. Kyoto University **65** (1987) 17.
13) PDG, Phys. Rev. D**50** (1994) 1173.
14) P.T.Springer et al., Phys. Rev. A**35** (1987) 679.
15) Ch. Weinheimer et al, Phys. Lett. B**300** (1993) 210.
16) F. X. Hartmann and R. A. Naumann, Phys. Rev. C**31** (1985) 1594.
17) J. U. Andersen et al., Phys. Lett. B**113** (1982) 72;
B. Jonson et al., Nucl. Phys. A**396** (1983) 479c.
18) P. A. Baisden et al., Phys. Rev. C**28** (1983) 337.

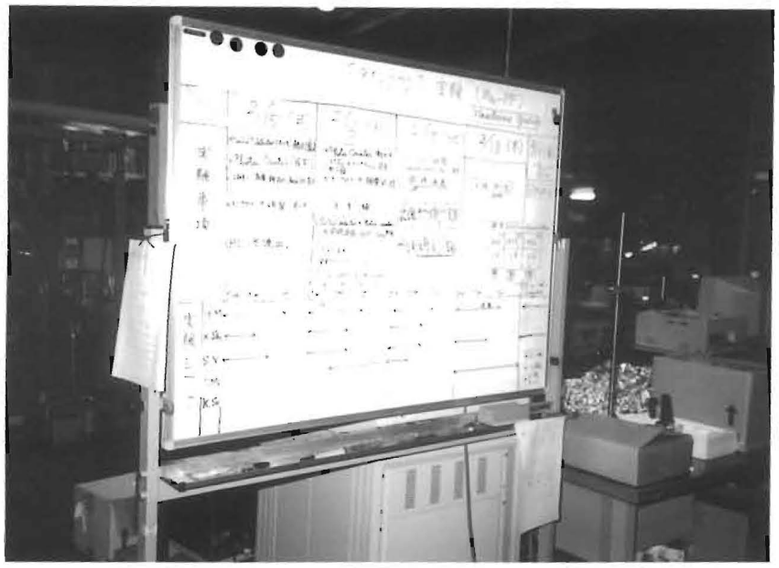

White board located near the BL-2A line of 2.5 GeV Photon Factory Storage Ring which indicates the schedule of experiments and shifts for participants in the February run of Experiment No. 91-272.

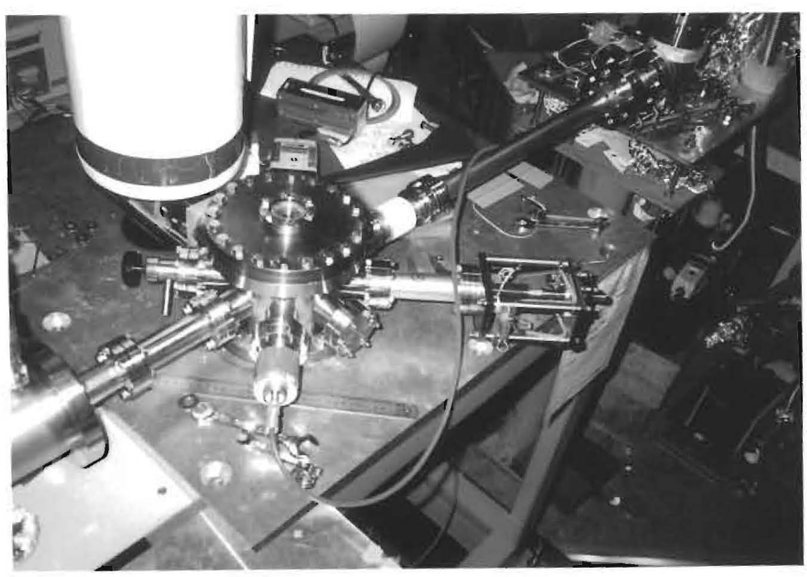

Target chamber seen from upstream.

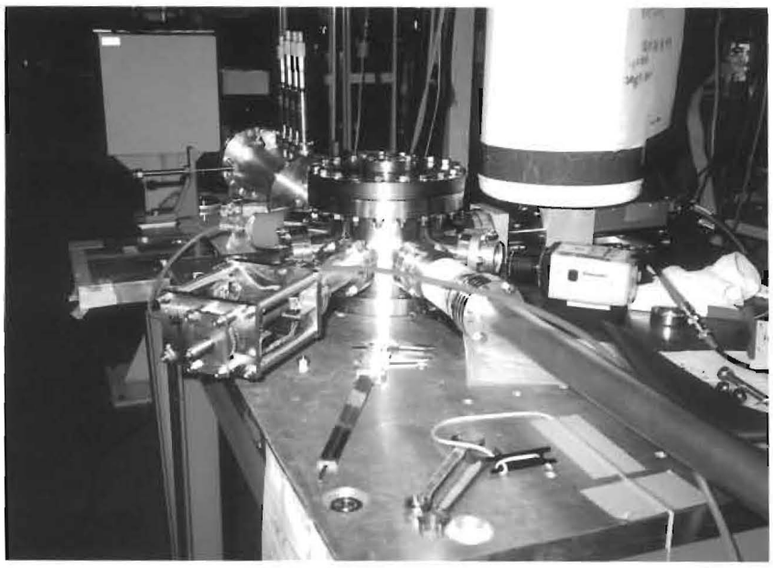

Target chamber, the Si(Li) detector, a linear feed through for the target system, and a part of the photon counter are seen.

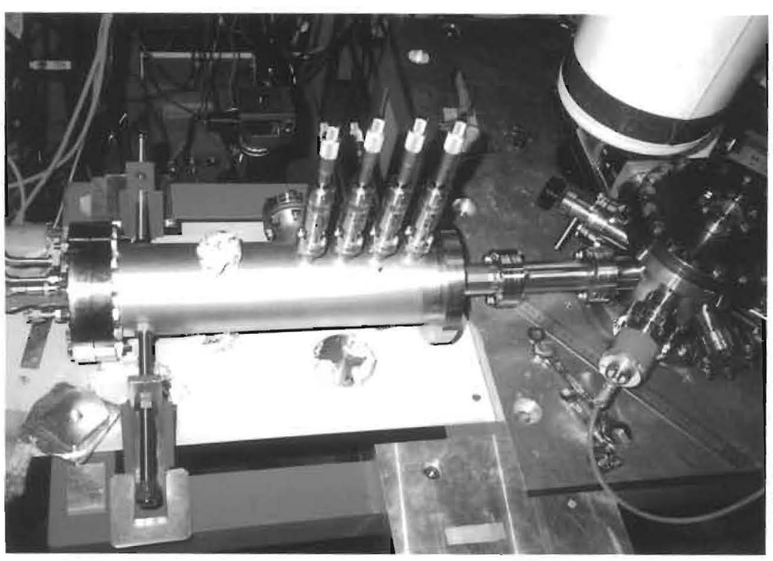

Photon counter with four linear feed throughs for Be absorbers.

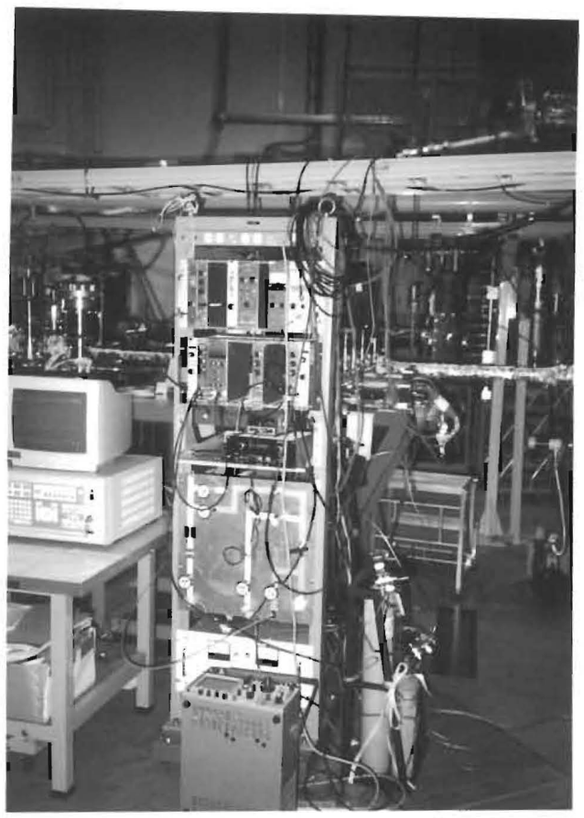

Electronics and the gas-filling system for the proportional counter.

Supplement 1

On the log *(ft)* values of Gamow-Teller Transitions around ^{163}Ho

M. Fujioka and S. Yasumi*

Cyclotron and Radioisotope Center, Tohoku University

**National Laboratory for High Energy Physics, KEK*

The recently performed experiment for the electron-neutrino rest mass gave the log *(ft)* value for ^{163}Ho electron capture, which lies in-between CERN's value and Princeton's value.

The Gamow-Teller matrix element(GTME) or the corresponding log *(ft)* value of nuclear beta decay is an important physical quantity related with the so-called quenching problem of the weak-interaction axial-vector coupling constant in nuclei[10].

Recently the result of an experiment on the electron-neutrino rest mass from the electron capture(EC) decay of ^{163}Ho[1] gave for the first time an experimental log *(ft)* value for this transition. A set of three independent quantities λ_{M1}, λ_{M2} and λ was measured in the experiment giving the information on three quantities $m_{\nu e}$, Q_{EC} and log *(ft)*. In the following we discuss the last quantity[1]; see Table 1 for the ^{163}Ho $\rightarrow$ ^{163}Dy spin -flip Gamow-Teller transition between the Nilsson orbitals of $p\frac{7}{2}[523] \rightarrow n\frac{5}{2}[523]$ in comparison with those of neighboring ones. It is noted that the log *(ft)* value of ^{163}Ho EC-decay had long been unknown due to the extremely small Q_{EC} value.

In the previous analyses of neutrino-mass experiments, only two quantities have been measured independently that necessitates an " estimate" for the log *(ft)* value for ^{163}Ho $\rightarrow$ ^{163}Dy . The CERN group used[2, 3] the value of 5.12 on the basis of systematics modified by a pairing-theoretical calculation, which we also adopted in our previous paper [4]. The Princeton group[5] on the other hand pointed out from their experiment on (d, p) reactions that the pairing-theoretical prediction overestimated the variation of log *(ft)* , and adopted the same value as for A=161 (i. e., 4.9). The pairing theory concerned Zeng et. al. [6] pointed out the importance of the so-called blocking effect which tends to suppress the variation of transition strength.

Meanwhile another quantity, the so-called N/M ratio, was measured by the CERN group[7] to be 2.4 ± 0.3 in apparent disagreement with 3.86 ± 0.12 obtained by the Princeton group[8].

The log *(ft)* value measured by us [1] for $^{163}Ho \rightarrow ^{163}Dy$ is shown in Table 1 in comparison with those [9] around this transition. It should be noted that our log *(ft)* value of 4.994 lies in-between CERN's value and Princetons's value. This should be explained by a more sophisticated theory of nuclear structure.

References

[1] S. Yasumi et.al., Phys. Lett. **B334**(1994)229.

[2] J. U. Anderson et.al., Phys. Letters **113B**(1982)72.

[3] J. U. Anderson et.al., CERN/PSCC/82-7, PSCC/M79, April, 1982.

[4] S. Yasumi et.al., Phys. Letters **122B**(1983)461.

[5] P. A. Baisden et.al., Phys. Rev. **C28**(1983)337.

[6] J. Y. Zeng et.al., Nucl. Phys. **A441**(1983)49.

[7] E. Laesgaard et.al., CERNEP/84-110; Proc. AMCO-7, Sept. 1984, Darmstadt-Seeheim.

[8] F. X. Hartmann, R. A. Nauman, Phys. Rev. **C1594**(1985) 1594.

[9] Tables of Isotopes 7th ed., John-Wilwy & Sons, 1987.

[10]H. Miyatake et.al., Nucl. Phys. **A470**(1987)328.

Table 1. Data of $p_{\frac{7}{2}}[523](\equiv N_{\pi 1}) \rightarrow n_{\frac{5}{2}}[523](N_{\nu 2})$ around ^{163}Ho

A	$t_{1/2}$	EC/β^-	Q_{EC}/β^- (keV)	Initial[a)]	Final[a)]	E^*_f(keV)	Q(keV)	Branch	log (*ft*)
157	12.6(2)m	EC	2540(50)	$_{67}Ho\ N_{\pi 1} \rightarrow Dy_{91}$	$N_{\nu 2}$	341	2199(50)	50%	4.9
159	33(1)m	EC	1853(9)	$_{67}Ho\ N_{\pi 1} \rightarrow Dy_{93}$	$N_{\nu 2}$	310	1543(9)	64%	4.9
161	3.64(8)m	β^-	1959(2)	$Gd_{97}\ N_{\pi 2} \rightarrow {}_{85}Tb$	$N_{\pi 1}$[b)]	417	1542(2)	85%	4.9[b)]
161	2.48(5)m	EC	853(3)	$_{67}Ho\ N_{\pi 1} \rightarrow Dy_{95}$	$N_{\nu 2}$	26	827(3)	75%	4.9
163	4569(27)y	EC	2.758(53)	$_{67}Ho\ N_{\pi 1} \rightarrow Dy_{97}$	$N_{\nu 2}$	0	2.758(53)	100%	4.994(16)
163	75.1(4)m	EC	1212(5)	$Er_{95}\ N_2 \rightarrow {}_{67}Ho$	$N_{\pi 1}$[b)]	0	1212(5)	99.8%	4.8[b)]
165	10.34(5)h	EC	377(2)	$Er_{97}\ N_2 \rightarrow {}_{67}Ho$	$N_{\pi 1}$[b)]	0	377(2)	100%	4.7[b)]

a) All the Nilsson states cited are the band head, i. e., $I_i = \Omega_i$ and $I_f = \Omega_f$

b) Statistical factor of Δ log (*ft*)= log (4/3) = 0.125 was corrected so that the values correspond to $N_{\pi 1} \rightarrow N_{\nu 2}$

c) The values are modified so that the errors be $\pm\ \sigma$.

Supplement 2

Milestones

February 23, 1981	Information on a new way of $m_{\nu e}$ -measurement from M. Yoshimura at KEK.
May 25, 1981	1st Workshop on $m_{\nu e}$
May 27, 1981	Proposal on a $m_{\nu e}$-measurement presented to KEK Director.
July 8, 1981	Proposal approved.
July 22, 1981	Seminar on $m_{\nu e}$ given by S.Y. at CYRIC, Tohoku University.
August 20, 1981	2nd Workshop.
October 21, 1981	$^{164}Dy_2O_3$ of about 7mg came to KEK form ORNL through JRIA.
November 4, 1981	3rd Workshop.
November 18, 1981	Neutrino Laboratory completed in Photon Factory, KEK.
December 10, 1981	Proton Irradiation on a Dysprosium-164 Metal Target at CYRIC, Tohoku University.
January 23, 1982	M X-rays of ^{163}Dy from ^{163}Ho observed at CYRIC, Tohoku University.
January 26-27, 1982	Holmium-163 Source came to KEK from Sendai.
January 29, 1982	Mini-workshop (theoretical).
March 27, 1982	4th Workshop.
April 3, 1982	Six Talks presented at the Meeting of the Physical Society of Japan.
June 15, 1982	Talk presented by S. Y. at Neutrino '82 June 14-19, 1982, Balatonfüred, Hungary.
June 25 and July 8, 1982	2nd Proton Irradiation on a ^{164}Dy Metal Target at CYRIC, Tohoku University.
July 15 (-October 27), 1982	Chemical Separations at Tohoku University.
July 31, 1982	5th Workshop at KEK.
October 18-20, 1982	Workshop on Monopoles and the Proton Decay at Kamioka.
November 16, 1982	Discussions with PF's people on the use of PF to measure $m_{\nu e}$ at the dining hall, KEK.
December 6, 1982	Letter of Intent presented to Photon Factory, KEK.

December 15, 1982	New ^{163}Ho Source (No. 14) came to KEK from Sendai. 6th Workshop at KEK.
December 23, 1982	Discussions with H. Taketani on a Measurement of the Q-value of ^{163}Ho using a Nuclear Reaction at Tokyo Institute of Technology.
March 4, 1983	PIXE Measurement for a New ^{163}Ho Source (No. 11) at CYRIC, Tohoku University.
March 17, 1983	The first paper on $m_{\nu e}$ appeared in Physics Letters B.
March 24, 1983	7th Workshop at KEK.
May 16, 1983	Seminar "Studies on the M-Shell of the Dysprosium Atom using Monochromatic X-Rays for a Measurement of $m_{\nu e}$"* given by S.Y. at the Photon Factory, KEK. (* Hereafter, this title is abbreviated to $m_{\nu e}$-PF Experiment).
June 21-23, 1983	Studies on the ^{163}Dy(p, n γ)^{163}Ho Reaction by H. Taketani et al. at Tokyo Institute of Technology.
July 23, 1983	Talk presented by S. Y. at the International Europhysics Conference on High Energy Physics, Brighton UK, July 20-27, 1983.
September 7, 1983	8th Workshop on $m_{\nu e}$ at KEK.
October 15-28, 1983 and November 8-18, 1983	Preliminary $m_{\nu e}$-PF Experiment.
November 4-5, 1983 and December 9-10, 1983	3rd Proton Irradiation on a ^{164}Dy Metal Target to produce ^{163}Ho at CYRIC, Tohoku University.
December 7-10, 1983	Workshop on GUTs and Cosmology at KEK.
December 10, 1983	Proposal on the $m_{\nu e}$-PF Experiment presented to the Photon Factory, KEK.
January 19, 1984	9th Workshop on $m_{\nu e}$ at KEK.
January 21, 1984	Meeting on the $m_{\nu e}$-PF Experiment.
January 31,1984	Proposal approved (No. 83-111).
February-March, 1984	$m_{\nu e}$-PF Experiment (No. 83-1111).
April 4, 1984	Talk given by S. Y. at the 39th Annual Meeting of the Physical Society of Japan, Fukuoka.
May 25 and June 24, 1984	Proton Irradiation in the 3rd Production Experiment of ^{163}Ho using the Reaction ^{164}Dy (p, 2n) ^{163}Ho at CYRIC, Tohoku University.

June 12, 1984	Short talk given by S. Y. at the ν 84 Conference, Nordkirchen near Dortmund, West Germany, June 11-16, 1984.
July 26, 1984	10th Workshop on $m_{\nu e}$ at KEK.
October 5, 1984	Mini-workshop on $m_{\nu e}$ at KEK.
October 25, 1984	Invited talk presented by S. Y. at the Telemark Conference on Neutrino Mass and Low Energy Weak Interactions, Telemark Lodge, Cable, Wisconsin, October 25-27, 1984.
November 2, 1984	Talk given by S. Y. at the 2nd Photon Factory Symposium, University of Tsukuba, Tsukuba, November 1-2, 1984.
December 14, 1984	Talk presented by S. Y. at the Workshop on Hadron-Lepton Interactions in the nucleus, Osaka University, Toyonaka, December 14-15, 1984.
December 21, 1984	Mini-workshop on $m_{\nu e}$ at KEK.
January-March, 1985	$m_{\nu e}$-PF Experiment using the Undulator Beam Line (BL-2) in Photon Factory, KEK (No. 83-111).
May-July, 1985	$m_{\nu e}$-PF Experiment (No. 83-111).
June 3, 1985	Half-life of ^{163}Ho was successfully measured by A. Masuda and O. Kawakami.
June 4, 1985	Eleventh Workshop on $m_{\nu e}$ at KEK.
July 20, 1985	Talk on $m_{\nu e}$ given by S.Y. at the International Europhysics Conference on High Energy Physics, Bari (Italy), July 18-24, 1985.
August 19-24, 1985	1985 International Symposium on Lepton and Photon Interactions at High Energies (Kyoto).
December 7, 1985	Twelfth Workshop on $m_{\nu e}$ at KEK.
December 26, 1985	Mini-workshop on $m_{\nu e}$ at KEK.
January 30, 1986	Talk given by S.Y. at the Sixth Moriond Workshop, Tignes-Savoie-France, Jan. 25-Feb. 1, 1986.
April 25, 1986	Mini-workshop on $m_{\nu e}$ at KEK.
June 12, 1986	Talk on $m_{\nu e}$ given by S.Y. at International Symposium on Nuclear Beta-Decays and Neutrino, Osaka, June 10-13, 1986.
July 3, 1986	Talk on $m_{\nu e}$ given by S.Y. at International Symposium on Weak and Electromagnetic Interactions in Nuclei, Heidelberg, July 1-5, 1986.

November 7, 1986	Thirteenth Workshop on $m_{\nu e}$ at KEK.
November 27, 1986	The second paper on $m_{\nu e}$ appeared in Physics Letters B.
April 21, 1987	Comment on $m_{\nu e}$ presented by S.Y. at the Eleventh International Conference on Particles and Nuclei, Kyoto, April 20-24, 1987.
September, 1987	Approval of Experiment No. 87-175.
September 24, 1987	Mini-workshop on Neutrino Mass from Electron Capture, for Prof. P. G. Hansen from Aarhus, at CYRIC, Tohoku University, Sendai.
March 18, 1988	Comment on the Half-life of ^{163}Ho given by O. Kawakami at XVI INS International Symposium on Neutrino Mass and Related Topics, Tokyo, March 16-18, 1988.
September 9, 1988	Fourteenth Workshop on $m_{\nu e}$ at KEK.
February 18-July 15, 1989	$m_{\nu e}$-PF Experiment (No. 87-175).
September 7, 1989	Talk on $m_{\nu e}$ given by S.Y. at International Europhysics Conference on High Energy Physics, Madrid, September 6-13, 1989.
September, 1989	Approval of Experiment No. 89-200.
November 21 - December 12, 1989	$m_{\nu e}$-PF Experiment (No. 89-200).
May 7-8, 1990	BL-2 Users' Meeting at Photon Factory, KEK.
June 1-4, 1990	$m_{\nu e}$-PF Experiment (No, 89-200).
June 16-17, 1990	the same as above
January 10, 1991	Fifteenth Workshop on $m_{\nu e}$ at KEK.
May 11 & 16, 1991	the same as above
June 27, 1991	Proposal of the next $m_{\nu e}$-PF Experiment.
October 4, 1991	Approval of $m_{\nu e}$-PF Experiment No. 91-272.
March 16-26, 1992	$m_{\nu e}$-PF Experiment (No. 91-272)
September 4, 1992	Seminar on $m_{\nu e}$ given by S. Y. at CYRIC, Tohoku University
December 15-21, 1992	$m_{\nu e}$-PF Experiment (No. 91-272)
February 16-20, 1993	the same as above
July 24, 1993	Talk on $m_{\nu e}$ given by S. Y. at the International Europhysics Conference on High Energy Physics, Marseille, France, July 22-28, 1993.
February 24, 1994	Seminar on $m_{\nu e}$ given by S. Y. at CYRIC.

March 29, 1994	Talk on $m_{\nu e}$ given by S. Y. at the annual meeting of the Physical Society of Japan in Fukuoka.
August 11, 1994	The third paper on $m_{\nu e}$ appeared in Physics Letters B.

Supplement 3

Publications

S. Yasumi, G. Rajasekaran, M. Ando, F. Ochiai, H. Ikeda, T. Ohta, P.M. Stefan, M. Maruyama, N. Hashimoto, M. Fujioka, K. Ishii, T. Shinozuka, K. Sera, T. Omori, G. Izawa, M. Yagi, K. Masumoto and K. Shima:
"Measurement of the Mass of the Electron Neutrino using the Electron Capture Decay Process of the Nucleus."
KEK Preprint 82-15 July 1982 E;
Proc. of Int. Conf. Neutrino '82 14-19 June 1982, Balatonfüred, Hungary, Vol. I, p.59.

S. Yasumi (Editor):
"Proc. of the 4th Workshop on the Mass of the Electron Neutrino."
KEK 82-8, September 1982 E.

S. Yasumi, G. Rajasekaran, M. Ando, F. Ochiai, H. Ikeda, T. Ohta, P.M. Stefan, M. Maruyama, N. Hashimoto, M. Fujioka, K. Ishii, T. Shinozuka, K. Sera, T. Omori, G. Izawa, M. Yagi, K. Masumoto and K. Shima:
"The Mass of the Electron Neutrino and Electron Capture in ^{163}Ho."
KEK 82-25, November 1982 E.

K. Ishii, M. Fujioka, K. Sera, T. Shinozuka and K. Katsube:
"Bonding of a Dysprosium Metal Target for the Production of ^{163}Ho."
Nucl. Instrum. and Meth., 205 (1983) 563.

S. Yasumi, G. Rajasekaran, M. Ando, F. Ochiai, H. Ikeda, T. Ohta, P.M. Stefan, M. Maruyama, N. Hashimoto, M. Fujioka, K. Ishii, T. Shinozuka, K. Sera, T. Omori, G. Izawa, M. Yagi, K. Masumoto and K. Shima:
"The Mass of the Electron Neutrino and Electron Capture in ^{163}Ho."
Phys. Lett., 122B (1983) 461.

S. Yasumi:
"Measurement of the Mass of the Electron Neutrino using Electron Capture in ^{163}Ho."
KEK 83-12, July 1983 T/E, p.135.

S. Yasumi (KEK-Osaka-Tohoku-Tsukuba-Kyoto-T.I.T. Collaboration):
"Measurement of the Mass of the Electron Neutrino using Electron Capture in ^{163}Ho."
Proc. of Int. Europhysics Conf. High Energy Physics, Brighton UK, July 1983, p.391.

S. Yasumi, F. Ochiai, M. Ando, H. Maezawa, H. Kitamura, K. Itoh, M. Maruyama, M. Fujioka, K. Ishii, T. Shinozuka, K. Sera, T. Omori, G. Izawa, M. Yagi, K. Masumoto, K. Shima, T. Mukoyama, Y. Inagaki and H. Taketani:
"Measurement of the Mass of the Electron Neutrino using Electron Capture in ^{163}Ho."
KEK Preprint 83-17, August 1983 E;
Rutherford Appleton Laboratory Library Database No. 0014.

S. Yasumi (Editor):
"Proc. of the 7th Workshop on the Mass of the Electron Neutrino."
KEK 83-15, September 1983 E.

K. Shima, S. Nagai, T. Mikumo and S. Yasumi:
"Measurement of the Low Energy Tail Spectra adjacent to the X-Ray Photopeak in Si(Li) X-Ray Detectors."
Nucl. Instrum. and Meth., 217 (1983) 515.

K. Sera, K. Ishii, M. Fujioka, G. Izawa and T. Omori:
"The Quantitative Analysis of ^{163}Ho Source by PIXE."
The 2nd Symposium on Ion Beam Technology - Ion Beam Analysis, Hosei University, December 2-3, 1983.

T. Mukoyama and H. Adachi:
"M-Shell X-Ray Emission Rates for Rare Earth Elements."
J. Phys. Soc. Japan, 53 (1984), 984.

S. Yasumi (Editor):
"Proc. of the 9th Workshop on the Mass of the Electron Neutrino."
KEK 83-24, March 1984 E.

S. Yasumi:
"Measurement of the Mass of the Electron Neutrino using Electron Capture in ^{163}Ho."

KEK Report 84-12, September 1984 H (Proc. Workshop on Grand Unified Theories and Cosmology, KEK, December 1983), p. 240.

S. Yasumi, F. Ochiai, M. Ando, H. Maezawa, H. Kitamura, M. Maruyama, M. Fujioka, K. Ishii, T. Shinozuka, K. Sera, T. Omori, G. Izawa, M. Yagi, K. Masumoto, K. Shima, T. Mukoyama, Y. Inagaki, H. Taketani, I. Sugai, and A. Masuda:
"Measurement of the Mass of the Electron Neutrino using Electron Capture in ^{163}Ho."
Proc. of 11th Int. Conf. on Neutrino Physics and Astrophysics, Nordkirchen near Dormund, June 11-16, 1984.

S. Yasumi, F. Ochiai, M. Ando, H. Maezawa, H. Kitamura, M. Maruyama, M. Fujioka, K. Ishii, T. Shinozuka, K. Sera, T. Omori, G. Izawa, M. Yagi, K. Masumoto, K. Shima, T. Mukoyama, Y. Inagaki, H. Taketani, I. Sugai, and A. Masuda:
"Measurement of the Mass of the Electron Neutrino using Electron Capture in ^{163}Ho."
KEK Preprint 84-9, September 1984 H.

S. Yasumi, F. Ochiai, M. Ando, H. Maezawa, H. Kitamura, M. Maruyama, M. Fujioka, K. Ishii, T. Shinozuka, K. Sera, T. Omori, G. Izawa, M. Yagi, K. Masumoto, K. Shima, T. Mukoyama, Y. Inagaki, H. Taketani, I. Sugai, A. Masuda, and O. Kawakami:
"Measurement of the Mass of the Electron Neutrino using Electron Capture in ^{163}Ho."
Neutrino Mass and Low Energy Weak Interactions, Telemark, 1984 edited by V. Barger and D. Cline, p.398.

S. Yasumi (Editor):
"Proc. of the 10th Workshop on the Mass of the Electron Neutrino."
KEK Report 84-19, 1985 H.

S. Yasumi, M. Ando, H. Maezawa, H. Kitamura, T. Ohta, F. Ochiai, A. Mikuni, M. Maruyama, M. Fujioka, K. Ishii, T. Shinozuka, K. Sera, T. Omori, G. Izawa, M.Yagi, K. Masumoto, K. Shima, T. Mukoyama, Y. Inagaki, I. Sugai, A. Masuda, and O. Kawakami:
"Measurement of the Mass of the Electron Neutrino using Electron Capture in ^{163}Ho."
Proc. Int. Europhysics Conf. on High Energy Physics, Bari, Italy, July 1985.

S. Yasumi, M. Ando, H. Maezawa, H. Kitamura, T. Ohta, F. Ochiai, A. Mikuni, M. Maruyama, M. Fujioka, K. Ishii, T. Shinozuka, K. Sera, T. Omori, G. Izawa, M.Yagi, K. Masumoto, K. Shima, T. Mukoyama, Y. Inagaki, I. Sugai, A. Masuda, and O. Kawakami:
"Measurement of the Mass of the Electron Neutrino using Electron Capture in ^{163}Ho."
Proc. Sixth Moriond Workshop, Tignes-Savoie-France, January 1986, p.579.

S. Yasumi, M. Ando, H. Maezawa, H. Kitamura, T. Ohta, F. Ochiai, A. Mikuni, M. Maruyama, M. Fujioka, K. Ishii, T. Shinozuka, K. Sera, T. Omori, G. Izawa, M. Yagi, K. Masumoto, K. Shima, T. Mukoyama, Y. Inagaki, I. Sugai, A. Masuda, and O. Kawakami:
"Measurement of the Mass of the Electron Neutrino using Electron Capture in ^{163}Ho."
Proc. Int. Symposium on Nuclear Beta Decays and Neutrino, Osaka, June 1986, p.377.

S. Yasumi, M. Ando, H. Maezawa, H. Kitamura, T. Ohta, F. Ochiai, A. Mikuni, M. Maruyama, M. Fujioka, K. Ishii, T. Shinozuka, K. Sera, T. Omori, G. Izawa, M. Yagi, K. Masumoto, K. Shima, T. Mukoyama, Y. Inagaki, I. Sugai, A. Masuda, and O. Kawakami:
"Measurement of the Mass of the Electron Neutrino using Electron Capture in ^{163}Ho."
Proc. Int. Symposium on Weak and Electromagnetic Interactions in Nuclei, Heidelberg, July 1-5, 1986, p.786.

S. Yasumi, M. Ando, H. Maezawa, H. Kitamura, T. Ohta, F. Ochiai, A. Mikuni, M. Maruyama, M. Fujioka, K. Ishii, T. Shinozuka, K. Sera, T. Omori, G. Izawa, M. Yagi, K. Masumoto, K. Shima, T. Mukoyama, Y. Inagaki, I. Sugai, A. Masuda, and O. Kawakami:
"The Mass of the Electron Neutrino using Electron Capture in ^{163}Ho."
Phys. Lett., B181 (1986) 169.

S. Yasumi and Y. Inagaki:
"Study on the Mass of the Electron Neutrino using Electron Capture Processes."
Physics Monthly, Vol. 8 No. 1 (1987) 45. (in Japanese)

Y. Inagaki, K. Shima and H. Maezawa:
"Response Functions of a Si(Li) Detector for 1.3-4.0 keV Monochromatic Photons."

Nucl. Instrum. and Meth., B27 (1987) 353.

S. Yasumi:
"Comment (on the Mass of the Electron Neutrino)."
Proc. the Eleventh Int. Conf. on Particles and Nuclei, Kyoto, April 1987, p.469 C.

O. Kawakami, A. Masuda, M. Fujioka, T. Omori and S. Yasumi:
"Measurement of the Half-life of ^{163}Ho by Isotope-Dilution Mass Spectrometry."
Proc. the Sixteenth INS Int. Symposium on Neutrino Mass and Related Topics, Tokyo, March 16-18, 1988, p.274.

O. Kawakami, A. Masuda, M. Fujioka, T. Omori and S Yasumi:
"Half-life of ^{163}Ho."
Phys. Rev., C38 (1988) 1857.

S. Yasumi, H. Maezawa, S. Kishimoto, M. Fujioka, K. Sera, T. Omori, K. shima, T. Mukoyama, Y. Inagaki and G. Izawa:
"Measurement of the Mass of the Electron Neutrino using Electron Capture in ^{163}Ho."
Nucl. Phys. B (Proc. Suppl.) , 16 (1990) 499.
(Proc. Int. Europhysics Conf. on High Energy Physics, Madrid, September 6-13, 1989.)

S. Yasumi, H. Maezawa, K. Shima, Y. Inagaki, T. Mukoyama, T. Mizogawa, K. Sera, S. Kishimoto, M. Fujioka, K. Ishii, T. Omori, G. Izawa and O. Kawakami:
"Measurement of the Mass of the Electron Neutrino using Electron Capture in ^{163}Ho" Proc. Int. Europhys. Conf. High Energy Physics, Marseille, France, 22-28 July 1993 p. 549.

S. Yasumi, H. Maezawa, K. Shima, Y. Inagaki, T. Mukoyama, T. Mizogawa, K. Sera, S. Kishimoto, M. Fujioka, K. Ishii, T. Omori, G. Izawa and O. Kawakami: The Mass of the Electron Neutrino from Electron Capture in ^{163}Ho" Phys. Lett. B334 (1994) 229.

S. Yasumi: "Measurement of the Mass of the Electron Neutrino using Orbital Electron Capture in ^{163}Ho" Butsuri 51 (1996) p.111 (in Japanese).